Title
Regulation of Autophagosome Biogenesis by the Autophagy Specific Class III Phosphatidylinostitol-3 Kinase Complex

Author
Wilz, Livia Margaret

Publication Date
2015

Peer reviewed|Thesis/dissertation

Regulation of Autophagosome Biogenesis by the Autophagy Specific Class III Phosphatidylinostitol-3 Kinase Complex

By

Livia Margaret Wilz

A dissertation submitted in partial satisfaction of the

requirements for the degree of

Doctor of Philosophy

in

Molecular and Cell Biology

in the

Graduate Division

of the

University of California, Berkeley

Committee in charge:

Professor Randy W. Schekman, Chair
Professor Jeremy W. Thorner
Professor James W. Hurley
Professor J. Christopher Anderson

Fall 2015

Abstract

Regulation of Autophagosome Biogenesis by the Autophagy Specific Class III Phosphatidylinostitol-3 Kinase Complex

by

Livia Margaret Wilz

Doctor of Philosophy in Molecular and Cell Biology

University of California, Berkeley

Professor Randy Schekman, Chair

Autophagy is a conserved pathway critical for homeostasis in all eukaryotic cells**.** Autophagy provides a mechanism for cells to respond to a large variety of cellular stresses through a vesicle-based degradation process. Most of the gene products and other factors required for the execution of autophagy have been elucidated**,** but the biochemical reactions by which these components work in concert to engulf cargo in a double membrane vesicle**,** called an autophagosome**,** is still unclear. In mammalian cells, the class III phosphatidylinositol 3-kinase complex I (PI3KC3-C1) is essential for early steps in autophagy because it generates a membrane lipid, phosphatidylinositol 3-phosphate (PtdIns3P), that is necessary to recruit downstream autophagy factors to cellular membranes. However, it was not known whether the PI3KC3-C1 also contributes to phagophore formation in other ways.

The research described in this dissertation focused on one of the subunits of PI3KC3-C1, Atg14L, which is essential for the complex to initiate autophagy. I used an *in vitro* reconstitution assay where I added back purified PI3KC3-C1 or various mutant derivatives of the complex to extracts derived from a Cas9-generated Atg14L-deficient cell line. As a biochemical readout for examining the functions of Atg14L, I used a cell-free reaction that reproduces a key early step in autophagosome membrane generation, lipidation of a cytoplasmic protein, LC3**.** In this assay, I found that Atg14L **(**and the other subunits of PI3KC3-C1**)** are required for LC3 lipidation, whereas mutants of the complex that abrogate its catalytic activity and membrane curvature-sensing capability did not support LC3 lipidation. In addition, PI3KC3-C1 activity, through Atg14L and its membrane curvature- sensing motif, is required for efficient membrane recruitment of the downstream PtdIns3P-binding effector, WIPI2, but not for recruitment of Atg16L, a key factor required for LC3 lipidation.

In an effort to find other cofactors that may also regulate PI3KC3-C1, I found that NRBF2 binds Atg14L and attenuates its autophagy-stimulating function and, hence, serves as a negative regulator of autophagy. Under fed conditions, however, NRBF2 is phosphorylated; phosphorylation null mutants show elevated autophagy under fed conditions. In another study, I uncovered that Atg14L acts as a vesicle tether that supports vesicle fusion when soluble N-ethylmaleimide-sensitive factor attachment protein receptors (SNAREs) are incorporated into the vesicle. The fusogenic activity of

Atg14L requires oligomerization through conserved cysteine repeats near the N-terminus of Atg14L.

Table of Contents

List of Figures

List of Tables

Acknowledgements

First, I would like to thank Randy for taking me into his lab when I was the most worried that I would not have a place to continue my PhD. His thoughtful and patient guidance has proven helpful throughout my entire time at Berkeley. He also fostered an environment within the lab of talented scientists I am proud to call my co-workers. I would like to thank all Schekman labmates for helpful conversation and continual guidance on both scientific and personal levels. I have learned so much from all of you. I would particularly like to thank Liang Ge for teaching his cell-free assay to me and guiding me as I mastered it myself. Lastly, I would like to thank our lab manager Bob Lesch, who keeps the lab running so smoothly so that we only have to focus on science and is a patient listener when we need it most.

I would also like to thank Qing for being the first to introduce me to autophagy, share his passion for the topic with me, and guide me through my first three years of my doctorate. I attribute my excitement about this field to when I met him for the first time. I would like to thank Zhong labmates for helpful conversation and guidance and to Weiliang Fan for teaching me the basics of cell biology and autophagy. I am grateful to Jeremy Thorner for emotional support as I switched labs and helpful discussion during committee meetings. I would also like to thank Jim Hurley for guidance and collaboration in purifying the PI3K complex, and particularly to Goran Stjeptanovic for patiently teaching me how to conduct a very complex biochemical purification that was pivotal to this project.

I would like to thank the UC Berkeley tissue culture facility for plating countless dishes of Atg5 KO MEFs for me, and the MCB GAO for logistical support. My classmates and friends throughout the MCB department were always eager to provide scientific guidance or, just as importantly, commiseration and release from the unique stresses that come from a PhD program. I have met some of my favorite people through this experience and am thankful for them.

My parents, siblings, in-laws, and extended family have eagerly supported me through everything I have wanted to do. I love each of them and am so grateful to have what seems like a village of cheerleaders and supporters in the Midwest who are always there for guidance if I should ask. My parents have always emphasized that I should do what makes me happy and to follow my dreams. I am so happy that their guidance brought me to this goal and supported me while I attained it. My dad helped me move across the country to Berkeley and my mom has been there to listen whenever I needed her. I am so proud to have been raised by two wonderful people.

Lastly, I have to thank my husband, Scott. He was my first chemistry partner when I fell in love with science and has been my best friend for almost half my life. He moved across the country and almost everyone he knew to be with me in California. As with any PhD, these past six years have been full of more frustrations than successes. He celebrated the wins with me, and more importantly, picked me up and urged me to keep going when I was the most discouraged. I am so happy with our life we have together and can't wait for our future.

Chapter 1: Macroautophagy as a Means of Maintaining Cellular Homeostasis

Regulated catabolism is critical for cellular homeostasis

Many nutrients that are essential for cellular survival are of limited availability or energetically costly to regularly build from scratch. Rather than export and discard anything that is toxic or not needed, cells are more economical with their waste and carefully break it down into basic building blocks that can be recycled into new macromolecules and organelles. Cells employ a few methods for recycling proteins, namely the proteasome, a cylindrical-shaped complex that proteolyzes unfolded proteins or the vacuole/lysosome that sequesters a variety of hydrolases in its membranous compartment that degrades soluble or insoluble protein and entire organelles.

If a specific protein is no longer needed or toxic to the cell because, for example, its regulatory function needs to be alleviated or it cannot fold properly, it can be targeted for degradation through the ubiquitin protease pathway (Bhattacharyya et al., 2014). A cascade of enzymatic events covalently attaches a chain of ubiquitin proteins to lysine residues on the target protein, marking it for degradation. Ubiquitylated proteins are then trafficked to the proteasome, the polyubiquitin chain is removed, and the proteins are unfolded into a polypeptide chain. This polypeptide chain is fed into the barrel-shaped catalytic component of the proteasome where the protease activity contained within can process it into small peptides that are easily degraded.

However, not all proteins can be degraded by the proteasome because they are aggregated, contained in a large complex, or incorporated into an entire organelle that needs to be removed. Moreover, under cytotoxic stress such as nutrient starvation or hypoxia, bulk degradation of cytosol and non-essential organelles can rapidly provide the amino acids and lipids required to construct proteins and organelles necessary for survival. In cases such as these, vesicle-based degradation is critical as vesicles can engulf a variety of cargo and traffic their contents to the vacuole/lysosome without having to alter their structure. Once inside the acidic lumen of the vacuole/lysosome, the menagerie of hydrolases enriched and activated within this compartment can easily degrade cargo into basic building blocks for recycling (Huang and Klionsky, 2002).

There are several ways by which vesicular-based degradation occurs. Extracellular or plasma membrane anchored proteins can be endocytosed and trafficked through the endosomes that eventually fuse with the vacuole/lysosome and deposit their content for degradation. Proteins can also be directly captured and engulfed by the vacuole/lysosome by microautophagy or chaperone-mediated autophagy (Huang and Klionsky, 2002; Kundu and Thompson, 2008). An alternative process called macroautopahgy (hereafter referred to as autophagy) encapsulates and degrades cytoplasmic content or other cellular components such as organelles by engulfing them in a double membrane vesicle called an autophagosome.

Autophagy is activated under a variety of cellular stress signals but the best-characterized method of autophagy induction is nutrient starvation. Upon activation, a cup-like structure called the phagophore forms from an existing organelle, possibly the

ER-Golgi intermediate compartment (ERGIC)(Ge et al., 2013) and engulfs specifically targeted cargo and/or bulk cytoplasm. Once the double membrane autophagosome is formed, it is transported to and fuses its outer membrane with the vacuole/lysosome and deposits the inner vesicle termed autophagic body into the lumen for degradation (Fig 1.1). Based on its capabilities to rapidly recycle unwanted factors under stress and target toxic organelles for degradation, autophagy is critical for maintaining cellular homeostasis (Huang and Klionsky, 2002; Levine and Klionsky, 2004; Mizushima and Yoshimori, 2007).

History and general autophagy mechanism

Autophagy was first observed and described by Christian de Duve and Robert Wattiaux in the 1960's after fixed and sectioned mammalian tissue were examined by electron microscopy (EM). Autophagosomes were described as double membrane structures associated with lysosomes that "contain mitochondria, endoplasmic reticulum… microbodies, glycogen particles and other cytoplasmic entities"(de Duve and Wattiaux, 1966). Future studies using animal systems and more EM uncovered that this process is related to nutrient availability because it is up regulated upon starvation or changes in mitochondrial membrane potential and inhibited by insulin (Klionsky, 2007; Yang and Klionsky, 2010).

It was not until the 1990's when the Ohsumi group characterized autophagy in the genetically tractable *S. cerevisiae* that the autophagy machinery was uncovered and detailed mechanistic studies could commence. Preliminary experiments demonstrated that when cells lacking critical vacuolar proteases are starved, autophagic bodies accumulate and fill the vacuole in a manner that can be visualized by differential interference contrast (DIC) microscopy (Takeshige et al., 1992). Using this phenotype as a marker for active autophagy, they conducted a screen and found 15 different genes that lose viability or cannot accumulate autophagic bodies upon starvation (Tsukada and Ohsumi, 1993). Other studies uncovered and further characterized the over 30 different autophagy (Atg) genes responsible for creating this double membrane vesicle that engulfs cargo targeted for degradation (Huang and Klionsky, 2002; Klionsky et al., 2003; Reggiori and Klionsky, 2002).

In *S. cerevisiae*, autophagosomes nucleate at a pre autophagosome structure (PAS) adjacent to the endoplasmic reticulum (ER) and vacuole (Huang and Klionsky, 2002; Suzuki and Ohsumi, 2010). The PAS is marked by pre aminopeptidase I (prApeI), a vacuolar hydrolase that requires autophagy machinery for trafficking to the vacuole (Baba et al., 1997). Under wild-type conditions, only one autophagosome forms at a time as visualized by the well-characterized autophagosome marker and substrate of the pathway, Atg8-PE (Kabeya et al., 2000; Kirisako et al., 1999; Mizushima, 2007; Suzuki et al., 2001). The other known autophagic machinery is not degraded upon autophagy induction. Consequently, these other factors are either localized only to the cytoplasmic leaflet of the autophagosome outer membrane or dissociate from the vesicle before it is sealed. Under non-starved conditions, a pathway similar to autophagy, the biosynthetic cytoplasm to vacuolar targeting (CVT) pathway, utilizes most of the same machinery as autophagy but targets and transports specific vacuolar hydrolases to the vacuole (Huang and Klionsky, 2002).

Autophagy progression can be monitored using a variety of standard techniques. Immunofluorescence of Atg8 puncta formation, PAS localization, or autophagic machinery colocalization is widely used in addition to the accumulation of autophagic bodies using DIC described above. Alternatively, time courses and immunoblotting can be used to track the covalent attachment of phosphatidylethanolamine (PE) to the small protein Atg8 to form Atg8-PE at the PAS, or the cleavage of GFP from GFP-Atg8-PE and maturation of prApe1 to mature Ape1 in the vacuole after autophagy is complete (Klionsky et al., 2007; Mizushima, 2007).

Autophagy is highly conserved across eukaryotes. However, in contrast to yeast or other single-celled organisms, autophagy in metazoans responds to a variety of different stimuli related to nutrient or hormonal levels, organelle malfunction and pathogen invasion (Levine and Klionsky, 2004). The mammalian ortholog of Atg8, LC3-I, is also conjugated to PE, becoming LC3-II. Autophagy progression in mammals can be monitored via immunoblotting for the conversion of LC3-I to LC3-II or degradation of key cargo such as p62/SQSTM1 (Klionsky et al., 2007; Mizushima, 2007). However, in contrast to *S. cerevisiae*, autophagy is constitutively active at low levels in metazoans but can be highly activated after induction by a variety of signals. In addition, many distinct autophagosomes can form at once in a metazoan cell in contrast to the single PAS observed in yeast. After autophagy induction, autophagosomes appear to form adjacent to or from the ER (Axe et al., 2008) or ER-Golgi intermediate compartment (ERGIC)(Ge et al., 2013), and migrate across the cell to the lysosome. En route to the lysosome, autophagosomes acidify and fuse with endosomes before they finally fuse with the lysosome to become an autolysosome where autophagic bodies are then degraded (Jahreiss et al., 2008).

Mechanisms of autophagy initiation

Autophagy regulation by mTORC1 and AMPK

Although mammalian autophagy responds to many different stress signals, it is primarily activated by cellular starvation as a result of either low amino acid or ATP levels. Autophagy response and regulation based on nutrient levels involves two master serine/threonine kinases, the mechanistic target of rapamycin complex 1 (mTORC1) and the AMP activated protein kinase (AMPK) that both phosphorylate and either inactivate or activate autophagy machinery, respectively, to allow the cell to respond to and recover from nutrient deprivation (Inoki et al., 2012).

mTORC1 is the master regulator of cellular nutrient status that activates biosynthetic pathways such as protein translation and inactivates catabolism pathways such as autophagy to coordinate cellular growth (Jewell et al., 2013; Zoncu et al., 2010). In mammalian cells, hormones such as insulin and growth factors stimulate mTORC1 by a signaling cascade that involves the RHEB GTPases, keeping autophagy inactive. In addition to responding to growth factors through RHEB, mTORC1 senses cellular amino acid levels through heterodimeric RagGTPases located on the cytoplasmic leaflet of the lysosome (Jewell et al., 2013). Under fed conditions, mTORC1 is active and tethered to the lysosome via a large complex of RagGTPases, the Ragulator and the vacuolar H^+-ATPase (Sancak et al., 2010; Sancak et al., 2008; Zoncu et al., 2011). The RagGTPases and vacuolar H+-ATPase sense amino acid levels within the lysosome. When amino acid

levels are low, mTORC1 is released from the membrane and inactivated. Consequently this activates a feedback loop to maintain nutrient level homeostasis where low amino acids inactivate mTORC1 and stimulate autophagy-mediated protein degradation. After autophagy progresses and amino acid levels are again high in lysosome, mTORC1 is reactivated and autophagy is inhibited (Jewell et al., 2013; Yu et al., 2010).

AMPK is another master regulator of cellular energy homeostasis activated after periods of starvation, hypoxia or ischemia. AMPK senses and responds to low ATP levels by binding AMP when its cellular concentration increases as a result of low or depleted ATP stores (Inoki et al., 2012). To conserve and rebuild cellular energy stores, AMPK shuts down anabolic pathways and activates catabolic pathways such as autophagy. AMPK regulates autophagy indirectly by phosphorylating and deactivating components of the mTORC1 pathway and directly by phosphorylating and activating specific autophagy machinery (Egan et al., 2011; Inoki et al., 2012; Kim et al., 2013; Kim et al., 2011; Mao and Klionsky, 2011).

Autophagy machinery

Two decades of research has resulted in the characterization of components of the autophagy machinery and defined functional groups that initiate and organize autophagosome formation (Fig 1.1). Additionally, several studies have looked at many autophagy factors at once and clarified the associations, membrane recruitment hierarchy, and the spatially distinct membrane localization of these factors (Behrends et al., 2010; Graef et al., 2013; Itakura and Mizushima, 2010; Kishi-Itakura et al., 2014; Koyama-Honda et al., 2013; Suzuki et al., 2013; Suzuki et al., 2007). This work has helped clarify how the over 30 characterized autophagy factors are organized genetically and temporally to orchestrate autophagosome formation. However, there are still many remaining questions regarding how these factors are recruited to the phagophore and manipulate it to form a complete autophagosome. Because autophagy is highly conserved across eukaryotes, most of the core autophagy machinery discovered in yeast have orthologs in higher eukaryotes (Kundu and Thompson, 2008; Levine and Klionsky, 2004). As my studies involved cultured mammalian cells, I refer to the names and describe the functions of the machinery in mammals. However, most autophagy machinery has conserved functions across eukaryotes.

Atg1p/ULK1 complex

The first functional complex activated upon autophagy induction is the Atg1p/ULK1 kinase complex. In *S. cerevisiae*, it exists as a pentamer with Atg1p, Atg13p, Atg17p, Atg29 pand Atg31p. In mammals, it exists as a tetramer with ULK1, Atg13, FIP200, and Atg101 (Noda and Fujioka, 2015). ULK1 and its paralog ULK2 are orthologs of the serine/threonine kinase Atg1p with some functional redundancies although ULK1 is the predominant regulator of autophagy (Chan et al., 2007; Young et al., 2006). Atg13p is stably bound to Atg1p (Stjepanovic et al., 2014) and serves as a signal modulator regulated by upstream kinases and Atg1p/ULK1 (Chang and Neufeld, 2009; Jung et al., 2009). Atg101 does not have any known homologs in yeast but maintains Atg13 stability in mammals (Hosokawa et al., 2009b; Mercer et al., 2009). FIP200 and Atg17 contain functional homologies as they both serve as a scaffold for the

PAS or nascent autophagosome but FIP200 is much larger than Atg17 and does not share much sequence similarity (Hara et al., 2008; Suzuki et al., 2007).

The ULK1 complex is the hub of autophagy activation, translating upstream nutrient sensing signals from mTORC1 and AMPK into autophagosome formation (Noda and Fujioka, 2015). Under fed conditions, ULK1 and Atg13 are inhibited and highly phosphorylated by mTORC1. After starvation, mTORC1 is inhibited and the ULK1 complex is rapidly dephosphorylated (Ganley et al., 2009; Hosokawa et al., 2009a; Jung et al., 2009). Either concurrently or in response to energy starvation, activated AMPK is phosphorylates and ULK1 which in turn phosphorylates itself and Atg13 (Egan et al., 2011; Kim et al., 2011; Mao and Klionsky, 2011). This kinase complex is responsible for recruiting and activating downstream factors such as the lipidation machinery (Gammoh et al., 2013; Nishimura et al., 2013), Atg9 vesicles (Mack et al., 2012; Young et al., 2006) and the PI3K complex (Jao et al., 2013; Russell et al., 2013) although the exact mechanism by which these are recruited is not clear.

Atg9

Atg9 is a multi-spanning transmembrane protein that positively regulates autophagy. After translation, it is trafficked through the Golgi and is localized in a distinct structure described as a reservoir of tubular/vesicular structures in yeast (Mari et al., 2010; Yamamoto et al., 2012) or in the trans-Golgi network and endosomes in mammals (Orsi et al., 2012; Young et al., 2006). Once autophagy is induced, the small 30-60 nm Atg9 positive vesicles translocate to the PAS or nascent autophagosome. Atg9 puncta localize near the PAS and also on the tips of the growing phagophore (Suzuki et al., 2013; Suzuki et al., 2007). It has been proposed that Atg9 vesicles may serve as a bulk membrane source for phagophore elongation (Yamamoto et al., 2012) or a few Atg9 vesicles may fuse and form the nucleation membrane for autophagosome formation. Structural and biochemical studies of the Atg1p/ULK1 complex suggest that this complex is capable of tethering small vesicles such as Atg9 vesicles and could initiate phagophore formation (Ge et al., 2014a; Hurley and Schulman, 2014; Ragusa et al., 2012). Imaging analyses in mammalian cells show Atg9 in vesicular structures near the phagophore that do not appear to stably associate with it. It is therefore unclear if Atg9 vesicles are ever a part of the early autophagosome (Orsi et al., 2012). It will be important to clarify the role that these dynamic Atg9 vesicles play in autophagy progression to better understand the membrane source and dynamics of autophagosome formation.

PI3KC3 complex

After localization and activation of the ULK1 complex and Atg9 vesicles, the next complex recruited to the phagophore is the class III phosphatidylinositol 3-kinase complex I (PI3KC3-C1) (Koyama-Honda et al., 2013; Suzuki et al., 2007). In *S. cerevisiae,* this complex consists of the sole phosphatidylinositol 3-kinase (PI3K), Vps34p; two regulatory and scaffolding factors, Vps15p and Vps30p/Atg6p; and an autophagy specific factor responsible for localization, Atg14p (Kihara et al., 2001a; Kihara et al., 2001b). This complex has high functional homology in mammals and consists of Vps34, Vps15 (p150), Beclin 1 and Atg14L/Barkor (Itakura et al., 2008; Matsunaga et al., 2009; Sun et al., 2008; Zhong et al., 2009).

In both yeast and mammalian systems, it appears that key role for the PI3K complex is to produce the signaling lipid phosphatidylinositol 3-phosphate (PtdIns3P). When cells are treated with PI3K inhibitors, such as 3-methyladenine (3-MA), LY294002 (LY), and wortmannin, autophagy progression, stable autophagy machinery membrane association and LC3-II lipidation are blocked (Itakura and Mizushima, 2010; Karanasios et al., 2013; Koyama-Honda et al., 2013; Petiot et al., 2000). In mammals, PI3K activity is required for budding of small vesicular autophagy precursors and phagophore formation (Axe et al., 2008; Ge et al., 2014b; Hamasaki et al., 2013; Kishi-Itakura et al., 2014). In yeast, the PI3K complex is localized to a punctate structure at one edge of the growing phagophore, creating PtdIns3P that is localized to the tips and inner membrane of the phagophore (Cheng et al., 2014; Graef et al., 2013; Obara and Ohsumi, 2008; Suzuki et al., 2013). The PI3KC3-C1 is responsible for creating the key signaling peptide, PtdIns3P and, because it stimulates the formation of small vesicular precursors, may also be critical for elongating the nascent phagophore.

Atg18-2/WIPI complex

One group of autophagy machinery proteins that are directly recruited to the phagophore as a result of PI3K activity are members of the WD repeat protein interacting with phosphoinositides (WIPI) family, orthologous to Atg18 in yeast. WIPI family proteins contain seven bladed β propeller repeats that are known to serve scaffolding functions (Proikas-Cezanne et al., 2015; Proikas-Cezanne et al., 2004). Two members of this family, WIPI1 and WIPI2, are PtdIns3P effectors that positively regulate autophagy activity (Mauthe et al., 2011; Polson et al., 2010; Proikas-Cezanne et al., 2007). Together with a constitutive binding partner, Atg2, they form the WIPI complex and are recruited to the tips of the growing phagophore in a PI3KC3-C1 dependent manner (Graef et al., 2013; Obara et al., 2008b; Proikas-Cezanne et al., 2015; Suzuki et al., 2013).

The WIPI complex is required for Atg9 recycling from the phagophore and for the progression of autophagy (Nagy et al., 2014; Reggiori et al., 2004). In addition, the WIPI complex is thought to facilitate phagophore elongation and possibly autophagosome closure as WIPI complex mutants, in particular Atg2 deletions, accumulate shorter, unsealed phagophores in yeast and mammalian systems (Kishi-Itakura et al., 2014; Suzuki et al., 2013; Velikkakath et al., 2012).

VMP1

Recently, an ER-localized multi-spanning transmembrane protein called vacuole membrane protein 1 (VMP1) has been uncovered as an early regulator of autophagy in mammals (Calvo-Garrido et al., 2008a; Calvo-Garrido et al., 2008b; Ropolo et al., 2007). VMP1 is localized at the phagophore early in the autophagy activation hierarchy before ULK1 or lipidation machinery membrane recruitment but is not required for their membrane localization (Itakura and Mizushima, 2010; Koyama-Honda et al., 2013). VMP1 associates with the PI3KC3-C1 by binding Beclin 1 (Molejon et al., 2013; Ropolo et al., 2007) and, similar to the WIPI complex, either VMP1 or the products it recruits to the membrane may be responsible for phagophore elongation and closure as VMP1 mutant cells show the accumulation of immature, unsealed phagophores similar to Atg2 deletion mutants (Kishi-Itakura et al., 2014).

Atg8p/LC3 lipidation machinery

Two ubiquitin-like proteins and their enzymatic conjugation systems are required to create the final autophagy marker consisting of a small protein covalently attached to PE (Geng and Klionsky, 2008; Mizushima et al., 2001). Although they share no sequence homology to ubiquitin, both Atg12 and Atg8/LC3 have a characteristic ubiquitin fold and are conjugated to another protein or lipid using an enzymatically similar mechanism (Ichimura et al., 2004; Ichimura et al., 2000; Matsushita et al., 2007; Sugawara et al., 2004). The final lipidation reaction product is either Atg8-PE in yeast or LC3-II in mammals. This lipidation system is highly conserved across eukaryotes although in mammals there are several different Atg8 orthologs outside of LC3, the GABARAP and GATE16 families, that undergo lipidation using the same enzymes and are also involved in autophagy (Sou et al., 2006; Weidberg et al., 2010).

The lipidation machinery is associated with the PAS and phagophore at an early stage, dependent on PtdIns3P production (Itakura and Mizushima, 2010; Koyama-Honda et al., 2013; Suzuki et al., 2007). The lipidation cascade begins when the first ubiquitin-like molecule, Atg12, is activated and forms a thioester bond with the E1-like protein, Atg7. Atg12 is transferred to the E2-like protein, Atg10, through another thioester bond and is then conjugated to Atg5 through an isopeptide bond without a canonical E3-like protein. In the second ubiquitin-like pathway, the C-terminal glycine of Atg8/LC3 is first exposed by the cysteine protease Atg4. Atg8 is then conjugated to Atg7 and then to another E2-like protein, Atg3 through thioester bonds. Lastly, the Atg5-12 conjugate forms a large complex with Atg16 that functions as an E3 for conjugating Atg8 through an amide bond to phosphatidylethanolamine and is associated with the membrane. Atg5-Atg12/Atg16 membrane localization determines the location of Atg8/LC3 lipidation (Fujita et al., 2008b; Geng and Klionsky, 2008; Hanada et al., 2007; Romanov et al., 2012).

LC3-II is located on both inner and outer membranes of the autophagosome (Kabeya et al., 2000), thus some portion of the LC3-II in the cell is degraded by the lysosome. However, LC3-II on the outside of the autophagosome is cleaved from PE and recycled by Atg4. The mechanistic purpose of LC3 lipidation in autophagosome biogenesis is not entirely clear but studies have suggested it is involved in autophagosome elongation and closure (Fujita et al., 2008a; Kabeya et al., 2000; Kaufmann et al., 2014; Kishi-Itakura et al., 2014; Mizushima et al., 2001).

However, another role for Atg8/LC3 is as a cargo receptor. LC3 binds proteins with an LC3 interacting region (LIR) motif, tethering cargo selected for degradation to the concave side of the phagophore (Carlsson and Simonsen, 2015; Lin et al., 2013; Rogov et al., 2014; Suzuki et al., 2014). The best characterized LIR motif-containing protein is p62 which accumulates in bodies around polyubiquinated cargo targeted for autophagic degradation that are then tethered to the autophagosome through the LIR motif (Bjørkøy et al., 2005; Katsuragi et al., 2015; Lin et al., 2013; Pankiv et al., 2007). The various Atg8 family orthologs in mammals may serve as distinct cargo receptors. For example, GABARAP binds another LIR motif aggregate scaffolding protein, ALFY, to also target its cargo for degradation (Lystad et al., 2014). Overall, it seems that the Atg8 family of proteins serves a variety of key functions for autophagy, principally by helping form the autophagosome and target specific cargo for degradation.

Autophagosome closure, maturation, fusion with lysosome

To date, it is not clear what factors are responsible for closing the autophagosome. It is possible that the ESCRT complex could be involved because autophagosome scission is topologically related to the scission event performed by ESCRT proteins to invaginate membrane and form vesicles within mutivesicular bodies (MVBs)(Hurley and Hanson, 2010). Genetic studies have demonstrated that ESCRT complex depletion accumulates autophagosomes and attenuates cargo degradation but it is not clear if these autophagy defects are a result of faulty phagophore closure or defects in endosome/autophagosome fusion later on in the process (Filimonenko et al., 2007; Lee et al., 2007; Rusten et al., 2007).

It is probable that autophagy machinery such as Atg2 and VMP1 may also function in autophagosome closure. EM and protease protection assays have shown that Atg2 and VMP1 null cells do not have sealed autophagosomes (Kishi-Itakura et al., 2014; Velikkakath et al., 2012). Consequently, it is possible that these factors could be directly responsible for fusing the two growing edges of the phagophore on their own or recruiting other fusion machinery.

Once autophagosome formation is complete, it must be transported to and fuse with the vacuole/lysosome for autophagy to be complete. Several different fusion machinery proteins are involved in the autophagosome maturation step including soluble N-ethylmaleimide-sensitive factor attachment protein receptors (SNAREs), RabGTPases, and the homotypic fusion and vacuole protein sorting (HOPS) tethering complex (Itakura et al., 2012; Jiang et al., 2014; Levine and Klionsky, 2004; Longatti and Tooze, 2009; Reggiori and Klionsky, 2006; Tooze et al., 2014). Autophagosome maturation is regulated to some extent by the PI3KC3-C2, an additional PI3K complex that contains the UV irradiation resistance associated gene (UVRAG) instead of Atg14L (Kim et al., 2015; Liang et al., 2008). In metazoans, once the autophagosome is complete, it matures and fuses with other autophagosomes and endosomes, becoming acidic along the way. Vesicle acidification is required for autophagy progression as treatment with drugs that abolish it such as chloroquine or bafilomycin A_1 cause the accumulation of LC3-II in immunoblots and LC3 positive vesicles in immunofluorescence and block degradation of autophagic cargo (Klionsky et al., 2008; Nakamura et al., 1997; Slater, 1993; Yamamoto et al., 1998). Because LC3-II is formed as a result of induced autophagy and is also a substrate for degradation, it is difficult to directly interpret autophagy activity after induction using LC3-II formation as a read out. To experimentally separate these two factors that regulate LC3-II levels, cells are often treated with these acidification inhibitors to block degradation. Therefore, after treatment, the amount of LC3-II or LC3 puncta present in the cell is directly related to the rate of LC3 lipidation (Klionsky et al., 2007; Mizushima and Yoshimori, 2007).

Autophagy in relation to disease

As a key regulator of cellular homeostasis and protein quality control, autophagy has been implicated in several different diseases including, cancer, neurodegeneration and infection. The mechanistic basis behind the role of autophagy in these conditions is reviewed below.

The first link between autophagy and cancer came with the discovery by the Levine group that Beclin 1 is a haploinsufficient tumor suppressor gene (Liang et al., 1999; Yue et al., 2003). In the years since that discovery, the role of autophagy in cancer is seen as much more complex. Autophagy plays a paradoxical role in cancer progression as different studies have found that autophagy can function as both a tumor suppressor and mechanism of tumor survival (Mathew et al., 2007; White and DiPaola, 2009). Loss-of-function mutations in autophagy genes have been associated with increased tumorigenesis. This is expected as autophagy maintains cellular homeostasis and mitigates metabolic stress that when uncontrolled can damage the genome and promote inflammation (Karantza-Wadsworth et al., 2007; Mathew et al., 2009). However, autophagy has also been shown contribute to cancer cell survival in solid tumors or tumors defective in apoptosis. Autophagy activation can help these cells better cope with metabolic stress based on limited nutrient availability or chemotherapies and prolong tumor survival (Amaravadi et al., 2007; Degenhardt et al., 2006). Consequently, many studies have been undertaken to either use available autophagy inhibitors or develop more specific ones that could block autophagy activity and tumor progression for use on their own on in combination with established chemotherapies (Kimura et al., 2013; Pasquier et al., 2015; Ronan et al., 2014). Overall, it appears that autophagy may play a dual role in cancer progression based on the stage at which autophagy is affected and the specific cancer type. Therefore, it is important to understand more about autophagy and its role in cancer before autophagy regulating therapeutics become standard in the clinic.

Because one of the primary roles of autophagy in maintaining cellular homeostasis is to clear protein aggregates, disorders characterized by protein misfolding and aggregation such as late-onset neurodegenerative disorders are often initiated or exacerbated by dysfunctional autophagy (Martinez-Vicente, 2015; Menzies et al., 2015). This can be best explained by focusing on the role of autophagy in the autosomal dominant polyQ expansion neurodegeneration disorder, Huntington's disease. Wild-type Htt protein has several different scaffolding functions in protein trafficking pathways and is subject to proteasome degradation (Ochaba et al., 2014). In contrast, mutant Htt characterized by the expansion of polyQ repeats near the N-terminus are not soluble and aggregate. Muntant Htt aggrates accumulate and are unable to be degraded by the proteasome. Some protein aggregates are regularly cleared by autophagy, but studies suggest that Htt is required for proper autophagic cargo recognition (Bjørkøy et al., 2005; Martinez-Vicente et al., 2010). Therefore, the toxic aggregates accumulate, further taxing cellular homeostasis and causing neuronal death. Cell death typically more catastrophic in neurons than in other organisms because they do not regenerate. Neurons from patients with other neurodegenerative conditions such as Alzheimer's disease show defects in lysosomal acidification and subsequent autophagosome accumulation (Lee et al., 2010; Liang and Jia, 2014; Martinez-Vicente, 2015), suggesting that blocks in autophagic flux and aggregate degradation may induce neuronal damage through a variety of mechanisms.

Clearance of damaged or old mitochondria via autophagy, also known as mitophagy, is critical for cell viability because damaged mitochondria left in the cytosol for too long can leak reactive oxygen species (ROS) damaging other nearby mitochondria, destroying cellular energy production and leading to cellular death (Durcan and Fon, 2015). Defects in mitochondrial clearance in neurons are related to neurodegeneration

disorders such as Parkinson's disease (PD). When mitochondrial damage disrupts membrane potential, the phosphatase and tensin homolog- induced putative kinase 1 (PINK1) accumulates on the mitochondrial outer membrane and phosphorylates the E3 ubiquitin ligase PARKIN (Matsuda et al., 2010; Narendra et al., 2010; Vives-Bauza et al., 2010). Activated PARKIN then polyubiquitinates many proteins on the mitochondrial surface, which recruits p62 and tethers the organelle to the autophagosome membrane for degradation (Geisler et al., 2010; Narendra et al., 2008). Autosomal recessive mutations that result in defective PINK1 or PARKIN have been related to early onset PD. However, only a small percentage of PD patients show these mutations, suggesting other mechanisms for PD occurrence, such as other mitophagy defects or α-synuclein accumulation as a result of defective chaperone mediated autophagy (Durcan and Fon, 2015; Martinez-Vicente, 2015). However, using what the field has learned about mitophagy from the mutations in PARKIN and PINK1, it may be possible to treat and prevent mitochondrial clearance disorders in the future.

Autophagy is involved in both the innate and adaptive immune responses after pathogen invasion. The type of pathogen and how it reacts to autophagic engulfment, xenophagy, determines if autophagy is beneficial or detrimental to pathogen clearance. For example, *Salmonella typhimurium* is engulfed by autophagosomes after infection and becomes sequestered in an autophagic compartment with limited nutrients that is then is degraded after fusion within the lysosome (Kundu and Thompson, 2008; Shibutani et al., 2015). Autophagy deficient cells are more sensitive to *Salmonella* infection; autophagosome enclosure helps the cell clear the pathogen more efficiently (Birmingham et al., 2006; Sun et al., 2008). In contrast, internalized *Legionella* bacteria slow autophagosome maturation and uses the distinct compartment as a replicative niche from which it emerges in much higher numbers (Amer and Swanson, 2005). For pathogens such as *Legionella*, autophagy deficient mutants clear the infection faster. Autophagy is also involved in the adaptive immune system by presenting exogenous antigens to the MHC Class II system via LC3 associated phagocytosis or endogenous pathogenic peptides to MHC Class I antigen after viral infection (Klionsky et al., 2007; Shibutani et al., 2015).

Overall, the integral role that autophagy plays in regulating cellular homeostasis is directly related to how organisms respond to stress and cope with disease and infection. It is clear that aberrant autophagy can be detrimental to the system under a variety of circumstances. Consequently, further understanding of the mechanism of autophagy initiation and regulation will be key to find more approaches to modulate autophagy and better treat and understand these and other disorders.

About this dissertation

This dissertation was completed under the guidance of two different professors at UC Berkeley. Chapter 2 was conducted from 2013 to 2015 under the guidance of Dr. Randy Schekman. Chapter 3 was conducted from 2010 to 2012 under the guidance of Dr. Qing Zhong. Although this work was done in two different labs with different approaches, both projects seek to answer a similar question, namely, what is the detailed mechanism of Atg14L and the PI3KC3-C1 in autophagy regulation and autophagosome biogenesis? Chapter 2 takes a more biochemical approach, using cell-free assays and

recombinantly expressed and purified protein complexes to directly observe differences in LC3 lipidation and autophagy factor membrane. Chapter 3 uses a more cell biological approach to characterize a recently discovered PI3KC3-C1 subunit, NRBF2, which binds Atg14L and attenuates its activity. Consequently, through two different approaches in two different labs, I continued to focus on the mechanism of autophagy regulation through the PI3KC3-C1 in this entire dissertation.

Tables

Table 1.1: List of Autophagy Factors Referenced in this Study

S. Cerevisiae	*H. Sapiens*	Function in Mammalian cells	Reference
Atg1	ULK1/ULK2	Initial regulatory kinase	(Noda and Fujioka, 2015)
Atg2	Atg2A/B	Phagophore closure?	(Romanyuk et al., 2011; Velikkakath et al., 2012)
Atg3	Atg3	E2 for LC3	(Geng and Klionsky, 2008)
Atg4	Atg4A/B	Cleaves pro-LC3 and LC3-II	(Geng and Klionsky, 2008)
Atg5	Atg5	Conjugated to Atg12 in a complex that is an E3 for LC3	(Geng and Klionsky, 2008; Mizushima et al., 2001)
Atg6/ Vps30	Beclin 1	Scaffold protein for PI3KC3, binds BCL2	(Levine et al., 2015)
Atg7	Atg7	E1 for Atg12 and LC3	(Geng and Klionsky, 2008)
Atg8	LC3/GABARAP/GATE	Cargo receptor and Autophagosome marker	(Geng and Klionsky, 2008; Kabeya et al., 2000)
Atg9	Atg9	Membrane source? Regulates autophagy initiation?	(Orsi et al., 2012)
Atg10	Atg10	E2 for Atg12	(Geng and Klionsky, 2008)
Atg12	Atg12	Conjugated to Atg5 and in a complex that is an E3 for LC3	(Geng and Klionsky, 2008)
Atg13	Atg13	Regulates ULK1	(Noda and Fujioka, 2015)
Atg14	Atg14L	Targets PI3KC3-C1 to autophagosome	(Itakura and Mizushima, 2009; Obara and Ohsumi, 2011)
Atg16	Atg16L	In a complex that is an E3 for LC3	(Fujita et al., 2008b; Geng and Klionsky, 2008; Mizushima et al., 1999)
~Atg17	FIP200	Scaffold for ULK1 complex	(Noda and Fujioka, 2015)
Atg18	WIPI 1/2	PtdIns3P effector, autophagosome	(Polson et al., 2010)

		elongation?	
Atg29	No known homolog		(Noda and Fujioka, 2015)
Atg32	No known homolog		(Noda and Fujioka, 2015)
Atg38	NRBF2	Regulates PI3KC3-C1	(Araki et al., 2013; Lu et al., 2014)
	Atg101	Stabilizes Atg13	(Noda and Fujioka, 2015)
Vps15	Vps15/p150	Regulates Vps34	(Backer, 2008)
Vps34	hVps34	Produces PtdIns3P	(Backer, 2008)
Vps38	UVRAG	Facilitates autophagosome formation and maturation	(Itakura and Mizushima, 2009; Liang et al., 2008)
	Bif-1	Remodels membrane in autophagosome formation	(Takahashi et al., 2007)
	Ambra1	Regulates Beclin 1	(Fimia et al., 2007)
	VMP1	Autophagosome closure?	(Calvo-Garrido et al., 2008a)
	Rubicon	Negatively Regulates PI3KC3-C2	(Matsunaga et al., 2009; Zhong et al., 2009)

Figures

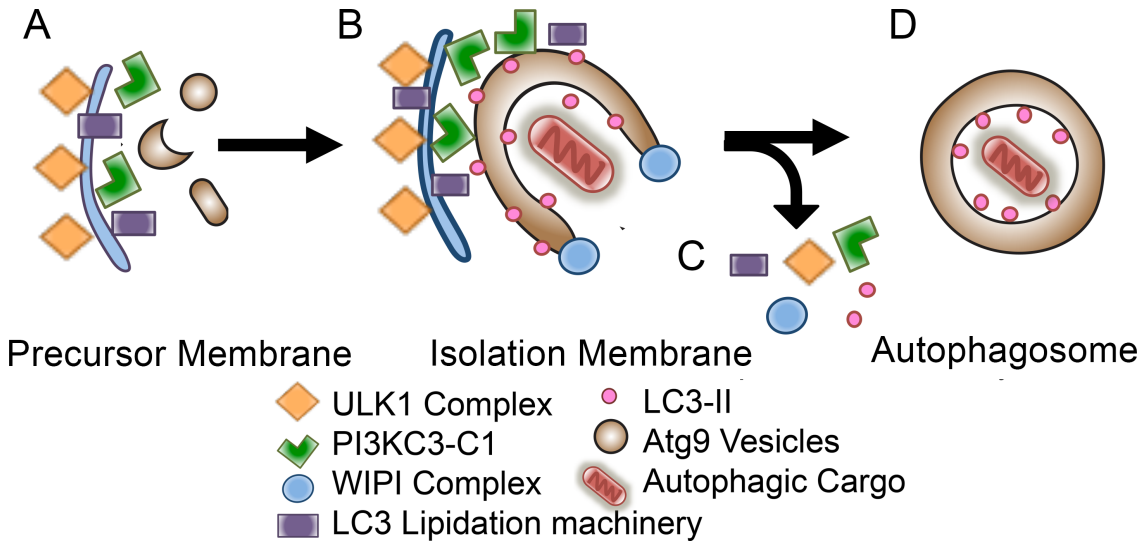

Figure 1.1: Current model of autophagosome formation
(A) Autophagy begins when early factors such as the ULK1 complex, PI3KC3-C1 and some components of the LC3 lipidation machinery such as Atg16L and Atg5 are activated and accumulate on the precursor membrane, possibly the ER or ERGIC. Small precursor vesicles, such as those bearing Atg9, are recruited to the membrane as a result of ULK1 activation. Additionally, COPII vesicles generated in a PI3KC3-C1-dependent manner accumulate near the initiation site. (B) The cup-shaped phagophore begins to form and elongate. The ULK1 complex, PI3KC3-C1 and lipidation machinery are localized on the edge of the phagophore. The WIPI PtdIns3P effector complex is located on the tips and LC3-II is distributed along the entire membrane. Cargo bound by LIR motif-factors (shown here, a damaged mitochondria surrounded by a cloud of p62 body) binds LC3-II on the concave surface. (C) Either prior to or immediately after autophagosome closure, most autophagy machinery dissociates from the membrane and Atg4 cleaves LC3-II on the cytosolic leaflet. (D) The final double membrane autophagosome with LC3-II and cargo enclosed is complete.

Chapter 2: The Atg14L ALPS motif and PI3KC3-C1 Activity is Required for LC3 Lipidation and WIPI Complex Recruitment

Introduction

The PI3KC3 complex 1 is a key component of autophagy initiation

The autophagy specific PI3KC3-C1 is a key positive regulator of autophagosome formation but the precise mechanism by which it regulates autophagy remains unclear. Many studies using chemical or genetic inhibition of Vps34 have shown that its enzymatic activity is required for LC3 lipidation and autophagy progression (Blommaart et al., 1997; Ge et al., 2013; Klionsky et al., 2007; Petiot et al., 2000). However because this complex is so large and contains other key regulatory proteins such as Beclin 1, Atg14L and Vps15, I suspect it could serve other functions in autophagy aside from its lipid kinase role for example recruiting other non-PtdIns3P effectors to the autophagosome or manipulating and forming the cup-shaped phagophore.

There are at least two predominant forms of the PI3KC3 heterotetramer present in yeast and mammalian cells (Itakura and Mizushima, 2009; Kihara et al., 2001b; Matsunaga et al., 2009). Both contain the core machinery of Vps15, Vps34 and Beclin 1. Complex one (PI3KC3-C1), which is primarily involved in autophagy initiation, contains the additional factor Atg14L (Itakura et al., 2008; Kihara et al., 2001b; Matsunaga et al., 2009; Sun et al., 2008; Zhong et al., 2009). Complex two (PI3KC3-C2), which is principally involved in late endosome and autophagosome maturation, contains UVRAG or yeast Vps38 in place of Atg14L (Kihara et al., 2001b) (Liang et al., 2008; McKnight et al., 2014). Both Atg14L and UVRAG associate with Beclin 1 through coiled-coil domain interactions and are thought to exchange places in the complex (Baskaran et al., 2014; Li et al., 2012; Noble et al., 2008; Sun et al., 2008). PI3KC3-C2 can also be divided into subcomplexes based on its association with other factors, the negative regulator of autophagosome and endosome maturation, Rubicon (Matsunaga et al., 2009; Sun et al., 2010b; Zhong et al., 2009), or the BAR domain-containing positive regulator of autophagy biogenesis, Bif-1/Endophilin B1 (Takahashi et al., 2007; Takahashi et al., 2009). Overall, these two PI3KC3 heterotetramers are thought to be complementary in their autophagy roles by producing PtdIns3P in two separate locations to initiate autophagy and promote autophagosome maturation, respectively (Itakura and Mizushima, 2009; Kihara et al., 2001b; Liang et al., 2008). However, some studies suggest that UVRAG is also involved in autophagy initiation, indicating there may be two separate roles for the PIKC3-C2 in the early and late stages of autophagy (Liang et al., 2006; Takahashi et al., 2007).

Two recent studies using single-particle electron microscopy and crystallography techniques uncovered the structures of the entire PI3KC3 heterotetramers from mammalian and yeast systems (Baskaran et al., 2014; Rostislavleva et al., 2015). Both studies revealed that the complex adopts a V-shaped structure with Beclin 1 and Atg14L/UVRAG (Vps38) on one branch and Vps34 and Vps15 primarily on the other. Because UVRAG (Vps38) is a larger protein, the PI3KC3-C2 also contains an extension on the apex of the V shape turning it into more of a Y shape (Baskaran et al., 2014;

Rostislavleva et al., 2015). The catalytic arm of the complex containing Vps34 is very mobile in solution, adopting different open and closed states based on activity. Preliminary work suggests that the tips of each branch may be key for membrane association based on the location of known membrane binding motifs and experiments using hydrogen deuterium exchange followed by mass spectrometry to detect localized changes in solution exposure after membrane association (Rostislavleva et al., 2015).

Vps34 is a member of PI3 kinase family that phosphorylates the 3' hydroxyl position on phosphatidylinositol to create a negatively charged signaling lipid, PtdIns3P (Backer, 2008). This protein contains a membrane association C2 domain, a HEAT domain and a kinase domain near its C-terminus (Fig 2.1A). Vps34 is the only PI3K in yeast, but in mammals there are three classes of PI3K with different substrates and regulatory functions. The well-characterized Class I enzyme catalyzes the formation of PtdIns(3,4,5)P_3 and consists of several regulatory subunits and isoforms. Class II consists of three isoforms and catalyzes the production of both PtdIns(3,4)P_2 and PtdIns3P. Vps34 is the only class III PI3 kinase; due to structural constraints in the substrate binding pocket it can only produce PtdIns3P (Backer, 2008). The presence of three different classes of PI3Ks in mammalian cells presents some difficulties experimentally because the known PI3K inhibitors, 3-methyladenine, LY294002 and wortmannin, bind and inhibit all classes of PI3 kinases to different extents (Walker et al., 2000; Wymann et al., 1996). Consequently, some care needs to be taken when using these inhibitors, especially because the Class I and III kinases differentially regulate autophagy. Furthermore, both Class II and III positively regulate autophagy, though Class III is the predominant positive regulator of the process (Backer, 2008; Devereaux et al., 2013). Two newly characterized selective inhibitors of Vps34 have been developed and should prove invaluable tools to block PtdIns3P production in autophagy in cells in the laboratory and in the clinic (Pasquier et al., 2015; Ronan et al., 2014).

Vps15, also known as p150, is a large protein consisting of an N-terminal myristoylation, a predicted serine/threonine kinase domain, and several HEAT and WD 40 domains (Fig 2.1A). Vps15 is stably associated with Vps34 and positively regulates it in both autophagy and endosomal maturation activity (Backer, 2008; Petiot et al., 2000). This protein has not been extensively studied in mammals but it is known to positively regulate stress-induced autophagy in drosophila and its autophagy and vesicle trafficking functions in yeast are well established (Anding and Baehrecke, 2015; Panaretou et al., 1997; Volinia et al., 1995). Vps15 is thought to regulate Vps34 via two mechanisms that may not be mutually exclusive. First, Vps15 contains a predicted protein kinase sequence required for its interaction with and lipid kinase activity of Vps34. However, current studies have been unable to uncover if Vps15 directly phosphorylates Vps34 or any other protein (Backer, 2008; Stack et al., 1995; Stack et al., 1993). Additionally, Vps15 may be a key for targeting Vps34 to the membrane by lipid anchor through its N-terminal myristoylation. Structural studies of the PI3KC3 complex also suggest that this large protein serves as a scaffold for heterotetramer folding (Baskaran et al., 2014; Rostislavleva et al., 2015).

Beclin 1 (Vps30/Atg6 in yeast) is a key regulator of the PI3KC3 complex that links Vps34 and Vps15 to the two membrane specificity factors, UVRAG and Atg14L. It

shares 24% sequence identity and 36% sequence similarity with Vps30p and contains a coiled-coil motif, BH3 domain, and an evolutionarily conserved domain (ECD) critical for its activity (Fig 2.1A) (Kang et al., 2011). Beclin 1 was originally discovered as a Bcl99-2 interacting protein through its BH3 domain and is a haploinsufficient tumor suppressor gene that positively regulates autophagy (Chan et al., 2007; Liang et al., 1999; Yue et al., 2003). This interchange between apoptosis and autophagy is highly regulated by post-translational modifications and Bcl-2 association (Kang et al., 2011; Zalckvar et al., 2009). Upon autophagy induction, Bcl-2 and Beclin 1 dissociate causing Beclin 1 to associate with the rest of the PI3KC3-C1 complex to initiate autophagy (Kim et al., 2013; Pattingre et al., 2005). Because it is also involved in apoptosis regulation, mutations in Beclin 1 are more detrimental compared to other autophagy related proteins. Beclin $1^{-/-}$ mice die at an early embryonic stage and Beclin $1^{+/-}$ mice develop tumors at an early age. In contrast, $Atg5^{-/-}$ or $Atg7^{-/-}$ mice do not have as severe a phenotype even though they are also autophagy deficient (Yue et al., 2003).

Atg14L as the autophagy-specific component of the PI3KC3-C1

The autophagy-specific component of the PI3KC3-C1 is Atg14L. It contains an N-terminal coiled-coil domain responsible for binding Beclin 1, cysteine repeats near the N-terminus responsible for ER localization, a C-terminal autophagosome targeting (BATS) domain, and a predicted amphipathic lipid packing sensor (ALPS) motif on its extreme C-terminus (Fig 2.1 A-B) (Fan et al., 2011; Matsunaga et al., 2010; Sun et al., 2008; Wilz et al., 2011). Atg14L is functionally orthologous to the yeast protein, Atg14p, although they only share 18% sequence homology and 32% sequence similarity (Kang et al., 2011; Sun et al., 2008). Atg14L binds the other components the PI3KC3-C1 through Beclin 1 and is required to recruit the complex to the nascent autophagosome membrane (Fan et al., 2011; Itakura et al., 2008; Kihara et al., 2001b). Under non-autophagic conditions, Atg14L associates with the ER through a zinc finger motif (Matsunaga et al., 2010). However, upon autophagy induction, Atg14L and the rest of the PI3KC3-C1 translocates to the phagophore and co-localizes with LC3, Atg16L, and ULK1 (Koyama-Honda et al., 2013; Matsunaga et al., 2010).

Four different groups discovered the mammalian ortholog of Atg14p as Atg14L (also called Barkor) and determined that it is a positive regulator of LC3 lipidation and autophagy activity (Itakura et al., 2008; Matsunaga et al., 2009; Sun et al., 2008; Zhong et al., 2009). Three studies used RNAi techniques; one used Atg14L KO ES cells. I sought to examine the role of Atg14L and the PI3KC3-C1 complex in more detail using a knock out cell line created using CRISPR-Cas9 techniques in conjunction with a cell-free lipidation reaction. Using a biochemical approach, I have been able to more directly relate the role that Atg14L plays in LC3 lipidation and autophagy factor membrane association.

Membrane curvature sensing with ALPS motifs

In addition to other domains and motifs throughout the PI3KC3-C1 complex that are responsible for membrane association, Atg14L contains a predicted ALPS motif at its C-terminus (Fig 2.1B). Previous work demonstrated that the BATS domain, encompassing the predicted ALPS motif, is required for recruiting the PI3KC3-C1 complex to the autophagosome membrane and for curvature sensing (Drin et al., 2007;

Fan et al., 2011; Gautier et al., 2008; Wilz et al., 2011). In this study, I focused on the ALPS motif of Atg14L to determine if it is necessary for proper PI3KC3-C1 targeting and LC3 lipidation activity.

ALPS motifs are short 20-40 residue peptides found on proteins targeted to highly curved organelle regions such as small vesicles or tubular structures (Antonny, 2011). As with other amphipathic alpha helices (AH) that bind to membrane, these motifs are typically unstructured in solution and adopt an alpha helical structure that lies parallel to the membrane between the polar and hydrophobic regions on one leaflet of a lipid bilayer (Antonny, 2011; Drin and Antonny, 2010). Half of the AH consists of large apolar side chains that form hydrophobic interactions with the hydrocarbon chains. The other half contains positively charged residues that form electrostatic interactions with negatively charged lipid head groups. It is thought that these two forces allow for strong membrane association. In contrast to canonical AH, the polar face of ALPS motifs predominantly constitutes glycine, threonine and serine, which will not form strong electrostatic bonds with lipid head groups (Bigay et al., 2005; Drin and Antonny, 2010; Drin et al., 2007). Consequently, because they lack electrostatic interactions, ALPS motifs cannot adsorb onto and induce curvature of flat membrane comparable to canonical AHs. Instead, driven primarily by hydrophobic interactions, the ALPS helix is more stably absorbed into the intrinsic lipid packing defects found in positively curved membrane (Antonny, 2011; Bigay et al., 2005; Doucet et al., 2015; Drin et al., 2007). Therefore, ALPS motifs serve as lipid packing and membrane curvature sensors and help proteins target appropriate membranes based on these physical characteristics.

I predict that the ALPS motif in Atg14L also serves as a membrane curvature sensor because the BATS domain preferentially binds highly curved membranes and its membrane binding ability is abolished when the bulky apolar side chains within the ALPS motif are mutated to positively charged residues (Fan et al., 2011). I do not expect the ALPS motif to be exclusively responsible for anchoring the PI3KC3-C1 to the membrane, particularly because the core PI3KC3 machinery also contains a membrane association domain and a lipid anchor (Backer, 2008; Baskaran et al., 2014; Rostislavleva et al., 2015). However, it is possible that the ALPS motif with its membrane curvature capabilities does contribute to targeting the PI3KC3-C1 complex to the appropriate pre-autophagosome membrane. Interestingly, one other autophagy factor, Atg3 has been shown to have an ALPS motif (Nath et al., 2014), and the Atg1 early autophagy tethering (EAT) domain senses membrane curvature (Ragusa et al., 2012), thus membrane curvature-sensing may be a conserved function for many different components of the autophagy machinery. I predict that the ALPS motif on Atg14L may be responsible for targeting the PI3KC3-C1 complex to the early autophagic membrane and to prime that membrane as a template for the lipidation of LC3.

Membrane recruitment of autophagy machinery and PI3P effectors in autophagy

There are two well-characterized families of PtdIns3P effectors involved in autophagosome biogenesis: DFCP1 and WIPI1 and WIPI 2 of the PROPPIN family. Membrane association of both of these complexes is regulated by PI3KC3-C1 activity. I will discuss both of these complexes in detail below.

DFCP1

Double FYVE domain-containing protein 1 (DFCP1) encoded by the gene *ZNFN2A1* was first predicted to be a PtdIns3P effector involved in autophagy because it localizes to the Golgi and ER instead of endosomes like most other FYVE domain containing proteins (Ridley et al., 2001). Upon initiation of autophagy, DFCP1 dynamically associates with the ER in a Vps34 and Beclin 1-dependent manner (Axe et al., 2008). Live imaging analyses show LC3 vesicles budding from a DFCP1 platform and suggest that the ER is a fundamental platform for autophagy initiation. Based on its omega-like shape, the DFCP1 positive platform and early autophagic membrane has been termed the omegasome. However, for consistency, I refer to any growing autophagosome membrane as a phagophore. Intriguingly, although DFCP1 appears to be a critical marker for PtdIns3P function and autophagosome formation, it is not essential for autophagy activity as DFCP1 depletion showed no clear autophagy defect (Axe et al., 2008).

WIPI1/2 and Atg2 complex

The WIPI1/2-Atg2 complex is also recruited to the autophagosome in a PtdIns3P-dependent manner. It is predicted that the WIPI complex is involved in phagophore elongation and closure as p62 is protease sensitive in Atg2 mutants and ultrastructural analyses show accumulated cup-shaped, unclosed phagophore structures (Kishi-Itakura et al., 2014; Velikkakath et al., 2012). Although the WIPI complex is key for autophagy activity, its direct role in LC3 lipidation is unclear. Genetic hierarchy studies suggest that Atg18 and Atg2 membrane recruitment in yeast is not required for Atg8-PE formation (Suzuki et al., 2007). Depletion of the two isoforms of Atg2 in mammals does not affect LC3 lipidation but reduces LC3 autophagic flux (Velikkakath et al., 2012). However, other studies show that WIPI1/2 depletion reduces LC3-I turnover, lipidation and puncta formation (Mauthe et al., 2011; Polson et al., 2010; Proikas-Cezanne et al., 2004), albeit not to the same extent as depletion of components of the lipidation machinery or even of the PI3KC3-C1 complex (Matsunaga et al., 2009; Sun et al., 2008). Consequently, it is unclear if the WIPI complex directly regulates LC3 lipidation or helps elongate the membrane, therefore providing more substrate for lipidation.

In vitro reconstitution of LC3 lipidation

Recently, our group has established a cell-free reaction that faithfully reconstitutes LC3 lipidation in a lysate consisting of membranes from Atg5 KO mouse embryonic fibroblasts (MEF) and cytosol from serum starved HEK293T cells (Fig 2.2)(Ge et al., 2013). After addition of nucleotide and recombinant LC3, we observed the formation of LC3-II, indicating that an early event in the autophagic pathway has been activated (Fig 2.3D)(Ge et al., 2013). The validity of the cell-free LC3 lipidation was confirmed by directly showing that lipidation responds to a variety of autophagy stimuli and depends on Vps34 activity, components of the lipidation machinery and ULK1 kinase. This reaction should prove valuable in the autophagy field because it allows one to directly reproduce and isolate the functions of factors that are responsible for LC3 lipidation activity, an early step in the autophagosome biogenesis pathway. Additionally, because autophagy is not fully reconstituted, observed LC3 lipidation activity is strictly LC3-II formation, not a balance of LC3-II formation and degradation through autophagy that occurs *in vivo*.

Demonstrating the value of this assay, the cell-free reaction was used to determine that the ER-Golgi intermediate compartment (ERGIC) is the major organelle that serves as a template for LC3 lipidation and is the likely initial autophagosome membrane source (Ge et al., 2013). Further analysis uncovered that the ERGIC is the donor membrane for PI3KC3-C1- dependent production of small COP II vesicles after starvation. These small vesicles are precursors for LC3 lipidation and likely at least one source of the autophagosome membrane (Ge et al., 2014b), further demonstrating the importance of the ERGIC in autophagosome biogenesis. Hence, this LC3 lipidation assay can be used to monitor autophagy activity in a variety of conditions involving manipulation of the membrane, cytosol and recombinant proteins added to the reaction.

The PI3KC3-C1 complex is also required for efficient lipidation machinery recruitment. Live-imaging studies show that Atg5 and Atg16L are associated with the phagophore at an early stage, but this association disappears with wortmannin treatment (Koyama-Honda et al., 2013). Consequently, the mechanism by which PtdIns3P production is translated into lipidation activity is unclear as no components of LC3 lipidation machinery are known PtdIns3P effectors, although the Atg5-Atg12/Atg16L complex does preferentially bind negatively charged membrane, including that enriched in PtdIns3P (Romanov et al., 2012). Several autophagy hierarchy studies show that the PI3KC3-C1 complex is required for autophagosome localization of both the Atg5-Atg12/Atg16 complex and Atg18/WIPI2, but that these two complexes are not dependent on each other (Suzuki et al., 2013; Suzuki et al., 2007). Hence, the PI3KC3-C1 complex appears to be a branch point in the recruitment of these two complexes possibly through separate mechanisms. WIPI2 directly binds PtdIns3P; the lipidation machinery could also directly bind PtdIns3P or simply require the stable presence of the PI3K3-C1 on the phagophore for another purpose. One study demonstrated that WIPI2b binds Atg16L1 and links PtdIns3P production to LC3 lipidation through this interaction, thus it is possible that WIPI2 and subsequent Atg16L recruitment is responsible for all PtdIns3P-dependent LC3 lipidation (Dooley et al., 2014). To clarify the mechanism of autophagosome membrane recruitment through Atg14L and the PI3KC3-C1, I adapted our *in vitro* LC3 lipidation reaction (Ge et al., 2013) to better understand the PI3KC3-C1 complex and more directly observe its role in LC3 lipidation, PtdIns3P production and membrane recruitment of downstream factors.

Using Atg14L-depleted cytosol and recombinant PI3KC3-C1 in our cell-free LC3 lipidation reaction, I found that Atg14L is directly responsible for *in vitro* LC3 lipidation, recruitment of the WIPI2 complex and PtdIns3P production. I determined that Vps34 catalytic activity and the ALPS motif of Atg14L are also necessary for these functions and that PI3KC3-C2 is inadequate to overcome the loss of Atg14L. Interestingly, addition of exogenous PtdIns3P into the LC3 lipidation reaction completely complemented Atg14L-depleted cytosol, suggesting that the primary role for the PI3KC3-C1 in LC3 lipidation is to produce PtdIns3P. Lastly, I also found that membrane association of Atg3 and Atg16L, the E2 and E3 of LC3 conjugation, respectively, do not correlate with lipidation activity and complementation with recombinant PI3KC3-C1.

Materials and Methods

Antibodies

Antibodies used in this study include: anti-T7-Tag monoclonal (69522-4, EMD Millipore, Billerica, MA), anti-Atg14L antiserum (PD026, MBL International, Woburn, MA) and anti-Atg2A antiserum (PD041, MBL), anti-Atg3 monoclonal (M133-3, MBL), anti-WIPI 2 monoclonal (MCA5780GA, AbD Serotec, Killington, UK) anti-GST antiserum (27-4577-01, GE Healthcare and Life Sciences, Pittsburgh, PA), anti-Ribophorin I antiserum (RPN I) was prepared as described in (Schindler and Schekman, 2009). Horseradish peroxidase-conjugated goat anti-mouse IgG, goat anti-rabbit IgG and donkey anti-goat IgG was from Jackson ImmunoResearch Laboratories, West Grove, PA.

Materials

Reagents used in this study include: Earle's Balanced Salt Solution (EBSS) (Thermo Fisher Scientific, Grand Island, NY), Protein-Assay Dye Reagent, (Bio-Rad Laboratories, Hercules, CA), Low retention tubes used for all lipid-containing samples (22-282LR, Olympus Plastics, San Diego, CA), OptiPrep Density Gradient Medium (Sigma, St. Louis, MO), wortmannin (Sigma), PC content assay was conducted as described in (Ge et al., 2011).

Plasmids

The plasmids encoding codon optimized VPS15, VPS34 and BECN1 DNAs were cloned into a pCAG vector with N-terminal twin STREP-FLAG and codon optimized UVRAG was cloned into pLEXm vector containing an N-terminal GST tag followed by a tobacco etch virus (TEV) cleavage site (Baskaran et al., 2014) were kindly provided by the James Hurley lab (University of California, Berkeley). The GST-FYVE and T7-LC3 plasmids were constructed by subcloning inserts provided by Nicholas Ktistakis (Babraham Institute, UK) as described in (Ge et al., 2013).

Primer extension PCR was used to construct codon optimized VPS34 kinase dead (KD) mutant with and N-terminal MBP tag, the primers with mutations underlined, R2: 5'-CGATCGGTACCATGGGCGAGGCTGAAAAG-3', F2: 5'-CCAGTACTGGCGCAAATGACTCGAGCGATC-3', FM: 5'-GCAGATTATCCAGATGCCTGGCGCCCACTC-3', and RM: 5'-CGCCAGGCATCTGGATAATCTGCTGCTGAC-3'were used in two subsequent rounds of PCR (R2+FM and F2+RM and then R2 +F2) and then digested with KPN I and XHO I for insertion into a pCAG vector with N-terminus MPB tag.

To create codon optimized either wild-type ATG14L or the ΔALPS mutant, I used the primer 5'- CGATCGGTACCATGGCTTCCCCATCTGG-3' with either 5'-GATCGCTCGAGTCACCTATGGCCTGTGTA G-3' for wild-type, 5'-GATCGCTCGAGTCAGGAAGCAATAGGGGG-3' for ΔALPS. The amplicons were digested with KpnI and Xho I and inserted into a pCAG vector with an N-terminus GST-tag followed by a TEV cleavage site.

To create the Atg14L CRISPR targeting plasmid, I first digested the pX330 Venus plasmid (48138, Addgene, Cambridge, MA) with Bbs1 the annealed primer set of 5'-CACCGTCTACTTCGACGGCCGCGAC-3' and 5'-AAACGTCGCGGCCGTCGAAGTAGAC-3' were ligated into the digested pX330 Venus vector.

Cell culture and transfection

MEF and HEK 293T cells were cultured in DMEM (Thermo Fisher Scientific, Waltham, MA) supplemented with 10% fetal bovine serum (FBS) (GE Healthcare and Life Sciences, Pittsburgh, PA) and 1% penicillin-streptomycin solution (Thermo Fisher Scientific). Cell transfection was performed using Lipofectamine 2000 (Invitrogen, Carlsbad, CA) or polyethylenimine (PEI) (Polysciences, Warrington, PA) according to protocols provided by manufacturers.

Recombinant protein purification

GST-FYVE peptide and 3X T7 LC3 were purified as described previously (Ge et al., 2013).

PI3KC3 purification from HEK 293T suspension cells

The PI3KC3 complex was purified as described in (Baskaran et al., 2014) with a few modifications detailed here. All HEK 293T cell pellets were lysed in 150 ml of HEK lysis buffer (50 mM Tris-HCl, pH 8.0, 200 mM NaCl, 2 mM $MgCl_2$, 10% (vol/vol) glycerol, 1% (vol/vol) Triton X-100, 1 mM TCEP, 50 mM NaF, 1 mM sodiumorthovanadate, 10 mM β-glycerophosphate, 5 mM sodium pyrophosphate, and EDTA-free Roche protease inhibitor tablet). The glutathione-Sepharose 4B and Strep-Tactin Sepharose beads were washed with PI3K wash buffer (50 mM Tris-HCl, pH 8.0, 200 mM NaCl, 2 mM $MgCl_2$, 1 mM TCEP, 50 mM NaF, 1 mM sodiumorthovanadate, 10 mM β-glycerophosphate, 5 mM sodium pyrophosphate). One additional step was conducted for the PI3KC3-C1 complex containing the Vps34 KD mutant. After elution from the glutathione-Sepharose column, the elution was passed over a column of 5 ml of packed amylose resin (M9676, Sigma) and the C1 complex was allowed to slowly bind through gravity. The Sepharose column was washed 5X 20 ml of wash buffer and eluted in 50 ml of 20 mM maltose in wash buffer. After this additional step, the PI3KC3 complex was treated with TEV enzyme and purified in the same manner as described previously for the rest of the complexes. Once purified, the peak fractions were pooled and mixed a 1:1 (vol/vol) ratio of 20% (vol/vol) glycerol in gel filtration buffer (20 mM Tris-HCl, pH 8.0, 200 mM NaCl, 2 mM $MgCl_2$, and 1 mM TCEP). Recombinant protein and PI3K freezing buffer (10% (vol/vol) glycerol in gel filtration buffer) was aliquoted into small fractions, snap frozen, stored at -80°C, and only limited to one freeze thaw cycle.

ADP-Glo kinase assay

The ADP-Glo kinase assay protocol for PI3KC3 activity was adapted from a published protocol (Baskaran et al., 2014) as detailed here. The ADP-Glo kinase assay (Promega, Madison, WI) was performed in 96 well PS F-Bottom white plates (Greiner Bio-One, Frickenhausen, Germany). The reaction was carried out using a 125 μM phosphatidylinositol (PI): phosphatidylserine (PS) (Avanti Polar Lipids, Alabaster, AL) substrate solution of small unilamellar vesicles in PI/PS buffer (50 mM HEPES pH 7.0, 50 mM $MnCl_2$, 0.5 mM TCEP). If solubilized lipids were used, the PI/PS buffer was supplemented with 1.0% Triton X-100. Recombinant PI3K was in PI3K freezing buffer at the concentration described. The reaction was initiated by adding 2.5 μl of 500 mM ATP and carried out for 1h at 37°C. The enzyme reaction was stopped and unconsumed ATP was depleted by the addition of 25 μl ADP-Glo Reagent supplemented with 10 mM

$MgCl_2$ and incubated at room temperature for 40 min. After ATP depletion, 50 µl of Kinase Detection Reagent was added to convert ADP into ATP and incubated at room temperature for 30 min. Luminescence was measured using an Infinite M1000 system (Tecan, Research Triangle Park, NC) with a 1000 ms integration time.

Creation of Atg14L knock out HEK 293T cells

Atg14L was knocked out (KO) of HEK 293T cells by using a target sequence followed by a PAM sequence to the first exon of Atg14L 5'-TCTACTTCGACGGCCGCGAC-3'. The optimal Atg14L target sequence was found using the CRISPR design tool from the Zhang lab at crispr.mit.edu and the algorithm described in (Hsu et al., 2013). HEK 293T cells were transfected with pX330 Venus Atg14L target sequence plasmid using the standard Lipofectamine 2000 (Thermo Fisher Scientific) protocol. After transfection (48h), the cells were subjected to flow cytometry on a BD Influx sorter (BD Biosciences, San Jose, CA) and the 530/40 filter for Venus positive cells. These cells were then diluted to 20 cells/ml and plated at a concentration of 2 cells per well in a 96 well dish. Cells were screened for single colonies and amplified until confluent in a 24 well dish. Cells were lysed in 50 µl of DirectPCR cell lysis reagent (Viagen Biotech, Los Angeles, CA) and 0.2 mg/ml proteinase K by heating at 65°C for 30 min and 35°C for another 30 min. The lysate was then subjected to semi-nested PCR using the primers 5'-GAAAAACAACAGTGCCCG -3', 5'-GTTGGGGATAAGTCATTCGG-3' and 5'-GTAGCAAAGCTCCGGTGC-3' and the amplicons were sequenced using the primer 5'-ATGGCGTCTCCCAGTGG-3'. Clones showing possible deletions were subjected to further screening for mutations on both chromosomes by ligating the sequenced amplicon into a TOPO vector and sequencing. To confirm that Atg14L protein was also not present in these cells, I lysed clones of interest in cell lysis buffer (20 mM Tris-HCl, pH 7.5, 150 mM NaCl, 0.5% NP-40 and 1 mM EDTA), mixed with 4X SDS loading dye (250 mM Tris-HCl, pH 6.8, 40% (v/v) glycerol, 350 mM β-mercaptoethanol, 30 mM SDS, 0.6 mM bromophenol blue) heated at 100 °C for 5 min followed by SDS-PAGE and immunoblot.

Cytosol preparation

The procedure for preparing cytosol from HEK 293T cells was conducted as previously described (Ge et al., 2013) with slight modifications. In detail, cells were starved in EBSS for 1h. After clarification via sedimentation, cytosol concentration was determined using Protein-Assay Dye Reagent (BioRad, Hercules, CA), diluted to 8.0 mg/ml, snap frozen and stored at -80°C until further use. Cytosol stocks were thawed for use and not refrozen.

Membrane preparation

Preparation of Atg5 KO membrane for lipidation reactions was performed as described in (Ge et al., 2013) with adaptations. Atg5 KO MEFS were grown to confluency and washed 1X with sterile PBS. Cells were then starved for 1h in 20 nM wortmannin in EBSS. Cells were collected by scraping into the media and centrifuged for 5 min at 600xg, 4°C and washed 1X with chilled PBS. Cells were lysed after resuspension in 2.7X cell pellet volume of membrane lysis buffer (20 mM HEPES pH 7.2, 1.0 mM EDTA, 250 mM sorbitol, 0.3 mM DTT, 1X Roche Protease inhibitor tablet, 1X Roche phosphatase inhibitor tablet) and passed through a 22 G needle to achieve ~ 85%

lysis, as assessed by Trypan Blue staining. Cellular debris was sedimented by centrifugation for 10 min at 3000xg, 4°C. The supernatant fraction was collected and the membrane pellet was washed again by resuspending it in the same volume of membrane lysis buffer. Both supernatant fractions were combined and centrifuged to collect the 25K pellet fraction by sedimentation at 25,000xg, 4°C. The membrane pellet was gently resuspended and washed one time in B88 lysis buffer (20 mM HEPES pH 7.2, 250 mM Sorbitol, 150 mM potassium acetate, 5 mM magnesium acetate, 0.3 mM DTT, 1X Roche Protease Inhibitor tablet, 1X Roche Phosphatase inhibitor tablet). The 25K membrane pellet was gently resuspended in 10% of the initial lysis volume in B88 lysis buffer. PC concentration was determined using the PC assay described in (Ge et al., 2011) and phosphatidylcholine (Avanti Polar Lipids) in 10% Triton was used as a standard. All membrane was stored at 4°C and used within 24h of preparation.

LC3-II lipidation reaction

The LC3-II lipidation reaction was adapted from (Ge et al., 2013). For each lipidation reaction, a final concentration of 2.4 mg protein/ml cytosol, 0.1 mg/ml (PC content final concentration) of 25 K membrane, ATP regeneration system (40 mM creatine phosphate, 0.2 mg/ml creatine phosphokinase, and 1 mM ATP), 0.15 mM GTP, and 10.0 ug protein/ml 3X T7-LC3 was mixed in a low retention tube and diluted to a final volume of 18 µl in B88 buffer (20 mM HEPES pH 7.2, 1.0 mM EDTA, 250 mM sorbitol).

In experiments containing recombinant PI3KC3, protein stocks were first diluted to equivalent concentrations in PI3K freezing buffer and then diluted to 12.5 nM in B88 buffer. Final recombinant protein concentrations are indicated. A balance solution was created using an equivalent ratio of PI3K freezing buffer diluted in B88. A similar protocol was used for every other type of reagent added to the lipidation reaction.

After preparation, samples were briefly agitated in a vortex mixer, centrifuged briefly to collect droplets and incubated for 70 min at 30°C. After incubation, membranes were sedimented at 20,000xg for 15 min, 4°C. The supernatant fraction (15 µl) was gently removed and the pellet was resuspended in 35 µl of 1X SDS buffer (4 X SDS buffer diluted in PBS) by shaking for 5 min in a bead beater. Samples were prepared for SDS-PAGE by heating at 65°C for 10 min. To best visualize T7-LC3-II turnover, samples were resolved on an 8-16% Criterion Tris-HCl Gel (3450039, BioRad), packed tightly in the transfer cassette using three sponges and transferred at 0.6 A for 90 min in transfer buffer.

PtdIns3P LC3-II lipidation reaction

To prepare liposomes, a 1 mg/mL stock of 18:0 PtdIns3P (Avanti Polar Lipids) 1 in chloroform was first dried to a thin layer in a glass round bottom tube overnight under a vacuum. The lipid was then resuspended in B88 by rotating at room temperature for 1h and gently pipetting. After resuspension, the liposomes were extruded through a B88 equilibrated 100 nM Whatman Nucleopore Track Etch Membrane filter (Sigma) 4X. After extrusion, the lipids are quickly added at the desired concentration to a mix of 0.1 mg/ml (PC content final concentration) of 25 K membrane, ATP regeneration system, 0.15 mM GTP and incubated for 1h at 30°C with sporadic gentle mixing.

After PtdIns3P incorporation, the membrane mixture was added to 2.4 mg/ml cytosol and 0.1 mg/ml 3X T7-LC3 to a final volume of 18 µ and incubated at 30°C for 70 min. The rest of the sample was treated as in a typical LC3-II lipidation reaction.

To test PtdIns3P incorporation, 0.75 mg/ml of GST-FYVE was added to a 20 µl sample of incubated membrane mix. This was incubated at 30°C for 70 min, centrifuged at 20,000xg for 15 min, 4°C and washed one time with B88 buffer. The final membrane pellet was resuspended in 35 µl of 1X SDS buffer and evaluated by SDS-PAGE and immunoblot.

Buoyant density membrane recruitment assay

Membrane recruitment assays were conducted using a 40 µl LC3-II lipidation reaction. After the first incubation, if noted, GST-FYVE was added to a concentration of 0.08 mg/ml, mixed and a 2.5% input sample was taken before incubation at 30°C for 1h. Samples were gently mixed with 50% OptiPrep in B88 to a final volume and concentration of 40% Opti Prep in 200 µl. Above that, 130 µl of 35%, 120 µl of 32%, and finally 20 µl of 0% Opti Prep in B88 were gently layered. Samples were centrifuged in a swinging bucket TLS-55 rotor (Beckman Coulter, Pasadena, CA) for 90 min at 165,000xg, 4°C with reduced braking. Fractions (90 µl) were removed by pipet from top to bottom for five total fractions. Samples were mixed with 4X SDS and prepared for SDS-PAGE and immunoblotting.

Results

Atg14L depleted cytosol cannot support LC3-II lipidation

Previous studies have suggested that Atg14L is critical for recruiting the PI3KC3-C1 to the early autophagosome membrane (Fan et al., 2011; Sun et al., 2008). Therefore, to better understand the role of the PI3KC3-C1 in autophagy initiation, I depleted Atg14L and observed the effects on an *in vitro* LC3 lipidation reaction. To make Atg14L null cytosol, I targeted the first exon of Atg14L in HEK293T cells using the CRISPR/Cas9 system (Cong et al., 2013; Jinek et al., 2013). I screened clones by sequencing and immunoblotting to detect isolates that introduced frame shift mutations on both alleles and resulted in Atg14L deficiency (Fig 2.3A) (Table 2.1).

Our previously established *in vitro* LC3 lipidation reaction uses an Atg5 KO MEF membrane fraction that does not support LC3 lipidation (Ge et al., 2013). However, these cells still contain Atg14L and an active PI3KC3-C1. I chemically depleted the PI3KC3-C1 from the membrane fraction rather than create an additional mutation the Atg5 KO MEF cell line. Atg5 KO MEFs were starved for 1h with 20 nM wortmannin to prime membranes for autophagy activation but also inhibit PtdIns3P production and block PI3KC3-C1 membrane association (Fig 2.3B). Wild-type cytosol with wortmannin-treated membrane supported LC3 lipidation. However, Atg14L-depleted cytosol showed more than an 80% drop in LC3-II production (Fig 2.3D-E).

Recombinant PI3KC3-C1 can complement Atg14L-depleted cytosol

To confirm that the block in LC3 lipidation was only from depleted PI3KC3-C1, I complemented the Atg14L-depleted LC3 lipidation reaction with recombinant PI3KC3-C1. I used the entire PI3KC3-C1 complex instead of just Atg14L because Atg14L is not stable when expressed as a monomer. In addition, the intact complex provided tighter

control on the amount of active Vps34 in the reaction. I used a published method to purify the entire PI3KC3-C1 heterotetramer from HEK 293T cells (Baskaran et al., 2014)(Fig 2.3C).

Recombinant PI3KC3-C1 complemented Atg14L-depleted cytosol in the LC3 lipidation reaction in a dose-dependent manner (Fig 2.3D-E). Lipidation observed with recombinant PI3KC3-C1 was a result of increased Vps34 activity because adding either wortmannin or GST-FYVE peptide that sequesters available PtdIns3P (Ge et al., 2013) reduced lipidation levels to what was observed in the absence of recombinant PI3KC3-C1 present (Fig 2.3F).

Recombinant PI3KC3-C2 can not complement Atg14L-depleted cytosol

There are two forms of the PI3KC3 complex present in mammalian cells (Itakura and Mizushima, 2009). Complex 1 is exclusively involved in autophagy initiation, however complex 2 has been observed to participate in both autophagosome initiation and maturation (He et al., 2013; Liang et al., 2008). Therefore, I used recombinant PI3KC3-C2 in the LC3 lipidation reaction to clarify if it can also stimulate LC3 lipidation and be used interchangeably with C1 in the production of PtdIns3P. I purified the PI3KC3-C2 (Fig 2.4A) and tested its catalytic activity. In an ADP-Glo kinase assay using either C1 or C2 with detergent-solubilized PI/PS as a substrate to remove any differences in membrane association, there is no significant difference in catalytic activity between the two complexes (Fig 2.4B). I then compared the LC3 lipidation efficiency of PI3KC3-C1 and –C2. PI3KC3-C1 showed a dose-dependent stimulation of LC3 lipidation in reactions with wild-type cytosol, whereas the PI3KC3-C2 did not (Fig 2.4C). With the Atg14L-depleted system, the PI3KC3-C1 was effective whereas the PI3KC3-C2 did not restore LC3 lipidation (Fig 2.4D), suggesting that these complexes cannot be used interchangeably for autophagy initiation.

Kinase dead PI3KC3-C1 cannot complement Atg14L-depleted cytosol

Although the wild-type PI3KC3-C1 complemented Atg14L-depleted cytosol, I was curious about other motifs, such as the Vps34 kinase domain, within the complex that may be essential to support LC3 lipidation or recruitment of other downstream autophagy factors. Chemical inhibitors of PtdIns3P production block LC3 lipidation in our system (Fig 2.3F)(Ge et al., 2013), but these inhibitors also block the class II PI3K. I purified recombinant PI3KC3-C1 with a kinase dead (KD) Vps34 (Fig 2.5A) in which two residues in the magnesium binding pocket were mutated to residues, D743A and N748I, that have been shown to abrogate catalytic activity (Fig 2.1A) (Miller et al., 2010). The KD PI3KC3-C1 mutant had negligible catalytic activity, even less than wortmannin treated wild-type PI3KC3-C1 (Fig 2.5B). When added to LC3 lipidation reactions at concentrations comparable to wild-type complex, the KD PI3KC3-C1 mutant did not stimulate LC3 lipidation (Fig 2.5C). Therefore, the PI(3) kinase activity of PI3KC3-C1 is necessary for LC3-II lipidaiton *in vitro*.

ΔALPS PI3KC3-C1 cannot complement Atg14L-depleted cytosol

In addition to catalytic activity, I wished to examine the role of the membrane curvature sensing capabilities of Atg14L in LC3 lipidation. Atg14L has a predicted membrane curvature sensor ALPS motif (Fig 2.1A-B). I purified the ΔALPS PI3KC3-C1 mutant (Fig 2.6A) and found that it had slightly attenuated PI3K catalytic activity on

small unilamellar vesicles (SUVs) (Fig 2.6B) but catalytic activity equal to the wild-type PI3KC3-C1 when using detergent-solubilized PI/PS as a substrate (Fig 2.6C). When added to the Atg14L-depleted lipidation reaction, the ΔALPS PI3KC3-C1 mutant did not complement LC3 lipidation defects (Fig 2.6D). The drop in LC3 lipidation was more severe than the loss of PI3K catalytic activity on SUVs (compare Fig 2.6 B and D), suggesting that the ability of Atg14L to sense membrane curvature is crucial to its activity in the lipidation reaction.

Given the role of the ALPS motif in our reaction, I evaluated the ability of the ΔALPS PI3KC3-C1 mutant complex to associate with membrane. I incubated wild-type and ΔALPS PI3KC3-C1 complexes with the 25K Atg5 KO membrane fraction used in LC3 lipidation reactions. This membrane fraction is enriched in ERGIC and other flat or tubular cellular membranes such as the ER and plasma membrane (Ge et al., 2013). PI3KC3-C1 activity is required to produce small, highly curved vesicles that are lipidation competent from this fraction (Ge et al., 2014b). The ALPS motif may be responsible for targeting the PI3KC3-C1 to highly curved regions of this fraction in order to stimulate COP II vesicle budding. I performed a buoyant density flotation reaction to determine relative membrane association. Proteins that are not tightly bound to the membrane remain in the dense OptiPrep layer after ultracentrifugation; membrane-associated material equilibrates at a lower buoyant density, separated from protein aggregates (Fig 2.6E). All components of the PI3KC3-C1 heterotetramer associated with membranes in the low-density fraction (Fig 2.6F). In contrast, the ΔALPS Atg14L subunit was partially recovered along with low-density membranes, the rest of the PI3KC3-C1 complex did not. This suggests that the ALPS motif is either responsible for targeting the PI3KC3-C1 to the appropriate membrane or that the ALPS motif and proper membrane association is required to maintain the intact complex.

PtdIns3P complements Atg14L deficient cytosol in LC3 lipidation reactions

If PtdIns3P is the ultimate and sole product of the PI3KC3-C1 relevant for LC3 lipidation, the lipid alone may be sufficient to complement Atg14L null lipidation defects. I incubated PtdIns3P vesicles with Atg5 KO 25K membrane and nucleotides followed by the addition of cytosol and recombinant T7-LC3-I for lipidation reactions. The extent of incorporation could be determined by further incubating the membrane with GST-FYVE peptide that specifically binds PtdIns3P (Fig 2.7A). PtdIns3P incorporation stimulated LC3 lipidation in a dose-dependent manner at a level above that seen with Atg14L-depleted cytosol, peaking around 100 μM of PtdIns3P (Fig 2.7B). This suggests that the primary role for Atg14L in this LC3 lipidation system is to activate Vps34.

Atg14L-depleted cytosol has attenuated recruitment of PtdIns3P effectors

I used the buoyant density flotation reaction to observe differences in membrane recruitment of autophagy factors influenced by mutant forms of the C1 complex (Fig 2.6D).

I first compared the relative recruitment of putative downstream autophagy factors using wild-type and Atg14L-depleted cytosol. I focused on the WIPI complex (Atg2A and WIPI2) because it is a PtdIns3P effector and as such, its recruitment should be directly related to relative PI(3)K activity. Atg14L-depleted cytosol had lower levels of WIPI complex components than wild-type overall, suggesting Atg14L is responsible

for its stability. Densitometry analysis and normalization to input and loading controls indicated that Atg14L-depleted cytosol did not efficiently recruit the WIPI complex to the lower density membranes compared to wild-type cytosol (Fig 2.8A).

The defect in WIPI complex membrane association observed with Atg14L-depleted cytosol was reversed with recombinant PI3KC3-C1 (Fig 2.8B and C). Atg2A and WIPI2 membrane association increased at least two-fold when recombinant PI3KC3-C1 was added to Atg14L-depleted cytosol. To measure PtdIns3P production, I added GST-FYVE peptide after the lipidation reaction was complete. Increased GST-FYVE membrane association can be used as a reporter for PtdIns3P production. PtdIns3P production increased in Atg14L-depleted cytosol with wild type PI3KC3-C1 (Fig 2.8B).

PI3KC3-C2 did not restore LC3 lipidation with Atg14L deficient cytosol, but it was catalytically active on solubilized lipids (Fig 2.4B). Therefore, it may be capable of producing PtdIns3P in the lipidation reaction. However, with Atg14L-depleted cytosol, the PI3KC3-C2 did not restore WIPI complex recruitment or increase PtdIns3P production (Fig 2.8B). Therefore, the PI3KC3-C2 cannot replace the PI3KC3-C1 in autophagy initiation functions such as PtdIns3P production, LC3 lipidation and WIPI complex recruitment.

The ΔALPS PI3KC3-C1 mutant also did not complement LC3 lipidation defects despite being catalytically active. It is not known if the lipidation defects observed with this mutant complex are a result of improper or low PtdIns3P production or defects in downstream recruitment because of weak PI3KC3-C1 membrane association. The ΔALPS PI3KC3-C1 mutant did not support WIPI complex membrane recruitment in comparison to wild-type (Fig 2.8B-C). The ΔALPS PI3KC3-C1 mutant also did not increase PtdIns3P production levels over that seen with Atg14L-depleted cytosol.

Lastly, the kinase dead Vps34 mutant, which was neither catalytically active nor restored LC3 lipidation beyond that seen with Atg14L-depleted cytosol also did not support WIPI complex recruitment (Fig 2.8C). The levels of WIPI2 recruitment in these reactions is even lower than just Atg14L-depleted cytosol, suggesting that the kinase dead mutant may interfere with WIPI complex to membrane.

The membrane association of both Atg3 and Atg16L, the E2 and E3 enzymes for LC3 conjugation (Hanada et al., 2007; Romanov et al., 2012), did not display any striking change in their membrane association that corresponded to lipidation activity (Fig 2.8C). Upon complementation with wild-type PI3KC3-C1, a condition that stimulated LC3-II lipidation, Atg16L and Atg3 membrane recruitment decreased slightly compared to Atg14L-depleted cytosol. However, Atg16L and Atg3 membrane association remained low upon the addition of all PI3KC3-C1 complexes, including the catalytically dead Vps34 and ΔALPS Atg14L mutants that cannot support LC3 lipidation. Because Atg16L and Atg3 membrane association does not correlate with LC3 lipidation levels, it seems that neither the PI3KC3-C1 nor the WIPI complex are responsible for recruiting LC3 lipidation machinery to the autophagosome.

Discussion

This work further clarifies that Atg14L is responsible for properly targeting the PI3KC3-C1 to the early autophagosome for PtdIns3P production. By using a cell-free assay, CRISPR/Cas9 genome editing and recombinant protein complementation, I established a system that lacks a functional PI3KC3-C1 and determined that it cannot support LC3 lipidation. This Atg14L-depleted system became a useful tool to answer other questions about the complex and how it relates to the rest of the autophagy machinery.

One value of the Atg14L-depleted system is to clarify the role of the PI3KC3-C2 in autophagy initiation. In yeast, there appears to be a distinct difference between C1 in autophagy initiation and C2 in autophagosome maturation (Kihara et al., 2001b). However, in mammals, some studies have shown that the PI3KC3-C2 regulates autophagy strictly through facilitating endosome and autophagosome maturation (Itakura and Mizushima, 2009; Kim et al., 2015; Liang et al., 2008; Sun et al., 2010b). Others, particularly those that study the PI3KC3-C2 in complex with Bif-1 suggest that it is also involved in Atg9 trafficking and is localized to the early autophagosome (He et al., 2013; Takahashi et al., 2007; Takahashi et al., 2011).

I used our assay and recombinant PI3KC3-C1 and –C2 heterotetramers (not including Bif-1) to help clarify these conflicting issues. I found that C2 does complement LC3 lipidation in the Atg14L-depleted system, thus the complexes have clear functional differences and cannot be used interchangeably as a source of PtdIns3P to initiate autophagy (Fig 2.4D). I also found that while C1 can stimulate LC3 lipidation in a wild-type LC3 lipidation reaction, C2 does not (Fig 2.4C). Although our recombinant PI3KC3-C2 does not contain Bif-1, this subunit only associates with UVRAG upon starvation (Takahashi et al., 2007), so Bif-1 present in the cytosol can bind C2 and stimulate autophagy activity in our *in vitro* reaction. Both PI3KC3-C1 and –C2 are activated upon glucose starvation-induced autophagy (Kim et al., 2013). Our results demonstrate that C2 does produce PtdIns3P in the Atg14L-depleted system (Fig 2.8B). Therefore, C2 not only can not be used interchangeably with C1, it is not active on LC3 lipidation-competent membranes in the 25K membrane fraction.

It was surprising that incorporating exogenous PtdIns3P into the 25K membrane fraction is sufficient to restore Atg14L-depleted lipidation defects (Fig 2.7B). Therefore, the primary role for Atg14L and the PI3KC3-C1 in LC3 lipidation is to produce PtdIns3P. I had hypothesized that other components of the PI3KC3-C1 would be required for recruiting the lipidation machinery to the phagophore because there are no known PtdIns3P effectors in the LC3 lipidation machinery yet membrane association of these factors still depends on Vps34 activity (Koyama-Honda et al., 2013; Suzuki et al., 2007). *In vitro* liposome sedimentation assays with the Atg5-Atg12/Atg16 complex show slightly enhanced liposome association with of PtdIns3P present, but this change was also observed with other negatively charged lipid head groups (Romanov et al., 2012). To explain how exogenous PtdIns3P can restore Atg14L-depleted lipidation defects, some other component of LC3 lipidation machinery must be an uncharacterized PtdIns3P effector or PI3KC3-C1 complex activity has a more indirect role in LC3 lipidation, such as providing and organizing a membrane source to support phagophore elongation and thus, LC3 lipidation.

Although PtdIns3P production appears to be the sole requirement for the PI3KC3-C1 in LC3 lipidation, kinase activity requires proper cellular localization. An attempt to complement our Atg14L-depleted system with a mutant complex lacking the ALPS membrane curvature sensor did not induce LC3 lipidation (Fig 2.6C). Although this mutant is catalytically active, it does not produce PtdIns3P or recruit the WIPI complex in an Atg14L-depleted system, suggesting that the PI3KC3-C1 is improperly targeted (Fig 2.8B). The ΔALPS mutant also does not stably bind the 25K Atg5 KO membrane as detected in a density flotation assay (Fig 2.6E). Because the PI3KC3-C1 contains a lipid anchor and other predicted membrane association domains on other subunits, (Fig 2.1A), I do not suspect that the ALPS motif is the only domain responsible for PI3KC3-C1 membrane association. Rather, the ALPS motif may be the membrane sensor that targets the appropriate membrane source before more stable PI3KC3-C1 membrane association occurs.

Atg14L and its C-terminal BATS domain encompassing the ALPS motif has been shown to preferentially bind smaller, more highly curved membranes (Fan et al., 2011). However, in this study, I have found that only the ALPS motif is necessary to support LC3 lipidation and proper PI3KC3-C1 membrane association. Vps34 activity is required to create small lipidation competent membrane precursors (Ge et al., 2014b). Imaging studies in yeast have also shown that PtdIns3P is enriched on the highly curved tips of the growing phagophore and that Atg14, Vps15 and Vps30 are enriched on one tip of this structure (Obara et al., 2008a; Suzuki et al., 2013). It is therefore likely that the ALPS motif targets the PI3KC3-C1 to highly curved membranes such as the tubular ERGIC structure or the tips of the phagophore to stimulate Vps34 activity for autophagosome formation.

I also used the Atg14L-depleted system to demonstrate how PI3KC3-C1 activity affects LC3 lipidation machinery membrane association. LC3 lipidation is only supported when Atg14L-depleted cytosol is complemented with wild-type PI3KC3-C1. However, membrane association of Atg3 and Atg16L, the E2 and E3 enzymes of LC3 conjugation, respectively, did not correlate with *in vitro* LC3 lipidation and PI3KC3-C1 activity (Fig 2.8C). One study demonstrated that WIPI2b binds Atg16L1 and this interaction is responsible for Atg16L-dependent LC3 lipidation (Dooley et al., 2014). However, this is not consistent with our observations as WIPI2 membrane association is correlated with PI3KC3-C1 activity. I lacked the reagents necessary to observe membrane recruitment of every factor in the LC3 lipidation cascade, but Atg3 and Atg16L in complex with the Atg5-Atg12 conjugate are involved in the final two steps of LC3 processing and Atg16L membrane association dictates where LC3 lipidation occurs (Romanov et al., 2012). Consequently, if increased PtdIns3P production is responsible for recruiting lipidation machinery and stimulating LC3 lipidation, it would likely affect membrane association of either Atg3 or Atg16L but that is not what we have observed.

The relationship between PI3KC3-C1 activity, LC3 lipidation and WIPI complex recruitment provides a hypothesis for autophagosome elongation and lipidation. PtdIns3P production is unmistakably responsible for WIPI complex recruitment. Atg2 in particular is thought to be involved in phagophore elongation and autophagosome closure (Kishi-Itakura et al., 2014; Suzuki et al., 2013; Velikkakath et al., 2012). PtdIns3P

produced by the PI3KC3-C1 enhances the production of small vesicles that bud from the ER-Golgi intermediate compartment (ERGIC) and are competent templates for LC3 lipidation (Ge et al., 2014b). Based on our observations, it is possible that the PI3KC3-C1 does not recruit and activate the lipidation machinery, rather it provides a platform and substrate for LC3 lipidation by stimulating the formation of small vesicles that are incorporated into the phagophore by the PtdIns3P bound WIPI complex. Therefore, PI3KC3-C1 activity indirectly stimulates LC3 lipidation by elongating the phagophore that can then support LC3 lipidation.

This study further clarified the importance of PtdIns3P production by the PI3KC3-C1 for LC3 lipidation and autophagy activity. Atg14L is responsible for properly targeting the PI3KC3-C1 to the phagophore and for LC3 lipidation, particularly through its membrane curvature sensor. However, despite the direct biochemical approach of this study, I was unable to determine the direct mechanism by which PtdIns3P production activates LC3 lipidation as the machinery is not recruited to the membrane in a PtdIns3P-dependent manner. Regardless, my biochemical approach has allowed a more direct path to examine the mechanistic link between PI3P production and an early event in the maturation of the phagophore membrane.

Figures

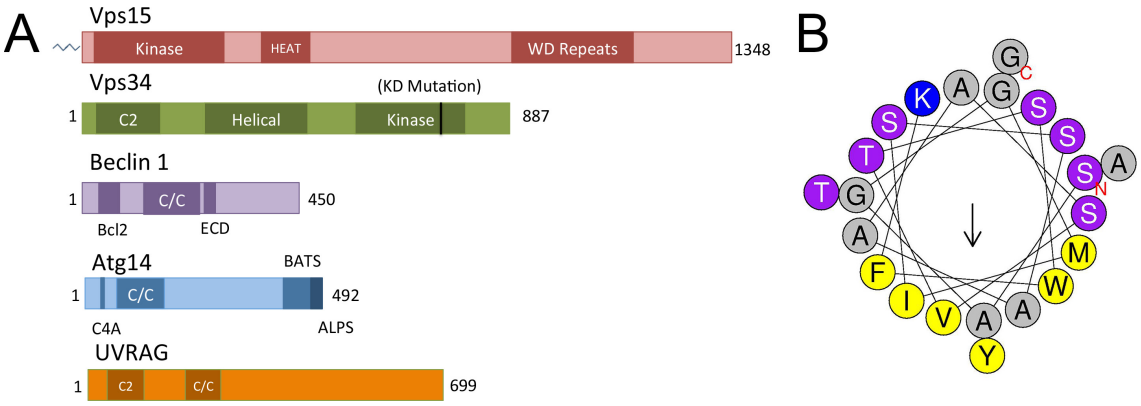

Figure 2.1: Schematic of domains in the PI3KC3 complex
(A) The domain structures of proteins associated with Vps34 in the PI3KC3 complex. Only mammalian proteins are shown. Key mutations used in this assay are noted. (B) Helical structure of the predicted ALPS motif of Atg14L analyzed using HELIQUEST, heliquest.ipmc.cnrs.fr (Gautier et al., 2008).

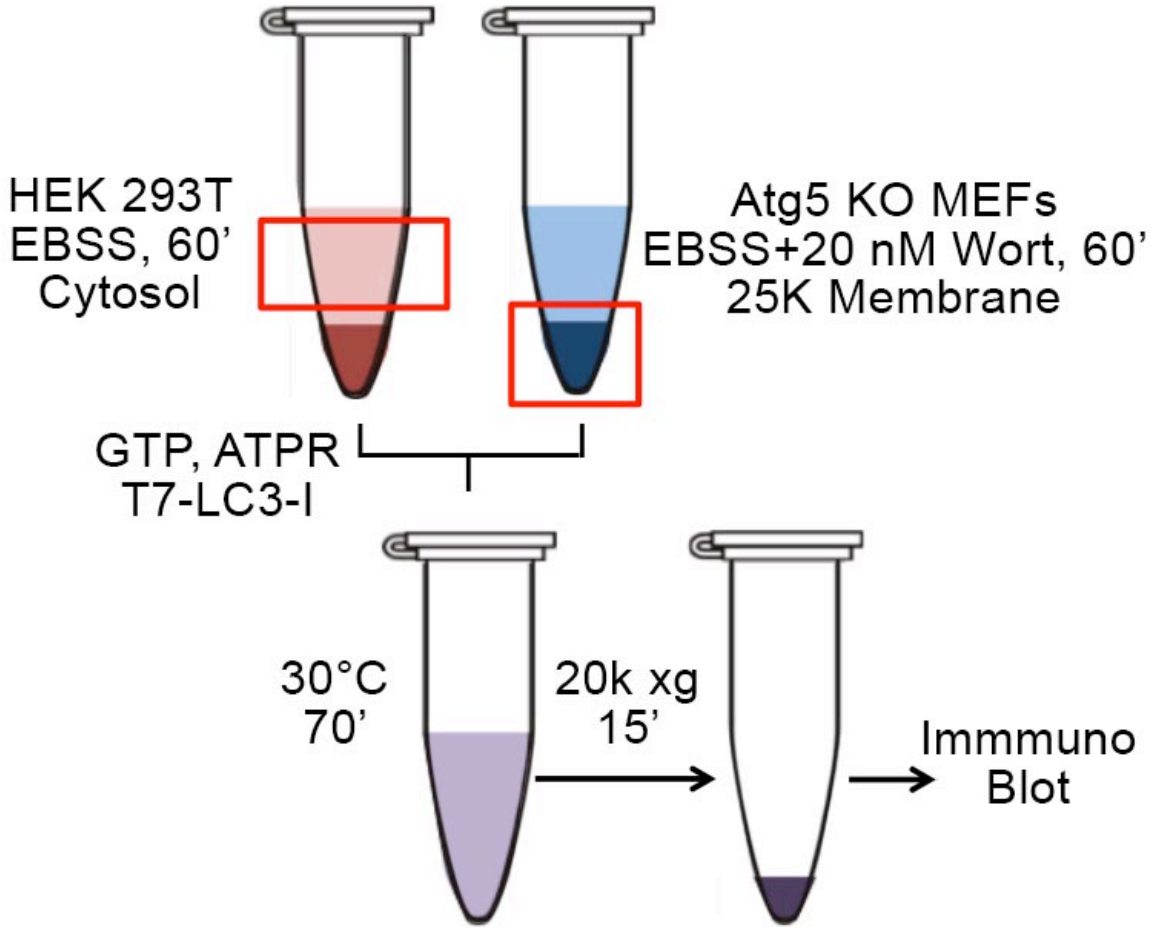

Figure 2.2: Schematic of *in vitro* LC3 lipidation reaction
(A) Cell-free reconstitution of LC3 lipidation. Membrane (25K pellet) fractions from Atg5 KO MEFs were treated with EBSS and 20 nM wortmannin (Wort), harvested, and incubated with indicated cytosol from EBSS starved HEK 293T cells, GTP, ATP regeneration system (ATPR), and recombinantly purified T7-LC3-I for 70 min. Membranes were centrifuged and evaluated by immunoblotting for analysis.

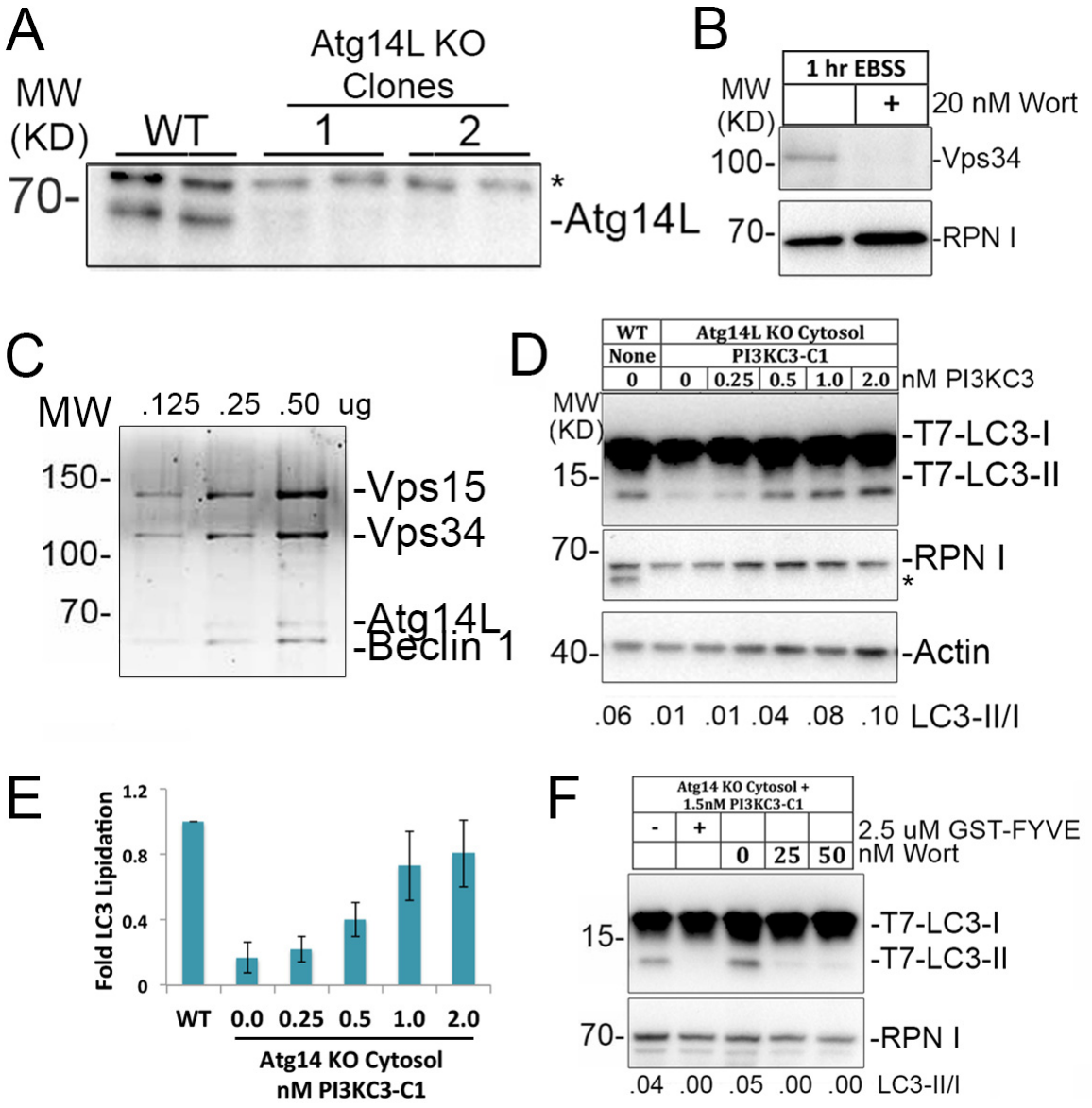

Figure 2.3: Atg14L-depleted cytosol does not support *in vitro* LC3 lipidation
(A) Immunoblot of cell lysate from two different CRISPR/Cas9 generated Atg14L knockout (KO) HEK 293T clones. Clone 2 was predominately used in this study. Asterisk indicates non-specific band. (B) Atg5 KO MEFs were starved in EBSS for 1h with 20 nM wortmannin (Wort) where indicated. Membrane (25K pellet) fractions were harvested and proteins evaluated by SDS-PAGE and immunoblotting. (C) A titration of recombinantly expressed and purified PI3KC3-C1 complex was visualized with SYPRO Red (Thermo scientific) staining. (D) LC3 lipidation reaction was performed as described in (Fig 2.2) with noted cytosol and titration of recombinant PI3KC3-C1. RPN I, ribophorin I. Asterisk indicates non-specific band. Relative LC3-II/I levels determined using band analysis in ImageJ. (E) Quantification of (D). N=6, error bars signify SEM. (F) Lipidation reaction was performed as in (C) in the absence or presence of indicated reagents. Relative LC3-II/I levels determined using band analysis in ImageJ.

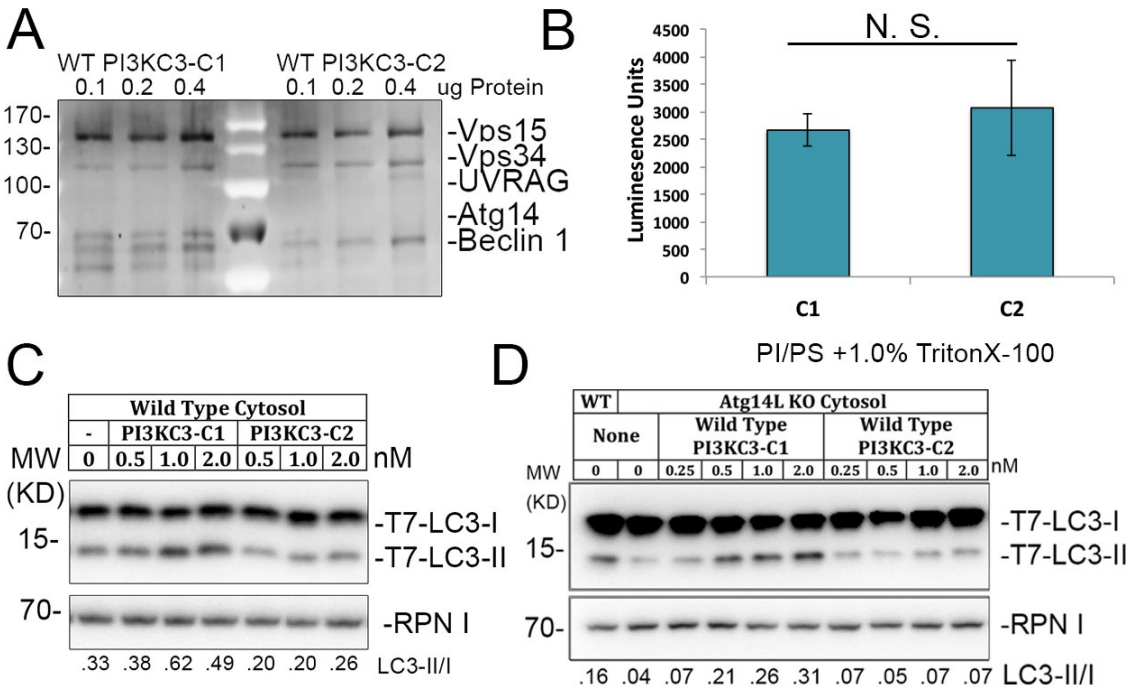

Figure 2.4: Recombinant PI3KC3-C2 does not complement Atg14L-depleted cytosol
(A) Titration of equal concentrations of recombinantly expressed and purified PI3KC3-C1 or PI3KC3-C2 complexes visualized with SYPRO Red staining. (B) ADP-Glo Kinase assay using 100 nM of indicated PI3KC3 complexes and PI/PS solubilized with 1.0% Triton X-100. N=6, error bars denote SEM. N.S.= not significant. (C-D) LC3 lipidation reaction using equivalent concentrations of PI3KC3-C1 or PI3KC3-C2 complexes over either (C) Wild-type or (D) Atg14L-depleted cytosol. Relative LC3-II/I levels were determined using band analysis in ImageJ.

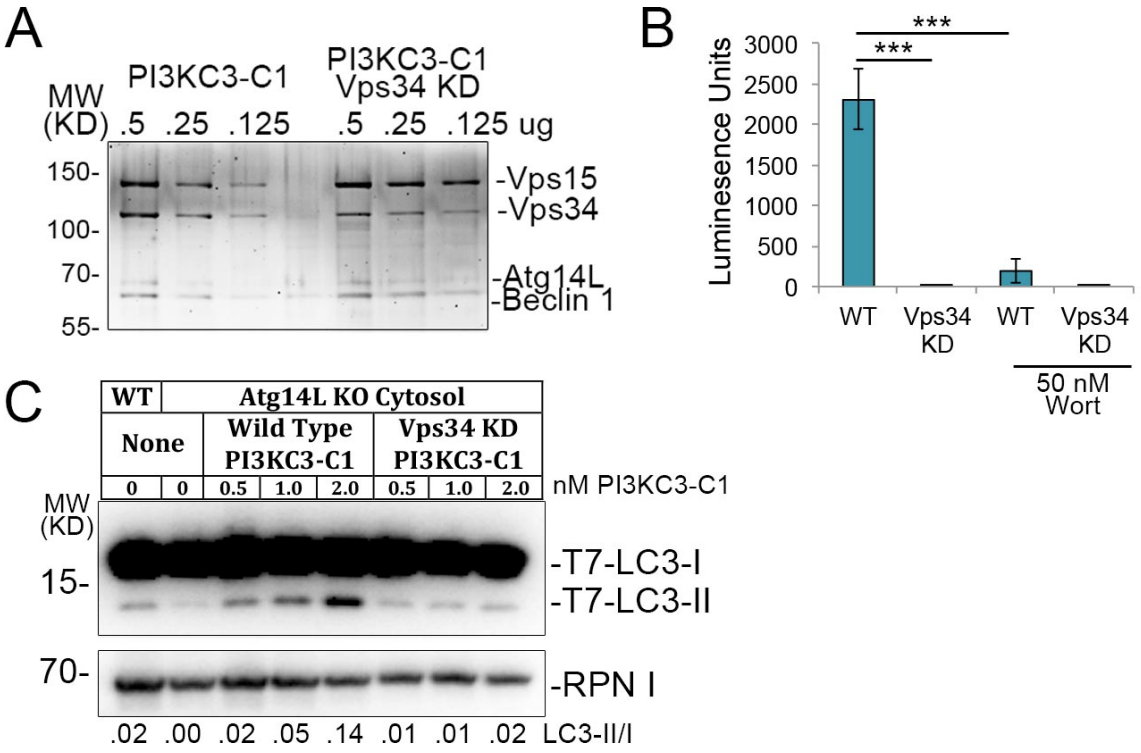

Figure 2.5: Kinase deficient PI3KC3-C1 does not complement Atg14L-depleted cytosol

(A) Titration of recombinantly expressed and purified wild-type or Vps34 KD PI3KC3-C1 mutant visualized with SYPRO Red staining. (B) ADP-Glo kinase assay using 100 nM of indicated PI3KC3-C1 complexes on PI/PS liposomes and 50 nM wortmannin (Wort) where indicated. N=3, error bars denote SEM, (**) P< 0.001. (C) LC3 lipidation reaction using equivalent concentrations of wild-type or Vps34 KD PI3KC3-C1 complexes. Relative LC3-II/I levels determined using band analysis in ImageJ.

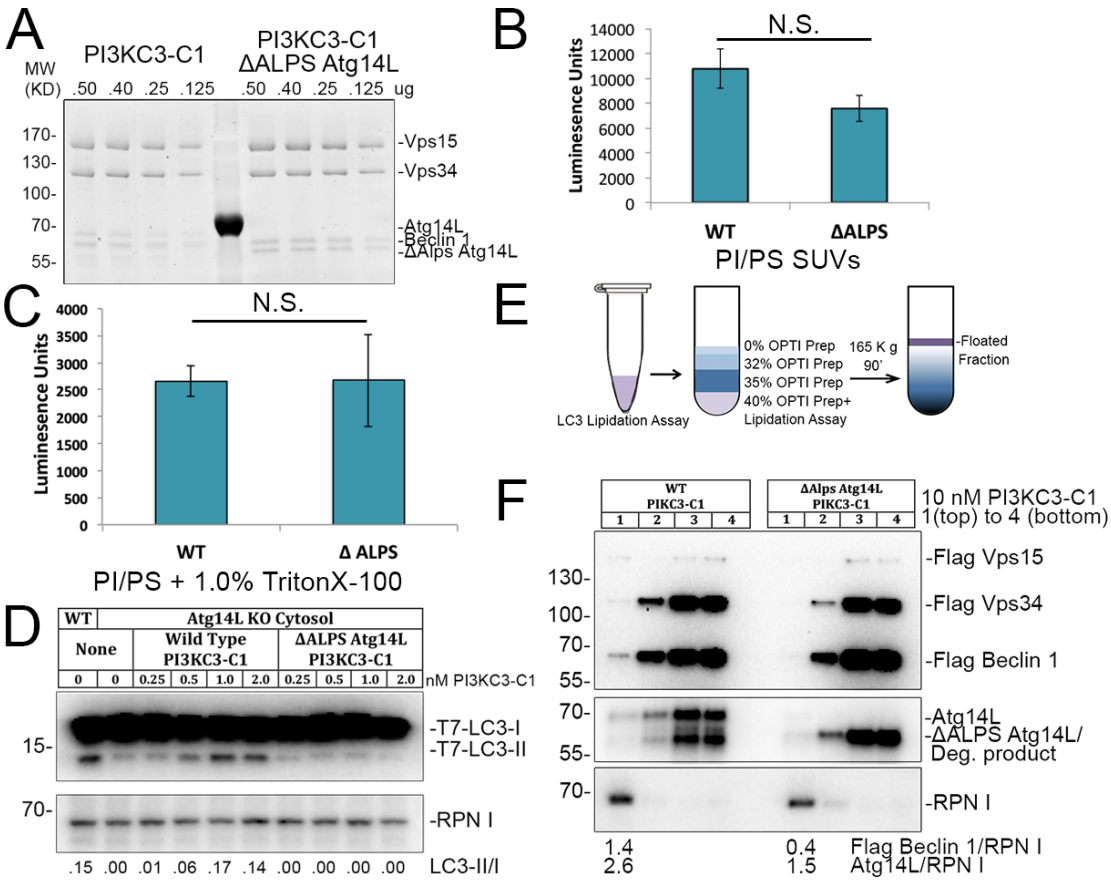

Figure 2.6:ΔALPS PI3KC3-C1 does not complement Atg14L-depleted cytosol
(A) Titration of equal concentrations of recombinantly expressed and purified wild-type or ΔALPS PI3KC3-C1 complex visualized with SYPRO Red staining. (B-C) An ADP-Glo kinase assay using 100 nM of indicated PI3KC3-C1 complexes on (B) small unilamellar vesicles (SUVs) made with PI/PS. N=3. (C) PI/PS lipids solubilized in 1.0% Triton X-100 N=6, error bars denote SEM, N.S.= not significant. (D) LC3 lipidation reaction using wild-type or ΔALPS PI3KC3-C1 mutant. Relative LC3-II/I levels determined using band analysis in ImageJ. (E) Schematic of a buoyant density membrane flotation assay. First, the samples are subjected to an LC3 lipidation reaction with cytosol and recombinant PI3KC3-C1 complexes, as indicated. The reaction mixture is then combined with a 50% OptiPrep solution to a final 40% concentration and 35%, 32% and 0% OptiPrep solutions are layered on top of that. After a 165,000xg centrifugation, the top low-density samples with visible membrane are then removed and evaluated by immunoblotting. (F) The ΔALPS PI3KC3-C1 mutant does not associate with lipidation reaction membrane. Wild-type and ΔALPS PI3KC3-C1 was mixed with the 25 K pellet Atg5 KO membrane fraction to a final concentration of 10 nM with 1X ATP regeneration system and 0.15 mM GTP. Samples were incubated at 30°C for 60 min and then subjected to an OptiPrep gradient centrifugation. Samples were taken sequentially from the top to bottom and evaluated by immunoblotting.

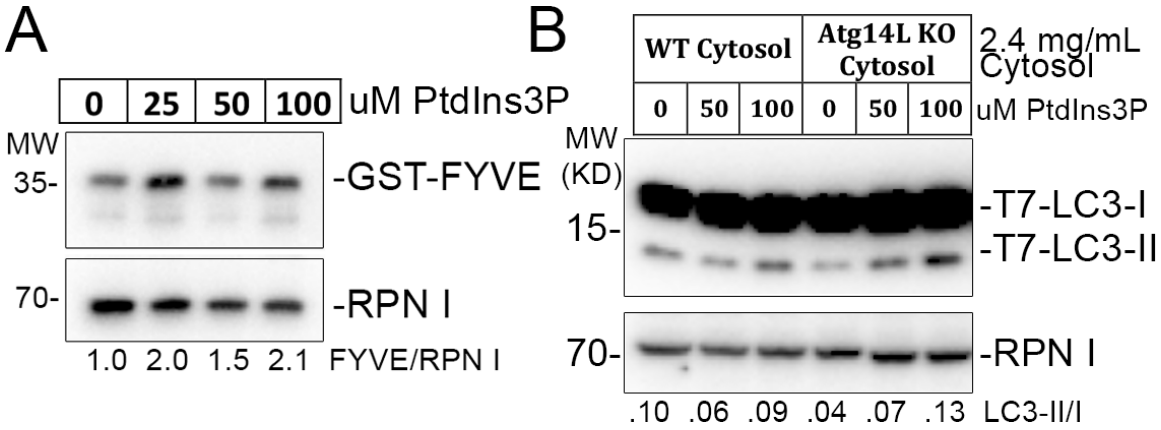

Figure 2.7: PtdIns3P addition complements lipidation defects with Atg14L-depleted cytosol

(A) Noted concentrations of PtdIns3P were incorporated into Atg5 KO membrane using a pre-lipidation reaction incubation step. The extent of PtdIns3P membrane incorporation was determined by mixing 0.07 mg protein/ml GST-FYVE peptide with the membrane and incubating for another 60 min. Following a membrane wash, samples were evaluated by SDS-PAGE and immunoblot. (B) The LC3 lipidation reaction performed with PtdIns3P incorporated membrane at the noted concentration and either wild-type or Atg14L-depleted cytosol. Relative LC3-II/I levels determined using band analysis in ImageJ.

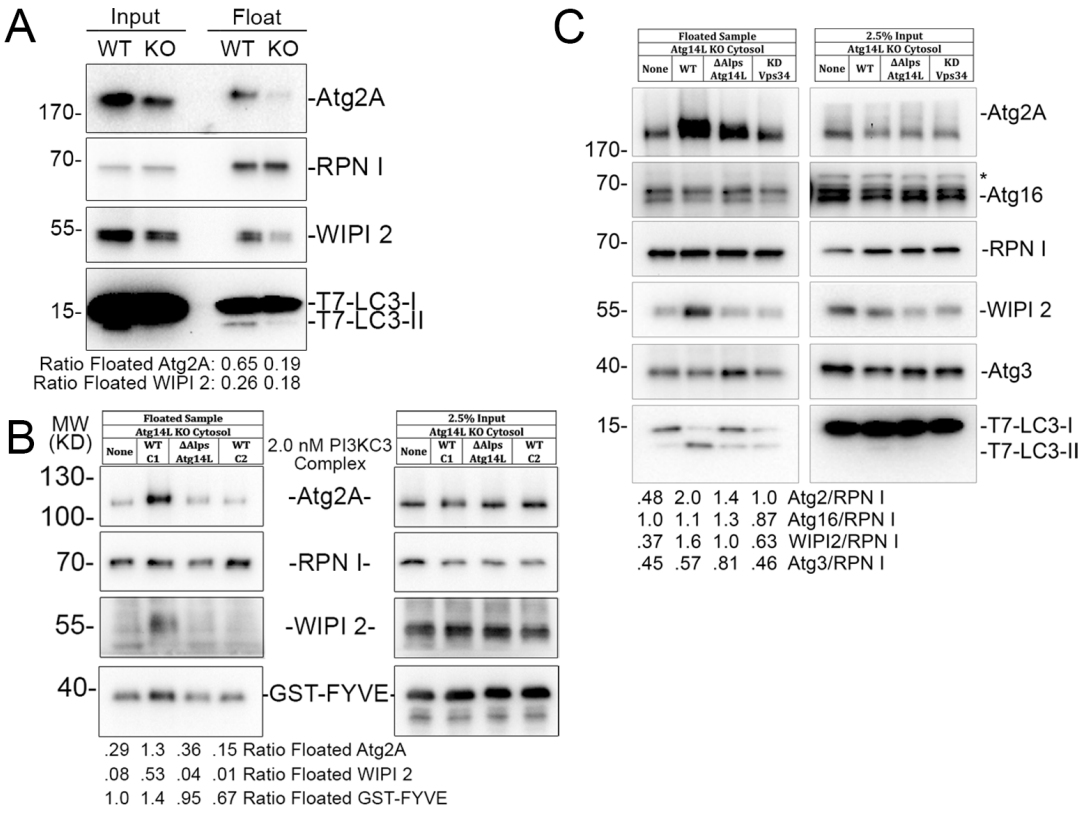

Figure 2.8: Atg14L-depleted cytosol has attenuated recruitment of PtdIns3P effectors

(A) Membrane buoyant density assay performed using either wild-type or Atg14L-depleted cytosol. Ratio of floated protein was determined by densitometry analysis using ImageJ and by normalizing the amount of protein associated with low-density membrane to loading controls and input fraction. (B) Reaction performed as in (A) except that after the lipidation reaction, GST-FYVE peptide was added and incubated for an additional 1h before density gradient sedimentation. Atg14L-depleted cytosol was used and complemented with either wild-type PI3KC3-C1, ΔALPS Atg14L PI3KC3-C1 or PI3KC3-C2. (C) Assay similar to that described in (A) but with Vps34 KD PI3KC3-C1.

Tables

Table 2.1 Mutation in CRISPR/Cas9 Targeted Atg14L Genomic Sequence	
Mutated Genomic Sequence Allele 1 Cas9 Target Sequence	WT: TCTACTTCGACGGCCGCGAC Cas9: TCTACTTCG----------CGAC
Mutated Genomic Sequence Allele 2	WT: TCTACTTCGACGGCCGCGACCGG Cas9: TCTACTTCGACGGCCGCG----------
Peptide Allele 1 Mutated Sequence * stop codon	MASPSGKGARALEAPGCGPRPLARDLVDSVDDAEGLYVAV ERCPLCNTTRRRLTCAKCVQSGDFVYFATGRGLSTRRKG*
Peptide Allele 2	MASPSGKGARALEAPGCGPRPLARDLVDSVDDAEGLYVAV ERCPLCNTTRRRLTCAKCVQSGDFVYFDGRDRRGLSTRRKG*

Chapter 3: NRBF2 negatively regulates autophagy through Atg14L and Atg14L vesicle tethering

Introduction

Identifying novel PI3KC3 subunits

The activity of the PI3KC3 complexes is regulated not only by membrane association and post-translational modifications but also through association with subunits outside of the core heterotetramer described earlier. Several groups have uncovered and characterized additional PI3KC3 effectors such as, AMBRA1, NRBF2, Bif-1 and Rubicon. These co-factors were not included in the Atg14L-depletion LC3 lipidation and complementation reaction (Chapter 2) as they are either not thought to be stably associated with the complex or are only present in specific cell types. However, I will review these co-factors here as this section focuses on initial characterization of one of them.

Ambra1 is a largely unstructured protein that positively regulates autophagy, neuronal system development and tumor suppression through its interaction with Beclin 1 (Cianfanelli et al., 2015b; Fimia et al., 2007). Ambra 1 is a haploinsufficient tumor suppressor gene; Ambra $1^{gt/gt}$ embryos show increased cell proliferation. Ambra 1, regulated by mTORC1 phosphorylation, stimulates degradation of proto-oncogene c-Myc (Cianfanelli et al., 2015a; Cianfanelli et al., 2015b). In addition to regulating cell growth, Ambra 1 is involved in neurological development as deficient embryos show defects in neural tube closure (Fimia et al., 2013; Fimia et al., 2007). Upon autophagic induction, Ambra1 binds Beclin 1 and stimulates its translocation to the ER. Ambra 1 also stabilizes ULK1 complex association and activates kinase activity by promoting Lys-63 ubiquitylation of ULK1 (Di Bartolomeo et al., 2010; Nazio et al., 2013). Therefore, Ambra1 provides an extra tier of regulation for autophagic induction through both the ULK1 and PI3KC3-C1 complexes. Because Ambra1 bridges autophagy, cancer and neuronal development, it is critical to better understand the function of this factor and PI3KC3-C1 activity in all of these disease models.

Rubicon (RUN domain and cysteine-rich domain containing, Beclin 1-interacting protein) negatively regulates endosome and autophagosome maturation by binding both UVRAG and Vps34 and inhibiting the PI3KC3-C2 (Matsunaga et al., 2009; Sun et al., 2010a; Sun et al., 2010b; Zhong et al., 2009). When active, Rubicon sequesters UVRAG from the C-VPS/HOPS complex and down-regulates Vps34 activity. This action leads to the accumulation of autophagosomes by blocking their fusion with endosomes and lysosomes. In contrast, Rubicon depletion enhances autophagosome maturation but does not alter the rate of autophagosome formation, suggesting that it only regulates the PI3KC3-C2 at a later step in autophagic flux (Matsunaga et al., 2009; Sun et al., 2010a; Zhong et al., 2009). The Rubicon/UVRAG association is regulated both by Rab7 and mTORC1 to attenuate autophagic activity when it is not needed (Kim et al., 2015; Sun et al., 2010a). This negative regulator of the PI3KC3-C2 and autophagic flux is a tantalizing target for chemical inhibition of autophagy.

Bif-1 (Endophilin-B1), contains an N-BAR (Bin-Amphiphysin-Rvs) domain and a C-terminal SH3 (Src Homology 3) domain and binds the PI3KC3-C2 through UVRAG

(Takahashi et al., 2007). Bif-1 stimulates synaptic endocytosis by inducing membrane curvature through its N-terminal AH and BAR domains and is localized on the Golgi, mitochondria, and plasma membranes (Gallop et al., 2006; Takahashi et al., 2009). Through its association with the PI3KC3-C2, Bif-1 positively regulates autophagy by stimulating Atg9 vesicle formation and trafficking to the phagophore. The Bif-1-bound PI3KC3-C2 is localized on early autophagosomes stained with Atg5, Atg9 and LC3 (He et al., 2013; Takahashi et al., 2007; Takahashi et al., 2011). These studies suggest that the PI3KC3-C2 and Bif-1 stimulate autophagy initiation and LC3-lipidation. However, work conducted in this dissertation (Fig 2.4) suggests that the PI3KC3-C2 does not stimulate cell-free LC3 lipidation. Accordingly, other studies demonstrate that UVRAG and the PI3KC3-C2 exclusively regulate autophagosome maturation (Itakura et al., 2008; Liang et al., 2008).

NRBF2 is a newly-discovered regulator of the PI3KC3-C1

Work in this dissertation has demonstrated that the PI3KC3-C1 is a critical autophagy regulator. My first goal in this dissertation was to characterize a newly uncovered PI3KC3-C1 subunit, NRBF2. Originally identified as a nuclear factor binding protein in rats, NRBF2 was not originally characterized as an autophagy protein (Yasumo et al., 2000). However, a tandem affinity purification (TAP) of Beclin 1 and Atg14L as described by Sun et al., 2008 uncovered an additional 40 KD protein that stably associated with the PI3KC3-C1. This protein was identified as NRBF2 through mass spectrometry. Further preliminary work using a reciprocal NRBF2 TAP confirmed that NRBF2 is a component of the PI3KC3-C1 (Fig 3.1A). This association was also confirmed in a large-scale yeast two-hybrid autophagy interaction study (Behrends et al., 2010).

Before my work on NRBF2, coauthors Qiming Sun and Weiliang Fan determined that NRBF2 directly binds the PI3KC3-C1 through Atg14L (Fig 3.2A) and established a doxycycline (DOX)-inducible NRBF2 shRNA cell line that efficiently depleted NRBF2 (Fig 3.1C). After their initial guidance, I continued characterizing NRBF2. Using autophagic flux, immunofluorescence and immunoprecipitation assays, I determined that NRBF2 negatively regulates autophagy through its association with Atg14L. I also uncovered two NRBF2 phosphorylation sites that induce NRBF2 autophagic inhibition and are relieved after autophagic induction.

Lastly, I contributed to an Atg14L vesicle tethering study that was published two years after I concluded my work in the Zhong group (Diao et al., 2015). This study demonstrates that Atg14L promotes tethering of protein-free liposomes and hemi- and full fusion of proteoliposomes incorporated with target (t)-SNAREs, Syntaxin 17, and SNAP29 and vesicle (v)-SNARE, VAMP8. These autophagic SNAREs bind Atg14L and regulate autophagosome maturation (Takáts et al., 2013). I uncovered that Atg14L may form a homo-oligomer and that cysteine repeats near the N-terminus of Atg14L are involved in this oligomerization. Coauthors on the Diao et al. study used this preliminary data to further demonstrate that Atg14L oligomerization through these cysteine repeats is required for Atg14L fusogenic activity.

Materials and Methods

Reagents

Antibodies used in this study include: mouse monoclonal anti-NRBF2 (2654C3a, Abcam, Cambridge, UK), anti-EGFP antiserum (ab6556), goat-anti-rabbit TRITC (ab6718), anti-Atg14L antiserum (5504, Cell Signaling, Danvers, MA), affinity-isolated anti-Th389 phospho-p70 S6 Kinase (SAB4503957), anti-LC3 antiserum (7543), anti-FLAG M2 monoclonal (F3165, Sigma, St. Louis, MO). Anti-Myc (9E10) and anti-β-tubulin antibodies were generated using hybridoma cells and described in (Chen et al., 2012). Horseradish peroxidase-conjugated goat anti-mouse IgG and goat anti-rabbit IgG are from Jackson ImmunoResearch Laboratories (West Grove, PA). Vectors used in this study are detailed in Table 3.1.

Cell culture, transfection, and cell lysate preparation

U_2OS and HEK 293T cells were cultured in DMEM (Thermo Fisher Scientific, Waltham, MA) supplemented with 10% fetal bovine serum (FBS) (GE Healthcare and Life Sciences, Pittsburgh, PA) and 1% penicillin-streptomycin solution (Thermo Fisher Scientific). Tet-approved FBS (Clontech Laboratories, Mountain View, CA) was used for doxycycline-inducible shRNA cells. Cell transfection was performed using Lipofectamine 2000 (Invitrogen, Carlsbad, CA) or PEI (Polysciences, Warrington, PA) according to protocols provided by manufacturers. Whole-cell lysates used for immunoprecipitation and immunoblotting were prepared in tandem affinity purification (TAP) buffer (20 mM Tris-HCl (pH 7.5), 150mM NaCl, 0.5% Igepal CA-360, 1 mM NaF, 1mM Na_3VO_4, 1 mM EDTA and a protease inhibitor cocktail) on ice. When used for immunoblotting, lysates were mixed with SDS loading buffer (200 mM Tris-HCl pH 6.8, 400 mM DTT, 16% β-mercaptoethanol, 8% SDS, 2X loading dye base (Amresco, Solon, OH) and 40% glycerol), heated in boiling water for 10 min and evaluated by SDS-PAGE and immunoblot.

Establishment of doxycycline-inducible overexpression cell lines

Inducible cell lines were established according to the protocol described in (Sun et al., 2008). Briefly, the pFRT/lacZeo vector was transfected into U_2OS^{TetR} cells constitutively expressing the Tet repressor protein. Single colonies were selected and screened for LacZ activity. Cell lines with moderate LacZ activity were selected in order to establish the overexpression cell line. The pCDNA5-NRBF2-FLAG vector was then transfected into these cells. Colony selection was performed with DMEM supplemented with 10% FBS, 0.5 μg/ml blasticidin, 50 μg /ml hygromycin and 1% penicillin/streptomycin. Single colonies were selected, amplified, and screened for inducible expression of the desired construct upon doxycycline (DOX) treatment.

Tandem affinity purification of Atg14L and NRBF2 complexes

Tandem affinity purification was performed as described in (Fan et al., 2011; Sun et al., 2008) with a few adaptations. Stable cell lines expressing either ZZ-Atg14L-FLAG or ZZ-NRBF2-FLAG after 1 mg/ml DOX induction were grown using standard media culture protocols described above and harvested at near confluence. The harvested cells were centrifuged and the cell pellet was washed 3X with chilled PBS. Cells were resuspended in 2.5X cell pellet volume of TAP lysis buffer, incubated on ice for 30 min, and briefly agitated in a vortex mixer. The homogenate was centrifuged for 20 min at 10,000xg, 4°C. The supernatant fraction was transferred to a fresh tube containing 0.8 ml

of packed IgG Sepharose (GE Healthcare) beads followed by gentle rotation overnight at 4°C. Bound protein was eluted after TEV protease cleavage and further purified by anti-FLAG M2 affinity gel (A2220, Sigma). Bound protein was eluted using 3X FLAG peptide (F4799 Sigma), resolved with SDS-PAGE on a 4-12% gradient gel (Invitrogen), and visualized by silver staining (Invitrogen). Distinct bands were excised and evaluated by mass spectrometry.

Purification of PI3KC3-FLAG subunits from HEK 293T cells

Purification of FLAG-tagged PI3KC3 subunits from HEK 293T cells was performed as described in (Chen et al., 2012; Sun et al., 2010a; Zhang et al., 2011) with a few adaptations. Transfected cells were collected and resuspended in 2.5X cell pellet volume of TAP lysis buffer. The supernatant fraction was separated from cellular debris after centrifugation for 10 min at 10,000xg, 4°C. Recombinant proteins were immunoprecipitated from the lysate after an overnight incubation with anti-FLAG M2 affinity gel at 4°C. Bound protein was eluted using 0.1 mg/ml 3X FLAG peptide.

GST pull-down reactions

The full-length GST-NRBF2 construct was expressed in BL21 (DE3) *E. coli* using standard protocols. Recombinant protein was purified using glutathione-Sepharose resin (GE Healthcare) as described in (Sun et al., 2008). For *in vitro* pull-down reactions, 10 μg of GST-NRBF2 protein was first adsorbed onto 10 μl glutathione beads and then incubated with noted recombinant proteins in TAP lysis buffer. After 2h rotation at 4°C, the beads were sedimented after a brief centrifugation and washed 3X in TAP lysis buffer. Sepharose beads and bound protein were mixed with SDS loading buffer, heated in boiling water and subjected to SDS-PAGE and evaluated by Coomassie staining.

Immunoprecipitation assays

Cells transfected with noted vectors were collected and lysed using TAP buffer as described earlier. The supernatant fraction was separated from cellular debris after centrifugation for 10 min at 10,000xg, 4°C. A 10% fraction of whole cell lysates (input) was removed from the supernatant fraction. The supernatant fraction was then incubated with anti-FLAG M2 affinity gel for 4h at 4°C. Beads were washed 3X with TAP buffer and bound protein was eluted with 3X FLAG peptide. Samples were then evaluated by SDS-PAGE and immunoblotting.

Creation of doxycycline-inducible NRBF2 shRNA cell lines

NRBF2 short hairpin RNA (shRNA) sequences were designed using "siRNA Target Finder" (Ambion, Carlsbad CA) and cloned into BglII and HindIII sites of the pSuperior.puro vector (Oligoengine, Seattle, WA). The shRNA sequences used are depicted below with the NRBF2 targeting sequence underlined:
GATCCCCGAGGCTATTTCTTGTCACATTCAAGAGATGTGACAAGAAATAGCCTCTTTTTA (sense);
AGCTTAAAAAGAGGCTATTTCTTGTCACATCTCTTGAATGTGACAAGAAATAGCCTCGGG (antisense). Inducible shRNA cell lines were generated by transfecting the pSuperior.puro vector containing NRBF2 shRNA sequences into U_2OS^{TetR} cells and selecting colonies using 1.0 μg/ml puromycin. Efficient NRBF2 knock down confirmed via immunoblotting was obtained after three days of incubation with 1.0 μg/ml DOX in fresh media each day.

Autophagy analysis

Autophagy was induced under two conditions, starvation or rapamycin treatment. For starvation, cells were washed 3X with PBS and incubated in EBSS for 1h at 37°C. For rapamycin (LC Laboratories, Woburn, MA) treatment, cells were incubated with either 500 nM rapamycin for 16h or 2 μM rapamycin for 4h in complete medium at 37°C. To block autophagic flux, either 400 nM bafilomycin A_1 (LC Laboratories, Woburn, MA) for 4h or 100 μM chloroquine (Sigma) for 2h was added to complete medium and incubated at 37°C.

Immunofluorescence

For immunofluorescence staining, cells were treated according to experimental requirements. Two days before collection and at least or 24h after transfection, cells were passaged onto to 6-well dishes containing coverslips. After another 24h, the cells were fixed using ice-cold methanol for 4 min at 4°C. Coverslips were washed 3X with PBS and incubated with blocking buffer (2.5% BSA + 0.1% Triton X-100 in PBS) for 2h at room temperature. Coverslips were incubated with appropriate primary antibodies 1:1000 in blocking buffer at 4°C overnight, washed with PBS buffer, incubated with appropriate secondary antibodies at 1:5000 in blocking buffer for 2h at room temperature, and mounted using Fluoroshield mounting medium with DAPI (ab104139, Abcam). Slides were imaged using a Zeiss Axio Observer Z1 fluorescent microscope and images were captured using Metamorph software (Molecular Devices, Sunnyvale, CA). Puncta were quantified using ImageJ particle analysis (NIH).

Calf intestinal alkaline phosphatase (CIP) assay

A cell lysate was prepared as described earlier in TAP lysis buffer lacking phosphatase inhibitors and EDTA. Samples were incubated for 30 min at 30°C with or without 1.0 U of CIP (NEB, Ipswich, MA) per μg of protein lysate. Addition of 4X SDS sample buffer and heating in boiling water for 10 min stopped the reaction. Samples were then subjected to SDS-PAGE and proteins evaluated by immunoblotting.

DSS crosslinking for Atg14L oligomers

To observe homo-oligomerization of Atg14L, I prepared cell lysates that were then treated with 0.25 μM of disuccinimidyl suberate (DSS), (Promega, Madison, WI) at 0.25 mM for 30 min on ice and then evaluated by SDS-PAGE and immunoblotting.

Results

NRBF2 is a novel PI3KC3-C1 subunit that negatively regulates autophagy

When mammalian Atg14L (also known as Barkor) was discovered through a tandem affinity purification (TAP) of ZZ-FLAG-Beclin 1 from fed U_2OS cells (Sun et al., 2008), an additional PI3KC3-C1 subunit, NRBF2, originally called p40, was also a part of this complex. A TAP of the ZZ-FLAG-Atg14L complex showed four associated proteins visible by silver staining that were identified by mass spectrometry as Vps15, Vps34, Beclin 1, and NRBF2 (Fig 3.1A)(Sun et al., 2008).

We used a reciprocal TAP from U_2OS cells stably expressing ZZ-FLAG-NRBF2 to confirm that NRBF2 is a subunit of the PI3KC3-C1. Similar to the Atg14L complex, NRBF2 predominately associated with the four other subunits of the PI3KC3-C1 (Fig. 3.1A). We concluded that NRBF2 is a *bona fide* subunit of the PI3KC3-C1 in fed cells.

NRBF2 is a 38 KD protein that contains a predicted microtubule interacting and trafficking (MIT) domain and coiled-coil motif (Fig 3.1B). At the time of our study, no known yeast homologs were identified, but a later close analysis by another group suggested that the NRBF2 is homologous to Atg38 in yeast (Araki et al., 2013). To characterize NRBF2, we created U_2OS cell lines stably expressing a DOX-inducible short hairpin RNA (shRNA) against NRBF2. After DOX treatment, NRBF2 protein levels were reduced to an undetectable level via immunoblot (Fig. 3.1C).

To characterize changes in autophagic flux related to NRBF2, LC3-II levels were monitored in NRBF2 KD cells after autophagic induction by starving cells in EBSS or blocking autophagosome maturation with bafilomycin A_1. In wild-type cells, LC3-II levels increased after starvation, when maturation was blocked with bafilomycin A_1, and after cells were both starved and treated with bafilomycin A_1. Because LC3-II is a marker and substrate of autophagy, the amount of LC3-II formed after blocking autophagosome maturation with bafilomycin A_1 is relative to the total amount of LC3-II produced in the cell. LC3-II levels were elevated in fed conditions in NRBF2 KD cells, a phenotype that became more apparent after bafilomycin A_1 addition. The increase in LC3-II formation in fed cells suggests that NRBF2 depletion stimulates autophagy.

Consistent with the observation that NRBF2 negatively regulates autophagy, the amount of LC3 puncta per cell was higher in fed NRBF2 KD cells than wild-type cells (Fig. 3.1D). The number of LC3 puncta per cell increased after rapamycin treatment in wild-type cells. The extent of LC3 puncta increase was attenuated in NRBF2 KD cells, likely because autophagy was already stimulated.

NRBF2 directly binds and negatively regulates Atg14L puncta formation

To test which component of the PI3KC3 complex binds NRBF2, we recombinantly expressed and purified Vps15, hVps34, Beclin 1, Atg14L, UVRAG, and Rubicon using FLAG-tagged constructs in HEK 293T cells. These purified proteins were incubated with GST-NRBF2 recombinantly expressed and purified from *E. coli*. Atg14L was the only PI3KC3 complex component that directly bound GST-NRBF2 (Fig 3.2A). Atg14L overexpression in fed cells activated autophagy and induced LC3-II formation. Co-expression of NRBF2-Myc with Atg14L-FLAG blocked this stimulation (Fig. 3.2B), suggesting that NRBF2 negatively regulates autophagy through Atg14L.

Atg14L immunofluorescence studies have shown that it localizes with LC3-stained phagophores (Sun et al., 2008). The number of Atg14L-EGFP puncta per cell increased in NRBF2 KD cells (Fig. 3.2C) and decreased when NRBF2-Myc was overexpressed (Fig. 3.2D), suggesting that NRBF2 negatively regulates Atg14L autophagosome localization. Accordingly, in fed cells, NRBF2-Myc tightly bound Atg14L in immunoprecipitation reactions, but this interaction weakened after autophagy induction (Fig. 3.4B lanes 3-6). Consequently, NRBF2 appears to be a stress-responsive negative regulator of the PI3KC3-C1 that directly antagonizes Atg14L.

NRBF2 is a phospho-protein regulated by autophagic induction

NRBF2 appeared as a doublet in immunoblots so it is possible that it is post-translationally modified. The slower-migrating band of the NRBF2 doublet disappeared after treating cells with rapamycin (Fig 3.3A) or lysate with calf intestinal phosphatase

(CIP)(Fig 3.3B). This suggests that NRBF2 is a phospho-protein regulated by mTORC1 inhibition. Rapamycin treatment rapidly reduced the presence of the slower-migrating NRBF2 phosphorylation band that was eventually replaced after sustained periods of autophagic induction. A closer analysis of NRBF2 mass spectrometry data revealed that NRBF2 is phosphorylated at S113 and S120 in fed cells.

I created an NRBF2-Myc construct that replaced both S113 and S120 with alanine (NRBF2 AA) and abolished the slower-migrating NRBF2 band on immunoblots (Fig 3.4A-B). In contrast, when S113 and S120 were mutated to phospho-mimetic aspartic acids (NRBF2 DD), the entire NRBF2 band migrated slower on immunoblots comparable to phosphorylated NRBF2 (Fig 3.4A-B). Therefore, NRBF2 is phosphorylated at these sites under fed conditions and dephosphorylated after autophagic induction.

NRBF2 phosphorylation negatively regulates autophagy

To analyze how NRBF2 phosphorylation regulates autophagy, I modified the DOX-inducible NRBF2 KD cell line to stably express Myc-tagged wild-type, AA or DD mutant NRBF2. In an autophagic flux reaction, both fed and bafilomycin A_1 treated NRBF2 KD cells increased LC3-II formation compared to wild-type cells. In contrast, in NRBF2 KD cells complemented with wild-type or the DD phospho-mimetic NRBF2, the increased LC3-II formation observed in fed NRBF2 KD cells with bafilomycin A_1 treatment was attenuated (Fig 3.4A). The phospho-null AA NRBF2 mutant did not restore NRBF2-depletion defects in NRBF2 KD cells. Rather, LC3-II levels were elevated under all conditions in cells expressing the AA NRBF2 mutant, suggesting that NRBF2 phosphorylation negatively regulates LC3-II formation.

I conducted immunoprecipitation reactions to determine if NRBF2 phosphorylation regulates its association with Atg14L. In cells expressing FLAG-NRBF2, the Atg14L/NRBF2 association weakens after starvation or rapamycin treatment (Fig 3.4B). The AA NRBF2 mutant bound Atg14L more tightly than wild-type NRBF2 and this interaction slightly weakens after autophagic induction. In contrast, under all conditions, the DD NRBF2 mutant bound Atg14L at a level comparable to the wild-type Atg14L/NRBF2 association after autophagy induction. This observation did not fit with my model based on my body of data that phosphorylated NRBF2 inhibits autophagy by binding and negatively regulating Atg14L. After autophagic induction, NRBF2 is dephosphorylated, it dissociates from Atg14L and autophagy progresses. This immunoprecipitation data with the NRBF2 phosphorylation mutants suggests that either the Atg14L/NRBF2 association is not inhibitory or that the AA mutant has a different role in autophagy.

I also monitored levels of LC3 puncta formation with the NRBF2 phosphorylation mutants. In wild-type cells, LC3 puncta accumulated after bafilomycin A_1 treatment because autophagosome maturation is blocked. Therefore, the total number of LC3 puncta per cell after bafilomycin A_1 treatment is relative to rate of autophagosome biogenesis. In NRBF2 KD cells, LC3 puncta levels after bafilomycin A_1 treatment were higher than wild-type cells and are not restored to wild-type levels when complemented with the AA NRBF2 mutant (Fig 3.4C and D). In contrast, after treating NRBF2 KD cells complemented with either wild-type NRBF2 or the DD NRBF2 mutant with bafilomycin A_1, LC3 puncta levels do not increase. These observations suggest that

NRBF2 depletion or dephosphorylation accelerates autophagosome formation and NRBF2 overexpression and phosphorylation blocks it.

Atg14L forms a homo-oligomer through its zinc-finger motif

In a parallel project, collaborators from the Brunger lab (Stanford University) observed that recombinantly expressed and purified Atg14L stimulates liposome tethering and lipid mixing (Diao et al., 2015). As vesicle tethering often requires oligomerization, I wanted to know if Atg14L was capable of self-association. In cells co-expressing two differently tagged Atg14L constructs, Atg14L-FLAG can immunoprecipitate Atg14L-EGFP (Fig. 3.5A), suggesting that at least two separate Atg14L subunits are present in a larger complex.

In accordance with the immunoprecipitation assays, when cell lysate is treated with a chemical cross-linker disuccinimidyl suberate (DSS) to preserve higher-order complex structures during SDS-PAGE, a slower-migrating Atg14L band appears on immunoblots and does not change after induction of autophagy (Fig 3.5B). I screened known Atg14L mutant constructs to uncover what domain may be responsible for oligomer formation and determined that mutating four evolutionarily conserved cysteines (C43,C46,C55,C58) near the N-terminus of Atg14L to alanine (C4A mutant) abolishes Atg14 oligomer formation under fed and rapamycin treated conditions (Fig 3.5B). These residues are responsible for Atg14L ER localization and autophagy function (Matsunaga et al., 2010). These observations were then used as a springboard for my co-authors to conduct several other experiments using the C4A Atg14L mutants to demonstrate that these residues are required for Atg14L oligomerization and vesicle tethering (Diao et al., 2015).

Discussion

In this study, I uncovered an additional PI3KC3-C1 subunit, NRBF2 that negatively regulates autophagosome formation, likely through association with Atg14L. The Atg14L/NRBF2 association is direct as it is observed in pull-down assays with recombinantly purified proteins and weakens upon autophagy induction. NRBF2 also negatively regulated Atg14L autophagosome association as Atg14L puncta formation is inversely related to NRBF2 expression levels.

NRBF2 phosphorylation at S113 and S120 tempers autophagosome formation in fed cells (Fig 3.4A). NRBF2 is phosphorylated at these two sites in non-stressed conditions and dephosphorylated after mTORC1 inhibition and autophagy induction. It is probable that NRBF2 is regulated by this master kinase as it also phosphorylates many other autophagy factors blocking autophagy progression under non-stressed conditions (Efeyan et al., 2015). Depleting NRBF2 or removing these phosphorylation sites increased LC3-II and LC3 puncta levels in fed cells treated with bafilomycin A_1 (Fig 3.4 A, C-D). In contrast, LC3 puncta levels remained low in cells overexpressing wild-type or the phospho-mimetic DD NRBF2 mutant. Consequently, excess NRBF2 or sustained phosphorylation at S113 and S120 attenuates autophagy.

When I immunoprecipitated Atg14L and the Myc-NRBF2 phosphorylation mutants, I uncovered that the AA NRBF2 mutant bound Atg14L very tightly (Fig 3.4B). In contrast, the phospho-mimetic DD NRBF2 mutant bound Atg14L weakly akin to wild-

type levels after autophagy induction. Therefore, NRBF2 phosphorylation negatively regulates Atg14L/NRBF2 association, LC3-II conjugation and LC3 puncta formation. This observation conflicts with data showing that under autophagic induction when NRBF2 is dephosphorylated, the Atg14L/NRBF2 association is weaker. Consequently, our hypothesis that phosphorylated NRBF2 negatively regulates autophagy in fed conditions by binding Atg14L and blocking autophagosome formation, LC3-II conjugation, and Atg14L puncta formation may be incorrect. It is possible that some of our observations used to form this model were incorrect or that NRBF2 regulates autophagy in a method not as straightforward as a brake removed after induction.

I discarded this project based on the conflict of observations and interpretations noted here and the knowledge that other groups were preparing manuscripts indicating that NRBF2 was both a positive (Cao et al., 2014; Lu et al., 2014) and negative regulator of autophagy (Zhong et al., 2014). Although the data presented here mostly appear to follow a simple model of negative regulation, data indicating that NRBF2 negatively regulated autophagy was not always the most consistent or reproducible observation. I repeated the NRBF2 depletion autophagic flux and LC3 puncta formation immunofluorescence experiments many times and although the most prominent result was that NRBF2 was a negative regulator, a significant amount of experiments conducted in the same manner would show either no effect or the opposite result. Therefore, uncertain that my observations were correct or too highly dependent on external factors such as cell passage number, I created a new strain of inducible NRBF2 depletion cell lines. These freshly generated cells no longer demonstrated the already subtle increases in autophagy activity after NRBF2 depletion as noted earlier (compare Fig 3.1 C-D to Fig 3.6 A-B). Consequently I decided that characterizing NRBF2 was no longer a valuable project.

After I ceased work on NRBF2, several studies have been published about its role in autophagy. Two studies from the Yue lab using siRNA and NRBF2$^{-/-}$ MEFs and Backer lab using only siRNA show that NRBF2 positively regulates autophagy in mammals (Cao et al., 2014; Lu et al., 2014). An additional study that identifies Atg38 as a yeast ortholog of NRBF2 also suggests that it positively regulates autophagy (Araki et al., 2013). Additionally, a study from the Wang group using siRNA to deplete NRBF2 shows that NRBF2 suppresses autophagy (Zhong et al., 2014) comparable to what I observed. In all studies, autophagy activity was measured using established techniques such as LC3 lipidation, p62 degradation, LC3 puncta and PtdIns3P production. However, the two studies from the Yue and Backer groups that suggest NRBF2 positively regulates autophagy do not use bafilomycin A_1 to measure differences in autophagy flux, presenting a possible difference in interpretations.

These conflicting observations of how NRBF2 regulates autophagy could be a result of different cell types, experimental conditions, or because NRBF2 defects can only be reliably observed in a knock out system. Regardless, all studies presented here indicate that NRBF2 is a component of the PI3KC3-C1, not –C2 and most show that it binds Atg14L.

In addition to the NRBF2 project, my work on Atg14L oligomerization contributed to an article regarding how Atg14L promotes membrane tethering and fusion

of autophagosomes to endolysosomes (Diao et al., 2015). This study uncovered that Atg14L promotes liposome tethering on its own. When combined with autophagic target (t)-SNAREs, Syntaxin 17, SNAP29 and the vesicle (v)-SNARE VAMP8, Atg14L promotes vesicle fusion and content mixing. Atg14L oligomerization mutants such as the C4A mutant I uncovered using the DSS crosslinking experiments can not bind the autophagic (t)-SNAREs, Syntaxin 17 and SNAP29. Accordingly, Atg14L with oligomerization mutants cannot promote vesicle fusion and content mixing and are defective in autophagic flux. These data suggest that Atg14L may be involved in autophagy initiation through its association with the PI3KC3-C1 complex and in later stages of autophagosome maturation through association with the autophagic SNAREs.

The work conducted by (Diao et al., 2015) suggests that Atg14L may positively regulate autophagy at two stages, autophagosome formation and maturation. Therefore, it is also possible that NRBF2 regulates Atg14L at one or both of these stages of autophagy. Our LC3 immunofluorescence reactions with NRBF2 depleted cells or those complemented with the phospho-null AA NRBF2 mutant rather strikingly show that autophagosomes accumulate after bafilomycin A_1 treatment, suggesting an increase in autophagosome formation. However, the LC3-II formation data does not support this hypothesis as strongly. The highly elevated LC3-II levels observed after complementation with the phospho-null mutant could also be interpreted as a block in autophagic flux, not increased autophagosome formation (Fig 3.4A). Because the phospho-null mutant tightly binds Atg14L (Fig 3.4B), it is possible that this mutant binds and blocks the tethering and autophagosome maturation activity of Atg14L; a phenotype that would accumulate LC3-II across all conditions such as what was observed.

Accordingly, one study characterizing NRBF2 suggested that it positively regulates both autophagosome biogenesis and maturation (Lu et al., 2014). The Yue group used NRBF2$^{-/-}$ MEFs and observed a block in LC3-II production upon rapamycin treatment but also a defect in autolysosome formation using the tandem-tagged GFP-RFP-LC3 (Kimura et al., 2007). It is possible that these two different ways that NRBF2 regulates autophagy can only be detected with a complete NRBF2 knock out, hence why it was missed in our study. Therefore, it may be pertinent to re-examine how NRBF2 phosphorylation regulates autophagy activity in NRBF2 knock out cells especially with this new knowledge that Atg14L also may function in autophagosome maturation.

Figures

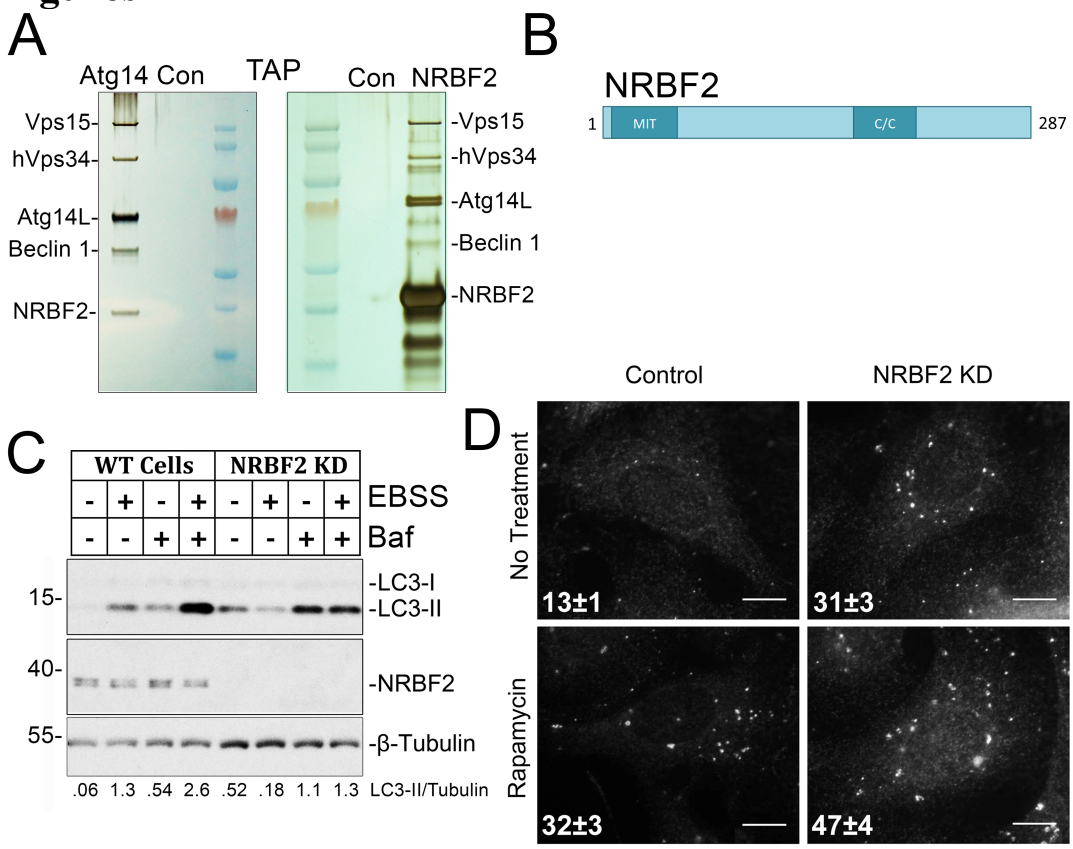

Figure 3.1: NRBF2 negatively regulates autophagy in fed cells
(A) Tandem affinity purification (TAP) of ZZ-Atg14L-3X FLAG (left panel) or ZZ-NRBF2-3X FLAG (right panel) in U_2OS cells that were subjected to SDS-PAGE and visualized using silver staining. Noted bands were identified using mass spectrometry. (B) Schematic of NRBF2 structural domains. MIT= microtubule interacting and trafficking domain. C/C=coiled-coil motif. (C) Relative LC3-II levels in DOX inducible NRBF2 depletion U_2OS cells (NRBF2 KD). Cells were treated with EBSS for 1h or 400 nM bafilomycin A_1 (Baf) for 4h as indicated. Relative LC3-II to β-tubulin was measured using band analysis in Image J. (D). LC3-positive vesicles per cell in either wild-type or DOX-induced NRBF2 KD cells with 2 μM rapamycin for 4 h as indicated. Data presented as average ± SEM. Scale bar = 10 μm N=50.

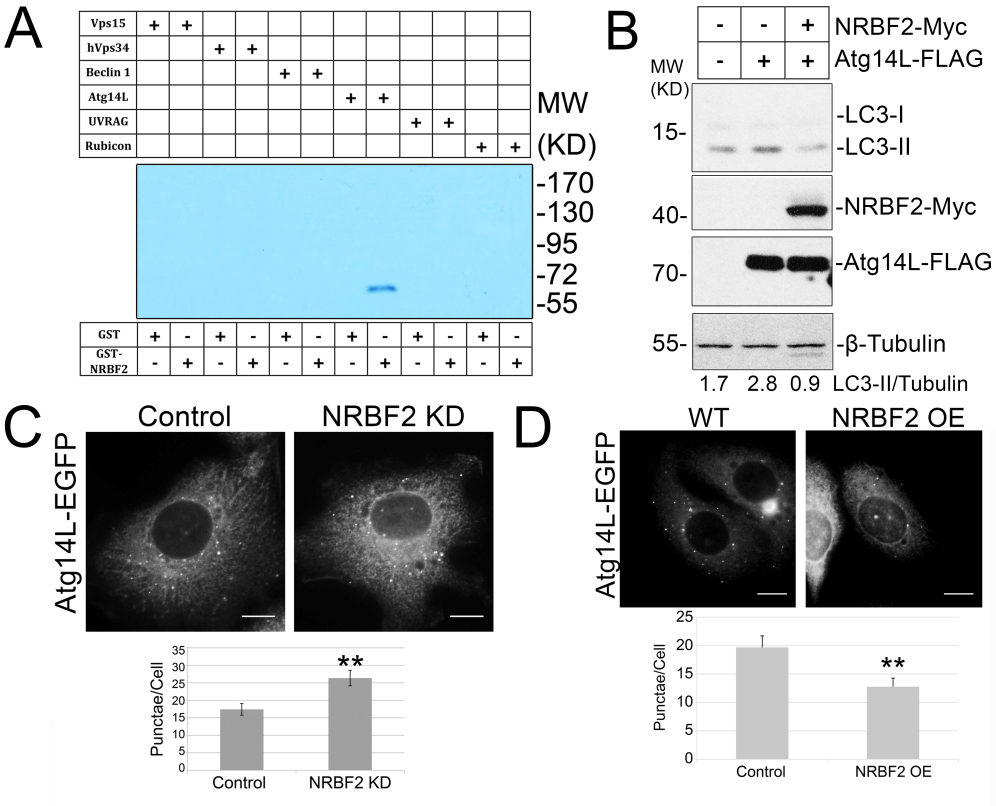

Figure 3.2: NRBF2 directly binds and negatively regulates Atg14L puncta formation

(A) Glutathione Sepharose pull-down reaction using noted recombinantly expressed and purified FLAG-tagged PI3KC3 complex components from HEK 293T cells and GST-NRBF2 from *E. coli*. (B) Relative LC3-II levels in DOX-induced (1.0 µg/ml, 16h) NRBF2-FLAG overexpression U_2OS cells (NRBF2 OE) transiently transfected with Atg14L-EGFP. (C-D). Immunofluorescence of Atg14L-EGFP in either (C) NRBF2 KD or (D) NRBF2 OE cells. Data presented as average ± SEM N=30 (**) P< 0.01.

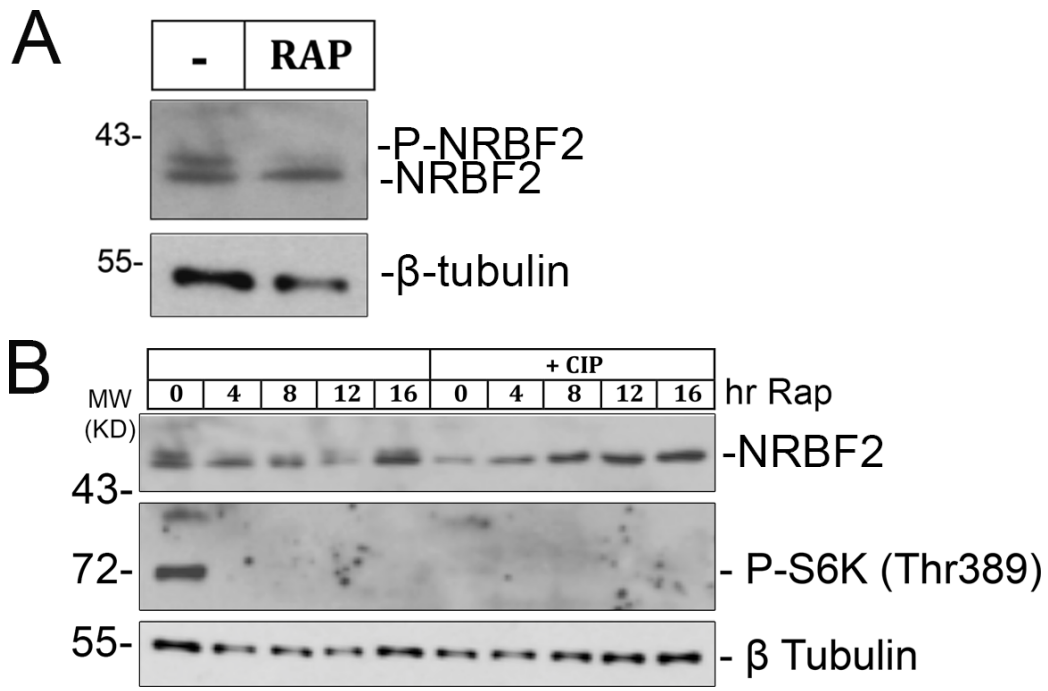

Figure 3.3: NRBF2 is a phospho-protein regulated by autophagic induction
(A) U_2OS cells treated with 2.0 μM rapamycin for 4h as indicated and evaluated by immunoblotting. (B) Time course of U_2OS cells with 2.0 μM rapamycin for the indicated time. Lysates were treated with or without calf intestinal alkaline phosphatase (CIP) and evaluated by immunoblotting.

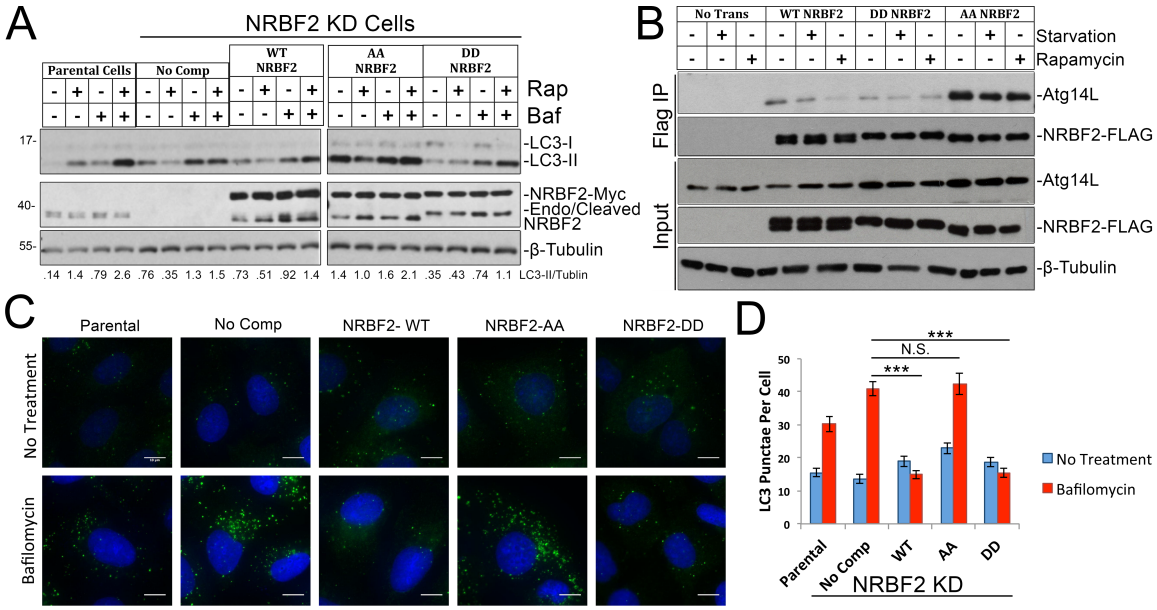

Figure 3.4: NRBF2 phosphorylation negatively regulates autophagosome formation
(A) Relative LC3-II levels in wild-type or NRBF2 KD cells that stably express NRBF2-Myc wild-type, AA or DD mutants. Cells were treated with 0.5 μM rapamycin for 16h and 400 nM bafilomycin A_1 (Baf) for 4h as indicated. (B) Immunoprecipitation of U_2OS cells transiently transfected with vector control or NRBF2-FLAG wild-type, AA, or DD mutants. Cells were starved in EBSS for 1h or incubated in 2 μM rapamycin for 4h as indicated. Lysates were subjected to immunoprecipitation with anti-FLAG resin. (C) LC3 immunofluorescence of cells as in (A) treated with 400 nM bafilomycin A_1 for 4h. Scale bar = 10 μm. (D) Quantitation of (C) presented as average ± SEM N=25 Not significant (N.S.), (***) P<0.001.

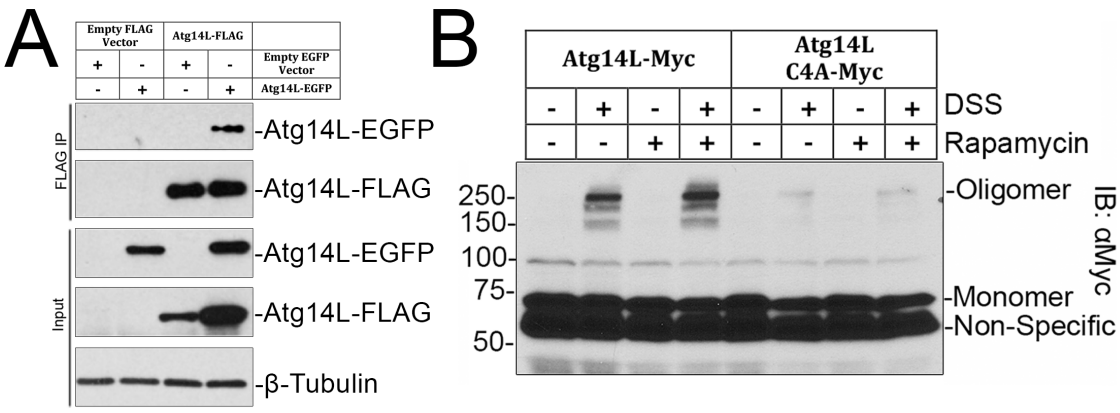

Figure 3.5: Atg14L self-association through N-terminal cysteine repeats
(A) HEK 293T cells were transiently transfected with vector controls, Atg14L-FLAG or Atg14L-EGFP. Lysates were subjected to immunoprecipitation with anti-FLAG resin and evaluated using immunoblots. (B) Atg14L oligomeric complex formation upon addition of DSS cross-linking reagent. HEK 293T cells were transiently transfected with Atg14L-Myc or Atg14LC4A-Myc and incubated with 0.5 μM rapamycin for 16h as indicated. Lysates were treated with cross-linking agent, disuccinimidyl suberate (DSS) at 0.25 mM for 30 min. Oligomeric complex formation observed as high molecular weight species.

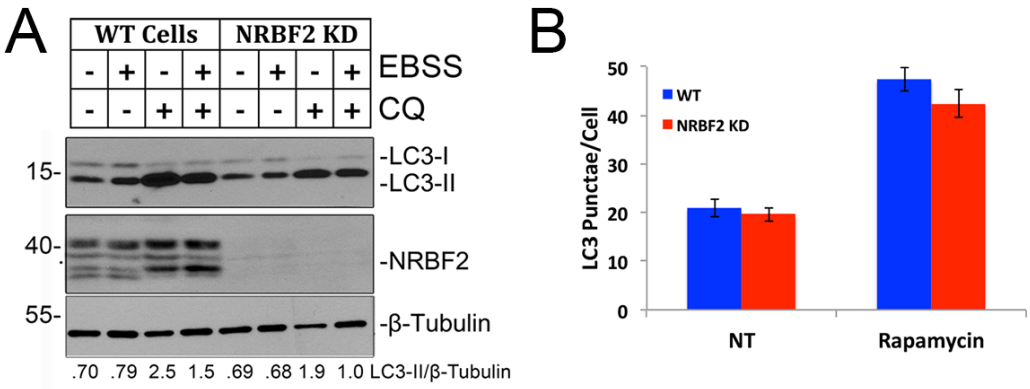

Figure 3.6 LC3-II conjugation and puncta formation with new NRBF2 KD clones
(A) Relative LC3-II levels in a regenerated DOX inducible NRBF2 depletion U_2OS cell line (NRBF2 KD). Cells were treated with EBSS for 1h or 100 μM chloroquine (CQ) for 2h as indicated. Relative LC3-II to β-tubulin was measured using band analysis in Image J. (B). Quantitation of LC3-positive vesicles per cell in either wild-type in a regenerated DOX-induced NRBF2 KD cells with 2 μM rapamycin for 4h as indicated. Data presented as average ± SEM. N=45.

Tables

Table 3.1: Plasmids used in NRBF2 Study

Construct Name	Vector	Gene	Restriction Sites	Use
Atg14L-EGFP	EGFP-N1	Atg14L	EcoR1+ SalI	Immunofluorescence
Atg14L-FLAG	modified framework of pCDNA4/FRT/TO-FLAG	Atg14L	EcoRV+ NotI	Autophagy Phenotype
ZZ-Atg14L-FLAG (1)	pCDNA5-ZZ-FLAG	Atg14L	EcoRV+ Not1	TAP purification
Atg14L-Myc	pCDNA3.1- Myc-6XHIS	Atg14L or C4A Mutant	Xba1 + Not1	Autophagy Phenotype and Crosslinking
ZZ-NRBF2-FLAG	pCDNA5-ZZ-FLAG	NRBF2	EcoRV+ Not1	TAP Purification
NRBF2-FLAG	modified framework of pCDNA5/FRT/TO-FLAG	NRBF2 or DD/AA Mutants	EcoRV+ NotI	NRBF2 Overexpression Cell Lines
NRBF2-Myc	pCDNA3.1- Myc-6XHIS	NRBF2 or DD/AA Mutants	Xba1 + Not1	Autophagy Phenotype
HA-NRBF2	modified framework of pCDNA4/FRT/TO-FLAG	NRBF2	EcoRV+ NotI	Map Binding Domains
Beclin 1-HA	modified framework of pCDNA4/FRT/TO-FLAG	Beclin 1	BamHI+ NotI	Autophagy Phenotype
DsRed-Beclin 1	pDSRed-C1	Beclin 1	EcoR1 + BamHI	Immunofluorescence

References

Amaravadi, R., Yu, D., Lum J, Bui, T., Gerard , E., Thomas-Tikhonenko, A., and Thompson, C.B. (2007). Autophagy inhibition enhances therapy-induced apoptosis in a Myc-induced model of lymphoma. J Clin Invest *117*, 326-336.

Amer, A.O., and Swanson, M.S. (2005). Autophagy is an immediate macrophage response to Legionella pneumophila. Cell Microbiol *7*, 765-778.

Anding, A.L., and Baehrecke, E.H. (2015). Vps15 is required for stress induced and developmentally triggered autophagy and salivary gland protein secretion in Drosophila. Cell Death Differ *22*, 457-464.

Antonny, B. (2011). Mechanisms of Membrane Curvature Sensing. Annu Rev Biochem *80*, 101-123.

Araki, Y., Ku, W.-C., Akioka, M., May, A.I., Hayashi, Y., Arisaka, F., Ishihama, Y., and Ohsumi, Y. (2013). Atg38 is required for autophagy-specific phosphatidylinositol 3-kinase complex integrity. J Cell Biol *203*, 299-313.

Axe, E.L., Walker, S.A., Manifava, M., Chandra, P., Roderick, H.L., Habermann, A., Griffiths, G., and Ktistakis, N.T. (2008). Autophagosome formation from membrane compartments enriched in phosphatidylinositol 3-phosphate and dynamically connected to the endoplasmic reticulum. J Cell Biol *182*, 685-701.

Baba, M., Osumi, M., Scott, S.V., Klionsky, D.J., and Ohsumi, Y. (1997). Two distinct pathways for targeting proteins from the cytoplasm to the vacuole/lysosome. J Cell Biol *139*, 1687-1695.

Backer, J.M. (2008). The regulation and function of Class III PI3Ks: novel roles for Vps34. Biochem J *410*, 1-17.

Baskaran, S., Carlson, L.-A., Stjepanovic, G., Young, L.N., Kim, D.J., Grob, P., Stanley, R.E., Nogales, E., and Hurley, J.H. (2014). Architecture and dynamics of the autophagic phosphatidylinositol 3-kinase complex. eLife *4*, 1-19.

Behrends, C., Sowa, M.E., Gygi, S.P., and Harper, J.W. (2010). Network organization of the human autophagy system. Nature *466*, 68-76.

Bhattacharyya, S., Yu, H., Mim, C., and Matouschek, A. (2014). Regulated protein turnover: snapshots of the proteasome in action. Nat Rev Mol Cell Biol *15*, 122-133.

Bigay, J., Casella, J.-F., Drin, G., Mesmin, B., and Antonny, B. (2005). ArfGAP1 responds to membrane curvature through the folding of a lipid packing sensor motif. EMBO J *24*, 2244-2253.

Birmingham, C.L., Smith, A.C., Bakowski, M.A., Yoshimori, T., and Brumell, J.H. (2006). Autophagy Controls Salmonella Infection in Response to Damage to the Salmonella-containing Vacuole. J Biol Chem *281*, 11374-11383.

Bjørkøy, G., Lamark, T., Brech, A., Outzen, H., Perander, M., Øvervatn, A., Stenmark, H., and Johansen, T. (2005). p62/SQSTM1 forms protein aggregates degraded by autophagy and has a protective effect on huntingtin-induced cell death. J Cell Biol *171*, 603-614.

Blommaart, E.F., Krause, U., Schellens, J.P., Vreeling-Sindelárová, H., and Meijer, A.J. (1997). The phosphatidylinositol 3-kinase inhibitors wortmannin and LY294002 inhibit autophagy in isolated rat hepatocytes. Eur J Biochem *243*, 240-246.

Calvo-Garrido, J., Carilla-Latorre, S., and Escalante, R. (2008a). Vacuole membrane protein 1, autophagy and much more. Autophagy *4*, 835-837.

Calvo-Garrido, J., Carilla-Latorre, S., Lázaro-Diéguez, F., Egea, G., and Escalante, R. (2008b). Vacuole membrane protein 1 is an endoplasmic reticulum protein required for organelle biogenesis, protein secretion, and development. Mol Biol Cell *19*, 3442-3453.

Cao, Y., Wang, Y., Abi Saab, W.F., Yang, F., Pessin, J.E., and Backer, J.M. (2014). NRBF2 regulates macroautophagy as a component of Vps34 Complex I. Biochem J *461*, 315-322.

Carlsson, S.R., and Simonsen, A. (2015). Membrane dynamics in autophagosome biogenesis. J Cell Sci *128*, 1-13.

Chan, E.Y.W., Kir, S., and Tooze, S.A. (2007). siRNA Screening of the Kinome Identifies ULK1 as a Multidomain Modulator of Autophagy. J Biol Chem *282*, 25464-25474.

Chang, Y.-Y., and Neufeld, T.P. (2009). An Atg1/Atg13 complex with multiple roles in TOR-mediated autophagy regulation. Mol Biol Cell *20*, 2004-2014.

Chen, D., Fan, W., Lu, Y., Ding, X., Chen, S., and Zhong, Q. (2012). A mammalian autophagosome maturation mechanism mediated by TECPR1 and the Atg12-Atg5 conjugate. Mol Cell *45*, 629-641.

Cheng, J., Fujita, A., Yamamoto, H., Tatematsu, T., Kakuta, S., Obara, K., Ohsumi, Y., and Fujimoto, T. (2014). Yeast and mammalian autophagosomes exhibit distinct phosphatidylinositol 3-phosphate asymmetries. Nat Commun *5*, 1-10.

Cianfanelli, V., De Zio, D., Di Bartolomeo, S., Nazio, F., Strappazzon, F., and Cecconi, F. (2015a). Ambra1 at a glance. J Cell Sci *128*, 2003-2008.

Cianfanelli, V., Fuoco, C., Lorente, M., Salazar, M., Quondamatteo, F., Gherardini, P.F., De Zio, D., Nazio, F., Antonioli, M., D'Orazio, M.*, et al.* (2015b). AMBRA1 links autophagy to cell proliferation and tumorigenesis by promoting c-Myc dephosphorylation and degradation. Nat Cell Biol *17*, 20-30.

Cong, L., Ran, F.A., Cox, D., Lin, S., Barretto, R., Habib, N., Hsu, P.D., Wu, X., Jiang, W., Marraffini, L.A.*, et al.* (2013). Multiplex genome engineering using CRISPR/Cas systems. Science *339*, 819-823.

de Duve, C., and Wattiaux, R. (1966). Functions of lysosomes. Annu Rev Physiol *28*, 435-492.

Degenhardt, K., Mathew, R., Beaudoin, B., Bray, K., Anderson, D., Chen, G., Mukherjee, C., Shi, Y., Gélinas, C., Fan, Y.*, et al.* (2006). Autophagy promotes tumor cell survival and restricts necrosis, inflammation, and tumorigenesis. Cancer Cell *10*, 51-64.

Devereaux, K., Dall'Armi, C., Alcazar-Roman, A., Ogasawara, Y., Zhou, X., Wang, F., Yamamoto, A., Camilli, P.D., and Di Paolo, G. (2013). Regulation of Mammalian Autophagy by Class II and III PI 3-Kinases through PI3P Synthesis. PLoS ONE *8*, e76405.

Di Bartolomeo, S., Corazzari, M., Nazio, F., Oliverio, S., Lisi, G., Antonioli, M., Pagliarini, V., Matteoni, S., Fuoco, C., Giunta, L.*, et al.* (2010). The dynamic interaction of AMBRA1 with the dynein motor complex regulates mammalian autophagy. J Cell Biol *191*, 155-168.

Diao, J., Liu, R., Rong, Y., Zhao, M., Zhang, J., Lai, Y., Zhou, Q., Wilz, L.M., Li, J., Vivona, S.*, et al.* (2015). ATG14 promotes membrane tethering and fusion of autophagosomes to endolysosomes. Nature *520*, 563-566.

Dooley, H.C., Razi, M., Polson, H.E.J., Girardin, S.E., Wilson, M.I., and Tooze, S.A. (2014). WIPI2 Links LC3 Conjugation with PI3P, Autophagosome Formation, and Pathogen Clearance by Recruiting Atg12-5-16L1. Mol Cell *55*, 238-252.

Doucet, C.M., Esmery, N., de Saint-Jean, M., and Antonny, B. (2015). Membrane Curvature Sensing by Amphipathic Helices Is Modulated by the Surrounding Protein Backbone. PLoS ONE *10*, e0137965.

Drin, G., and Antonny, B. (2010). Amphipathic helices and membrane curvature. FEBS Lett *584*, 1840-1847.

Drin, G., Casella, J.-F., Gautier, R., Boehmer, T., Schwartz, T.U., and Antonny, B. (2007). A general amphipathic alpha-helical motif for sensing membrane curvature. Nat Struct Mol Biol *14*, 138-146.

Durcan, T.M., and Fon, E.A. (2015). The three 'P's of mitophagy: PARKIN, PINK1, and post-translational modifications. Genes Dev *29*, 989-999.

Efeyan, A., Comb, W.C., and Sabatini, D.M. (2015). Nutrient-sensing mechanisms and pathways. Nature *517*, 302-310.

Egan, D.F., Shackelford, D.B., Mihaylova, M.M., Gelino, S., Kohnz, R.A., Mair, W., Vasquez, D.S., Joshi, A., Gwinn, D.M., Taylor, R.*, et al.* (2011). Phosphorylation of

ULK1 (hATG1) by AMP-Activated Protein Kinase Connects Energy Sensing to Mitophagy. Science *331*, 456-461.

Fan, W., Nassiri, A., and Zhong, Q. (2011). Autophagosome targeting and membrane curvature sensing by Barkor/Atg14(L). Proc Natl Acad Sci USA *108*, 7769-7774.

Filimonenko, M., Stuffers, S., Raiborg, C., Yamamoto, A., Malerod, L., Fisher, E.M.C., Isaacs, A., Brech, A., Stenmark, H., and Simonsen, A. (2007). Functional multivesicular bodies are required for autophagic clearance of protein aggregates associated with neurodegenerative disease. J Cell Biol *179*, 485-500.

Fimia, G.M., Corazzari, M., Antonioli, M., and Piacentini, M. (2013). Ambra1 at the crossroad between autophagy and cell death. Oncogene *32*, 3311-3318.

Fimia, G.M., Stoykova, A., Romagnoli, A., Giunta, L., Di Bartolomeo, S., Nardacci, R., Corazzari, M., Fuoco, C., Ucar, A., Schwartz, P.*, et al.* (2007). Ambra1 regulates autophagy and development of the nervous system. Nature *447*, 1121-1125.

Fujita, N., Hayashi-Nishino, M., Fukumoto, H., Omori, H., Yamamoto, A., Noda, T., and Yoshimori, T. (2008a). An Atg4B Mutant Hampers the Lipidation of LC3 Paralogues and Causes Defects in Autophagosome Closure. Mol Biol Cell *19*, 4651-4659.

Fujita, N., Itoh, T., Omori, H., Fukuda, M., Noda, T., and Yoshimori, T. (2008b). The Atg16L Complex Specifies the Site of LC3 Lipidation for Membrane Biogenesis in Autophagy. Mol Biol Cell *19*, 2092-2100.

Gallop, J.L., Jao, C.C., Kent, H.M., Butler, P.J.G., Evans, P.R., Langen, R., and McMahon, H.T. (2006). Mechanism of endophilin N-BAR domain-mediated membrane curvature. The EMBO Journal *25*, 2898-2910.

Gammoh, N., Florey, O., Overholtzer, M., and Jiang, X. (2013). Interaction between FIP200 and ATG16L1 distinguishes ULK1 complex–dependent and –independent autophagy. Nat Struct Mol Biol *20*, 144-149.

Ganley, I.G., Lam, D.H., Wang, J., Ding, X., Chen, S., and Jiang, X. (2009). ULK1-ATG13-FIP200 Complex Mediates mTOR Signaling and Is Essential for Autophagy. J Biol Chem *284*, 12297-12305.

Gautier, R., Douguet, D., Antonny, B., and Drin, G. (2008). HELIQUEST: a web server to screen sequences with specific alpha-helical properties. Bioinformatics *24*, 2101-2102.

Ge, L., Baskaran, S., Schekman, R., and Hurley, J.H. (2014a). The protein-vesicle network of autophagy. Curr Opin Cell Biol *29*, 18-24.

Ge, L., Melville, D., Zhang, M., and Schekman, R. (2013). The ER-Golgi intermediate compartment is a key membrane source for the LC3 lipidation step of autophagosome biogenesis. eLife *2*, 1-23.

Ge, L., Qi, W., Wang, L.-J., Miao, H.-H., Qu, Y.-X., Li, B.-L., and Song, B.-L. (2011). Flotillins play an essential role in Niemann-Pick C1-like 1-mediated cholesterol uptake. Proc Natl Acad Sci USA *108*, 551-556.

Ge, L., Zhang, M., and Schekman, R. (2014b). Phosphatidylinositol 3-kinase and COPII generate LC3 lipidation vesicles from the ER-Golgi intermediate compartment. eLife *3*, 1-13.

Geisler, S., Holmström, K.M., Skujat, D., Fiesel, F.C., Rothfuss, O.C., Kahle, P.J., and Springer, W. (2010). PINK1/Parkin-mediated mitophagy is dependent on VDAC1 and p62/SQSTM1. Nat Cell Biol *12*, 119-131.

Geng, J., and Klionsky, D.J. (2008). The Atg8 and Atg12 ubiquitin-like conjugation systems in macroautophagy. . EMBO reports *9*, 859-864.

Graef, M., Friedman, J.R., Graham, C., Babu, M., and Nunnari, J. (2013). ER exit sites are physical and functional core autophagosome biogenesis components. Mol Biol Cell *24*, 2918-2931.

Hamasaki, M., Furuta, N., Matsuda, A., Nezu, A., Yamamoto, A., Fujita, N., Oomori, H., Noda, T., Haraguchi, T., Hiraoka, Y.*, et al.* (2013). Autophagosomes form at ER–mitochondria contact sites. Nature *495*, 389-393.

Hanada, T., Noda, N.N., Satomi, Y., Ichimura, Y., Fujioka, Y., Takao, T., Inagaki, F., and Ohsumi, Y. (2007). The Atg12-Atg5 Conjugate Has a Novel E3-like Activity for Protein Lipidation in Autophagy. J Biol Chem *282*, 37298-37302.

Hara, T., Takamura, A., Kishi, C., Iemura, S.i., Natsume, T., Guan, J.L., and Mizushima, N. (2008). FIP200, a ULK-interacting protein, is required for autophagosome formation in mammalian cells. J Cell Biol *181*, 497-510.

He, S., Ni, D., Ma, B., Lee, J.-H., Zhang, T., Ghozalli, I., Pirooz, S.D., Zhao, Z., Bharatham, N., Li, B.*, et al.* (2013). PtdIns(3)P-bound UVRAG coordinates Golgi-ER retrograde and Atg9 transport by differential interactions with the ER tether and the beclin 1 complex. Nat Cell Biol *15*, 1206-1219.

Hosokawa, N., Hara, T., Kaizuka, T., Kishi, C., Takamura, A., Miura, Y., Iemura, S.-i., Natsume, T., Takehana, K., and Yamada, N. (2009a). Nutrient-dependent mTORC1 association with the ULK1–Atg13–FIP200 complex required for autophagy. Mol Biol Cell *20*, 1981-1991.

Hosokawa, N., Sasaki, T., Iemura, S.-i., Natsume, T., Hara, T., and Mizushima, N. (2009b). Atg101, a novel mammalian autophagy protein interacting with Atg13. Autophagy *5*, 973-979.

Hsu, P.D., Scott, D.A., Weinstein, J.A., Ran, F.A., Konermann, S., Agarwala, V., Li, Y., Fine, E.J., Wu, X., Shalem, O.*, et al.* (2013). DNA targeting specificity of RNA-guided Cas9 nucleases. Nat Biotechnol *31*, 827-832.

Huang, W.-P., and Klionsky, D.J. (2002). Autophagy in Yeast: A Review of the Molecular Machinery. Cell Struct Funct *27*, 409-420.

Hurley, J.H., and Hanson, P.I. (2010). Membrane budding and scission by the ESCRT machinery: it's all in the neck. Nat Rev Mol Cell Biol *11*, 556-566.

Hurley, J.H., and Schulman, B.A. (2014). Atomistic Autophagy: The Structures of Cellular Self-Digestion. Cell *157*, 300-311.

Ichimura, Y., Imamura, Y., Emoto, K., Umeda, M., Noda, T., and Ohsumi, Y. (2004). In Vivo and in Vitro Reconstitution of Atg8 Conjugation Essential for Autophagy. J Biol Chem *279*, 40584-40592.

Ichimura, Y., Kirisako, T., Takao, T., Satomi, Y., Shimonishi, Y., Ishihara, N., Mizushima, N., Tanida, I., Kominami, E., and Ohsumi, M. (2000). A ubiquitin-like system mediates protein lipidation. Nature *408*, 488-492.

Inoki, K., Kim, J., and Guan, K.-L. (2012). AMPK and mTOR in Cellular Energy Homeostasis and Drug Targets. Annu Rev Pharmacol Toxicol *52*, 381-400.

Itakura, E., Kishi, C., Inoue, K., and Mizushima, N. (2008). Beclin 1 forms two distinct phosphatidylinositol 3-kinase complexes with mammalian Atg14 and UVRAG. Mol Biol Cell *19*, 5360-5372.

Itakura, E., Kishi-Itakura, C., and Mizushima, N. (2012). The Hairpin-type Tail-Anchored SNARE Syntaxin 17 Targets to Autophagosomes for Fusion with Endosomes/Lysosomes. Cell *151*, 1256-1269.

Itakura, E., and Mizushima, N. (2009). Atg14 and UVRAG: Mutually exclusive subunits of mammalian Beclin 1-PI3K complexes. Autophagy *5*, 534-536.

Itakura, E., and Mizushima, N. (2010). Characterization of autophagosome formation site by a hierarchical analysis of mammalian Atg proteins. Autophagy *6*, 764-776.

Jahreiss, L., Menzies, F.M., and Rubinsztein, D.C. (2008). The Itinerary of Autophagosomes: From Peripheral Formation to Kiss-and-Run Fusion with Lysosomes. Traffic *9*, 574-587.

Jao, C.C., Ragusa, M.J., Stanley, R.E., and Hurley, J.H. (2013). A HORMA domain in Atg13 mediates PI 3-kinase recruitment in autophagy. Proc Natl Acad Sci USA *110*, 5486-5491.

Jewell, J.L., Russell, R.C., and Guan, K.-L. (2013). Amino acid signalling upstream of mTOR. Nat Rev Mol Cell Biol, 133-139.

Jiang, P., Nishimura, T., Sakamaki, Y., Itakura, E., Hatta, T., Natsume, T., and Mizushima, N. (2014). The HOPS complex mediates autophagosome-lysosome fusion through interaction with syntaxin 17. Mol Biol Cell.

Jinek, M., East, A., Cheng, A., Lin, S., Ma, E., and Doudna, J. (2013). RNA-programmed genome editing in human cells. eLife *2*, e00471.

Jung, C.H., Jun, C.B., Ro, S.-H., Kim, Y.-M., Otto, N.M., Cao, J., Kundu, M., and Kim, D.-H. (2009). ULK-Atg13-FIP200 complexes mediate mTOR signaling to the autophagy machinery. Mol Biol Cell *20*, 1992-2003.

Kabeya, Y., Mizushima, N., Ueno, T., Yamamoto, A., Kirisako, T., Noda, T., Kominami, E., Ohsumi, Y., and Yoshimori, T. (2000). LC3, a mammalian homologue of yeast Apg8p, is localized in autophagosome membranes after processing. The EMBO Journal *19*, 5720-5728.

Kang, R., Zeh, H.J., Lotze, M.T., and Tang, D. (2011). The Beclin 1 network regulates autophagy and apoptosis. Cell Death Differ *18*, 571-580.

Karanasios, E., Stapleton, E., Manifava, M., Kaizuka, T., Mizushima, N., Walker, S.A., and Ktistakis, N.T. (2013). Dynamic association of the ULK1 complex with omegasomes during autophagy induction. J Cell Sci *126*, 5224-5238.

Karantza-Wadsworth, V., Patel, S., Kravchuk, O., Chen, G., Mathew, R., Jin, S., and White, E. (2007). Autophagy mitigates metabolic stress and genome damage in mammary tumorigenesis. Genes Dev *21*, 1621-1635.

Katsuragi, Y., Ichimura, Y., and Komatsu, M. (2015). p62/SQSTM1 functions as a signaling hub and an autophagy adaptor. FEBS J, 1-7.

Kaufmann, A., Beier, V., Franquelim, H.G., and Wollert, T. (2014). Molecular mechanism of autophagic membrane-scaffold assembly and disassembly. Cell *156*, 469-481.

Kihara, A., Kabeya, Y., Ohsumi, Y., and Yoshimori, T. (2001a). Beclin-phosphatidylinositol 3-kinase complex functions at the trans-Golgi network. EMBO reports *2*, 330-335.

Kihara, A., Noda, T., Ishihara, N., and Ohsumi, Y. (2001b). Two distinct Vps34 phosphatidylinositol 3-kinase complexes function in autophagy and carboxypeptidase Y sorting in Saccharomyces cerevisiae. J Cell Biol *152*, 519-530.

Kim, J., Kim, Y.C., Fang, C., Russell, R.C., Kim, J.H., Fan, W., Liu, R., Zhong, Q., and Guan, K.-L. (2013). Differential Regulation of Distinct Vps34 Complexes by AMPK in Nutrient Stress and Autophagy. Cell *152*, 290-303.

Kim, J., Kundu, M., Viollet, B., and Guan, K.-L. (2011). AMPK and mTOR regulate autophagy through direct phosphorylation of Ulk1. Nat Cell Biol *13*, 132-141.

Kim, Y.-M., Jung, C.H., Seo, M., Kim, E.K., Park, J.-M., Bae, S.S., and Kim, D.-H. (2015). mTORC1 phosphorylates UVRAG to negatively regulate autophagosome and endosome maturation. Mol Cell *57*, 207-218.

Kimura, S., Noda, T., and Yoshimori, T. (2007). Dissection of the autophagosome maturation process by a novel reporter protein, tandem fluorescent-tagged LC3. Autophagy *3*, 452-460.

Kimura, T., Takabatake, Y., Takahashi, A., and Isaka, Y. (2013). Chloroquine in Cancer Therapy: A Double-Edged Sword of Autophagy. Cancer Res *73*, 3-7.

Kirisako, T., Baba, M., Ishihara, N., Miyazawa, K., Ohsumi, M., Yoshimori, T., Noda, T., and Ohsumi, Y. (1999). Formation process of autophagosome is traced with Apg8/Aut7p in yeast. J Cell Biol *147*, 435-446.

Kishi-Itakura, C., Koyama-Honda, I., Itakura, E., and Mizushima, N. (2014). Ultrastructural analysis of autophagosome organization using mammalian autophagy-deficient cells. J Cell Sci *127*, 4089-4102.

Klionsky, D.J. (2007). Autophagy: from phenomenology to molecular understanding in less than a decade. Nat Rev Mol Cell Biol *8*, 931-937.

Klionsky, D.J., Cregg, J.M., Dunn, W.A., Emr, S.D., Sakai, Y., Sandoval, I.V., Sibirny, A., Subramani, S., Thumm, M., Veenhuis, M.*, et al.* (2003). A unified nomenclature for yeast autophagy-related genes. Dev Cell *5*, 539-545.

Klionsky, D.J., Cuervo, A.M., and Seglen, P.O. (2007). Methods for monitoring autophagy from yeast to human. Autophagy *3*, 181-206.

Klionsky, D.J., Elazar, Z., Seglen, P.O., and Rubinsztein, D.C. (2008). Does bafilomycin A1 block the fusion of autophagosomes with lysosomes? Autophagy *4*, 849-850.

Koyama-Honda, I., Itakura, E., Fujiwara, T.K., and Mizushima, N. (2013). Temporal analysis of recruitment of mammalian ATG proteins to the autophagosome formation site. Autophagy *9*, 1491-1499.

Kundu, M., and Thompson, C.B. (2008). Autophagy: Basic Principles and Relevance to Disease. Annu Rev Pathol: Mech Dis *3*, 427-455.

Lee, J.-A., Beigneux, A., Ahmad, S.T., Young, S.G., and Gao, F.-B. (2007). ESCRT-III Dysfunction Causes Autophagosome Accumulation and Neurodegeneration. Curr Biol *17*, 1561-1567.

Lee, J.-H., Yu, W.H., Kumar, A., Lee, S., Mohan, P.S., Peterhoff, C.M., Wolfe, D.M., Martinez-Vicente, M., Massey, A.C., Sovak, G.*, et al.* (2010). Lysosomal proteolysis and autophagy require presenilin 1 and are disrupted by Alzheimer-related PS1 mutations. Cell *141*, 1146-1158.

Levine, B., and Klionsky, D.J. (2004). Development by self-digestion: molecular mechanisms and biological functions of autophagy. Dev Cell *6*, 463-477.

Levine, B., Liu, R., Dong, X., and Zhong, Q. (2015). Beclin orthologs: integrative hubs of cell signaling, membrane trafficking, and physiology. Trends Cell Biol *25*, 533-544.

Li, X., He, L., Che, K.H., Funderburk, S.F., Pan, L., Pan, N., Zhang, M., Yue, Z., and Zhao, Y. (2012). Imperfect interface of Beclin1 coiled-coil domain regulates homodimer and heterodimer formation with Atg14L and UVRAG. Nat Commun *3*, 662-611.

Liang, C., Feng, P., Ku, B., Dotan, I., Canaani, D., Oh, B.-H., and Jung, J.U. (2006). Autophagic and tumour suppressor activity of a novel Beclin1-binding protein UVRAG. Nat Cell Biol *8*, 688-698.

Liang, C., Lee, J.-s., Inn, K.-S., Gack, M.U., Li, Q., Roberts, E.A., Vergne, I., Deretic, V., Feng, P., Akazawa, C*., et al.* (2008). Beclin1-binding UVRAG targets the class C Vps complex to coordinate autophagosome maturation and endocytic trafficking. Nat Cell Biol *10*, 776-787.

Liang, J.-H., and Jia, J.-P. (2014). Dysfunctional autophagy in Alzheimer's disease: pathogenic roles and therapeutic implications. Neurosci Bull *2*, 308-316.

Liang, X.H., Jackson, S., Seaman, M., Brown, K., Kempkes, B., Hibshoosh, H., and Levine, B. (1999). Induction of autophagy and inhibition of tumorigenesis by beclin 1. Nature *402*, 672-676.

Lin, X., Li, S., Zhao, Y., Ma, X., Zhang, K., He, X., and Wang, Z. (2013). Interaction Domains of p62: A Bridge Between p62 and Selective Autophagy. DNA Cell Biol *32*, 220-227.

Longatti, A., and Tooze, S.A. (2009). Vesicular trafficking and autophagosome formation. Cell Death Differ *16*, 956-965.

Lu, J., He, L., Behrends, C., Araki, M., Araki, K., Jun Wang, Q., Catanzaro, J.M., Friedman, S.L., Zong, W.-X., Fiel, M.I*., et al.* (2014). NRBF2 regulates autophagy and prevents liver injury by modulating Atg14L-linked phosphatidylinositol-3 kinase III activity. Nat Commun *5*, 1-15.

Lystad, A.H., Ichimura, Y., Takagi, K., Yang, Y., Pankiv, S., Kanegae, Y., Kageyama, S., Suzuki, M., Saito, I., Mizushima, T*., et al.* (2014). Structural determinants in GABARAP required for the selective binding and recruitment of ALFY to LC3B-positive structures. EMBO reports *15*, 557-565.

Mack, H.I., Zheng, B., Asara, J.M., and Thomas, S.M. (2012). AMPK-dependent phosphorylation of ULK1 regulates ATG9 localization. Autophagy *8*, 1197-1214.

Mao, K., and Klionsky, D.J. (2011). AMPK Activates Autophagy by Phosphorylating ULK1. Circul Res *108*, 787-788.

Mari, M., Griffith, J., Rieter, E., Krishnappa, L., Klionsky, D.J., and Reggiori, F. (2010). An Atg9-containing compartment that functions in the early steps of autophagosome biogenesis. J Cell Biol *190*, 1005-1022.

Martinez-Vicente, M. (2015). Autophagy in neurodegenerative diseases: From pathogenic dysfunction to therapeutic modulation. Semin Cell Dev Biol *40*, 115-126.

Martinez-Vicente, M., Talloczy, Z., Wong, E., Tang, G., Koga, H., Kaushik, S., de Vries, R., Arias, E., Harris, S., Sulzer, D*., et al.* (2010). Cargo recognition failure is responsible for inefficient autophagy in Huntington's disease. Nat Neurosci *13*, 567-576.

Mathew, R., Karantza-Wadsworth, V., and White, E. (2007). Role of autophagy in cancer. Nat Rev Cancer *7*, 961-967.

Mathew, R., Karp, C.M., Beaudoin, B., Vuong, N., Chen, G., Chen, H.-Y., Bray, K., Reddy, A., Bhanot, G., Gélinas, C*., et al.* (2009). Autophagy Suppresses Tumorigenesis through Elimination of p62. Cell *137*, 1062-1075.

Matsuda, N., Sato, S., Shiba, K., Okatsu, K., Saisho, K., Gautier, C.A., Sou, Y.s., Saiki, S., Kawajiri, S., Sato, F*., et al.* (2010). PINK1 stabilized by mitochondrial depolarization recruits Parkin to damaged mitochondria and activates latent Parkin for mitophagy. J Cell Biol *189*, 211-221.

Matsunaga, K., Morita, E., Saitoh, T., Akira, S., Ktistakis, N.T., Izumi, T., Noda, T., and Yoshimori, T. (2010). Autophagy requires endoplasmic reticulum targeting of the PI3-kinase complex via Atg14L. J Cell Biol *190*, 511-521.

Matsunaga, K., Saitoh, T., Tabata, K., Omori, H., Satoh, T., Kurotori, N., Maejima, I., Shirahama-Noda, K., Ichimura, T., Isobe, T*., et al.* (2009). Two Beclin 1-binding proteins, Atg14L and Rubicon, reciprocally regulate autophagy at different stages. Nat Cell Biol *11*, 385-396.

Matsushita, M., Suzuki, N.N., Obara, K., Fujioka, Y., Ohsumi, Y., and Inagaki, F. (2007). Structure of Atg5-Atg16, a complex essential for autophagy. J Biol Chem *282*, 6763-6772.

Mauthe, M., Jacob, A., Freiberger, S., Hentschel, K., Stierhof, Y.-D., Codogno, P., and Proikas-Cezanne, T. (2011). Resveratrol-mediated autophagy requires WIPI-1-regulated LC3 lipidation in the absence of induced phagophore formation. Autophagy *7*, 1448-1461.

McKnight, N.C., Zhong, Y., Wold, M.S., Gong, S., Phillips, G.R., Dou, Z., Zhao, Y., Heintz, N., Zong, W.-X., and Yue, Z. (2014). Beclin 1 Is Required for Neuron Viability and Regulates Endosome Pathways via the UVRAG-VPS34 Complex. PLoS Genet *10*, e1004626.

Menzies, F.M., Fleming, A., and Rubinsztein, D.C. (2015). Compromised autophagy and neurodegenerative diseases. Nat Rev Neurosci *16*, 345-357.

Mercer, C.A., Kaliappan, A., and Dennis, P.B. (2009). A novel, human Atg13 binding protein, Atg101, interacts with ULK1 and is essential for macroautophagy. Autophagy *5*, 649-662.

Miller, S., Tavshanjian, B., Oleksy, A., Perisic, O., Houseman, B.T., Shokat, K.M., and Williams, R.L. (2010). Shaping Development of Autophagy Inhibitors with the Structure of the Lipid Kinase Vps34. Science *327*, 1638-1642.

Mizushima, N. (2007). Autophagy: process and function. Genes Dev *21*, 2861-2873.

Mizushima, N., Noda, T., and Ohsumi, Y. (1999). Apg16p is required for the function of the Apg12p-Apg5p conjugate in the yeast autophagy pathway. The EMBO Journal *18*, 3888-3896.

Mizushima, N., Yamamoto, A., Hatano, M., Kobayashi, Y., Kabeya, Y., Suzuki, K., Tokuhisa, T., Ohsumi, Y., and Yoshimori, T. (2001). Dissection of autophagosome formation using Apg5-deficient mouse embryonic stem cells. J Cell Biol *152*, 657-668.

Mizushima, N., and Yoshimori, T. (2007). How to interpret LC3 immunoblotting. Autophagy *3*, 542-545.

Molejon, M.I., Ropolo, A., Re, A.L., Boggio, V., and Vaccaro, M.I. (2013). The VMP1-Beclin 1 interaction regulates autophagy induction. Sci Rep *3*, 1-11.

Nagy, P., Hegedűs, K., Pircs, K., Varga, Á., and Juhasz, G. (2014). Different effects of Atg2 and Atg18 mutations on Atg8a and Atg9 trafficking during starvation in Drosophila. FEBS Lett, 408-413.

Nakamura, N., Matsuura, A., Wada, Y., and Ohsumi, Y. (1997). Acidification of vacuoles is required for autophagic degradation in the yeast, Saccharomyces cerevisiae. J Biochem *121*, 338-344.

Narendra, D., Tanaka, A., Suen, D.F., and Youle, R.J. (2008). Parkin is recruited selectively to impaired mitochondria and promotes their autophagy. J Cell Biol *183*, 795-803.

Narendra, D.P., Jin, S.M., Tanaka, A., Suen, D.-F., Gautier, C.A., Shen, J., Cookson, M.R., and Youle, R.J. (2010). PINK1 Is Selectively Stabilized on Impaired Mitochondria to Activate Parkin. PLoS Biol *8*, e1000298.

Nath, S., Dancourt, J., Shteyn, V., Puente, G., Fong, W.M., Nag, S., Bewersdorf, J., Yamamoto, A., Antonny, B., and Melia, T.J. (2014). Lipidation of the LC3/GABARAP family of autophagy proteins relies on a membrane-curvature-sensing domain in Atg3. Nat Cell Biol *16*, 415-424.

Nazio, F., Strappazzon, F., Antonioli, M., Bielli, P., Cianfanelli, V., Bordi, M., Gretzmeier, C., Dengjel, J., Piacentini, M., Fimia, G.M.*, et al.* (2013). mTOR inhibits

autophagy by controlling ULK1 ubiquitylation, self-association and function through AMBRA1 and TRAF6. Nat Cell Biol *15*, 406-416.

Nishimura, T., Kaizuka, T., Cadwell, K., Sahani, M.H., Saitoh, T., Akira, S., Virgin, H.W., and Mizushima, N. (2013). FIP200 regulates targeting of Atg16L1 to the isolation membrane. EMBO Reports *14*, 284-291.

Noble, C.G., Dong, J.-M., Manser, E., and Song, H. (2008). Bcl-xL and UVRAG cause a monomer-dimer switch in Beclin1. J Biol Chem *283*, 26274-26282.

Noda, N.N., and Fujioka, Y. (2015). Atg1 family kinases in autophagy initiation. Cell Mol Life Sci *72*, 3083-3096.

Obara, K., Noda, T., Niimi, K., and Ohsumi, Y. (2008a). Transport of phosphatidylinositol 3-phosphate into the vacuole via autophagic membranes in Saccharomyces cerevisiae. Genes Cells *13*, 537-547.

Obara, K., and Ohsumi, Y. (2008). Dynamics and function of PtdIns(3)P in autophagy. Autophagy *4*, 952-954.

Obara, K., and Ohsumi, Y. (2011). Atg14: A Key Player in Orchestrating Autophagy. Int J Cell Biol *2011*, 1-7.

Obara, K., Sekito, T., Niimi, K., and Ohsumi, Y. (2008b). The Atg18-Atg2 Complex Is Recruited to Autophagic Membranes via Phosphatidylinositol 3-Phosphate and Exerts an Essential Function. J Biol Chem *283*, 23972-23980.

Ochaba, J., Lukacsovich, T., Csikos, G., Zheng, S., Margulis, J., Salazar, L., Mao, K., Lau, A.L., Yeung, S.Y., Humbert, S.*, et al.* (2014). Potential function for the Huntingtin protein as a scaffold for selective autophagy. Proc Natl Acad Sci USA *47*, 16889-16894.

Orsi, A., Razi, M., Dooley, H.C., Robinson, D., Weston, A.E., Collinson, L.M., and Tooze, S.A. (2012). Dynamic and transient interactions of Atg9 with autophagosomes, but not membrane integration, are required for autophagy. Mol Biol Cell *23*, 1860-1873.

Panaretou, C., Domin, J., Cockcroft, S., and Waterfield, M.D. (1997). Characterization of p150, an adaptor protein for the human phosphatidylinositol (PtdIns) 3-kinase. Substrate presentation by phosphatidylinositol transfer protein to the p150.Ptdins 3-kinase complex. J Biol Chem *272*, 2477-2485.

Pankiv, S., Clausen, T.H., Lamark, T., Brech, A., Bruun, J.-A., Outzen, H., Øvervatn, A., Bjørkøy, G., and Johansen, T. (2007). p62/SQSTM1 binds directly to Atg8/LC3 to facilitate degradation of ubiquitinated protein aggregates by autophagy. J Biol Chem *282*, 24131-24145.

Pasquier, B., El-Ahmad, Y., Filoche-Romme, B., Dureuil, C., Fassy, F., Abecassis, P.-Y., Mathieu, M., Bertrand, T., Benard, T., Barrière, C.*, et al.* (2015). Discovery of (2S)-8-[(3R)-3-methylmorpholin-4-yl]-1-(3-methyl-2-oxobutyl)-2-(trifluoromethyl)-3,4-

dihydro-2H-pyrimido[1,2-a]pyrimidin-6-one: a novel potent and selective inhibitor of Vps34 for the treatment of solid tumors. J Med Chem *58*, 376-400.

Pattingre, S., Tassa, A., Qu, X., Garuti, R., Liang, X.H., Mizushima, N., Packer, M., Schneider, M.D., and Levine, B. (2005). Bcl-2 Antiapoptotic Proteins Inhibit Beclin 1-Dependent Autophagy. Cell *122*, 927-939.

Petiot, A., Ogier-Denis, E., Blommaart, E.F., Meijer, A.J., and Codogno, P. (2000). Distinct classes of phosphatidylinositol 3′-kinases are involved in signaling pathways that control macroautophagy in HT-29 cells. J Biol Chem *275*, 992-998.

Polson, H.E.J., de Lartigue, J., Rigden, D.J., Reedijk, M., Urbé, S., Clague, M.J., and Tooze, S.A. (2010). Mammalian Atg18 (WIPI2) localizes to omegasome-anchored phagophores and positively regulates LC3 lipidation. Autophagy *6*, 506-522.

Proikas-Cezanne, T., Ruckerbauer, S., Stierhof, Y.-D., Berg, C., and Nordheim, A. (2007). Human WIPI-1 puncta-formation: A novel assay to assess mammalian autophagy. FEBS Lett *581*, 3396-3404.

Proikas-Cezanne, T., Takacs, Z., Dönnes, P., and Kohlbacher, O. (2015). WIPI proteins: essential PtdIns3P effectors at the nascent autophagosome. J Cell Sci *128*, 1-11.

Proikas-Cezanne, T., Waddell, S., Gaugel, A., Frickey, T., Lupas, A., and Nordheim, A. (2004). WIPI-1α (WIPI49), a member of the novel 7-bladed WIPI protein family, is aberrantly expressed in human cancer and is linked to starvation-induced autophagy. Oncogene *23*, 9314-9325.

Ragusa, M.J., Stanley, R.E., and Hurley, J.H. (2012). Architecture of the Atg17 complex as a scaffold for autophagosome biogenesis. Cell *151*, 1501-1512.

Reggiori, F., and Klionsky, D.J. (2002). Autophagy in the Eukaryotic Cell. Eukaryot Cell *1*, 11-21.

Reggiori, F., and Klionsky, D.J. (2006). Atg9 sorting from mitochondria is impaired in early secretion and VFT-complex mutants in Saccharomyces cerevisiae. J Cell Sci *119*, 2903-2911.

Reggiori, F., Tucker, K.A., Stromhaug, P.E., and Klionsky, D.J. (2004). The Atg1-Atg13 complex regulates Atg9 and Atg23 retrieval transport from the pre-autophagosomal structure. Dev Cell *6*, 79-90.

Ridley, S.H., Ktistakis, N., Davidson, K., Anderson, K.E., Manifava, M., Ellson, C.D., Lipp, P., Bootman, M., Coadwell, J., Nazarian, A.*, et al.* (2001). FENS-1 and DFCP1 are FYVE domain-containing proteins with distinct functions in the endosomal and Golgi compartments. J Cell Sci *114*, 3991-4000.

Rogov, V., Dötsch, V., johansen, T., and Kirkin, V. (2014). Interactions between autophagy receptors and ubiquitin-like proteins form the molecular basis for selective autophagy. Mol Cell *53*, 167-178.

Romanov, J., Walczak, M., Ibiricu, I., Schüchner, S., Ogris, E., Kraft, C., and Martens, S. (2012). Mechanism and functions of membrane binding by the Atg5-Atg12/Atg16 complex during autophagosome formation. The EMBO Journal *31*, 4304-4317.

Romanyuk, D., Polak, A., Maleszewska, A., Sieńko, M., Grynberg, M., and Żołądek, T. (2011). Human hAtg2A protein expressed in yeast is recruited to preautophagosomal structure but does not complement autophagy defects of atg2Δ strain. Acta Biochim Pol *58*, 365-374.

Ronan, B., Flamand, O., Vescovi, L., Dureuil, C., Durand, L., Fassy, F., Bachelot, M.-F., Lamberton, A., Mathieu, M., Bertrand, T.*, et al.* (2014). A highly potent and selective Vps34 inhibitor alters vesicle trafficking and autophagy. Nat Chem Biol *12*, 1013-1019.

Ropolo, A., Grasso, D., Pardo, R., Sacchetti, M.L., Archange, C., Re, A.L., Seux, M., Nowak, J., Gonzalez, C.D., Iovanna, J.L.*, et al.* (2007). The pancreatitis-induced vacuole membrane protein 1 triggers autophagy in mammalian cells. J Biol Chem *282*, 37124-37133.

Rostislavleva, K., Soler, N., Ohashi, Y., Zhang, L., Pardon, E., Burke, J.E., Masson, G.R., Johnson, C., Steyaert, J., Ktistakis, N.T.*, et al.* (2015). Structure and flexibility of the endosomal Vps34 complex reveals the basis of its function on membranes. Science *350*, aac7365.

Russell, R.C., Tian, Y., Yuan, H., Park, H.W., Chang, Y.-Y., Kim, J., Kim, H., Neufeld, T.P., Dillin, A., and Guan, K.-L. (2013). ULK1 induces autophagy by phosphorylating Beclin-1 and activating VPS34 lipid kinase. Nat Cell Biol *15*, 741-750.

Rusten, T.E., Vaccari, T., Lindmo, K., Rodahl, L.M.W., Nezis, I.P., Sem-Jacobsen, C., Wendler, F., Vincent, J.-P., Brech, A., Bilder, D.*, et al.* (2007). ESCRTs and Fab1 Regulate Distinct Steps of Autophagy. Curr Biol *17*, 1817-1825.

Sancak, Y., Bar-Peled, L., Zoncu, R., Markhard, A.L., Nada, S., and Sabatini, D.M. (2010). Ragulator-Rag complex targets mTORC1 to the lysosomal surface and is necessary for its activation by amino acids. Cell *141*, 290-303.

Sancak, Y., Peterson, T.R., Shaul, Y.D., Lindquist, R.A., Thoreen, C.C., Bar-Peled, L., and Sabatini, D.M. (2008). The Rag GTPases bind raptor and mediate amino acid signaling to mTORC1. Science *320*, 1496-1501.

Shibutani, S.T., Saitoh, T., Nowag, H., Münz, C., and Yoshimori, T. (2015). Autophagy and autophagy-related proteins in the immune system. Nat Immunol *16*, 1014-1024.

Slater, A.F.G. (1993). Chloroquine: Mechanism of drug action and resistance in plasmodium falciparum. Pharmacol Ther *57*, 203-235.

Sou, Y.-S., Tanida, I., Komatsu, M., Ueno, T., and Kominami, E. (2006). Phosphatidylserine in addition to phosphatidylethanolamine is an in vitro target of the mammalian Atg8 modifiers, LC3, GABARAP, and GATE-16. J Biol Chem *281*, 3017-3024.

Stack, J.H., DeWald, D.B., Takegawa, K., and Emr, S.D. (1995). Vesicle-mediated protein transport: regulatory interactions between the Vps15 protein kinase and the Vps34 PtdIns 3-kinase essential for protein sorting to the vacuole in yeast. J Cell Biol *129*, 321-334.

Stack, J.H., Herman, P.K., Schu, P.V., and Emr, S.D. (1993). A membrane-associated complex containing the Vps15 protein kinase and the Vps34 PI 3-kinase is essential for protein sorting to the yeast lysosome-like vacuole. EMBO J *12*, 2195-2204.

Stjepanovic, G., Davies, C.W., Stanley, R.E., Ragusa, M.J., Kim, D.J., and Hurley, J.H. (2014). Assembly and dynamics of the autophagy-initiating Atg1 complex. Proceedings of the National Academy of Sciences of the United States of America.

Sugawara, K., Suzuki, N.N., Fujioka, Y., Mizushima, N., Ohsumi, Y., and Inagaki, F. (2004). The crystal structure of microtubule‐associated protein light chain 3, a mammalian homologue of Saccharomyces cerevisiae Atg8. Genes Cells *9*, 611-618.

Sun, Q., Fan, W., Chen, K., Ding, X., Chen, S., and Zhong, Q. (2008). Identification of Barkor as a mammalian autophagy-specific factor for Beclin 1 and class III phosphatidylinositol 3-kinase. Proc Natl Acad Sci USA *105*, 19211-19216.

Sun, Q., Westphal, W., Wong, K.N., Tan, I., and Zhong, Q. (2010a). Rubicon controls endosome maturation as a Rab7 effector. Proc Natl Acad Sci USA *107*, 19338-19343.

Sun, Q., Zhang, J., Fan, W., Wong, K.N., Ding, X., Chen, S., and Zhong, Q. (2010b). The RUN Domain of Rubicon Is Important for hVps34 Binding, Lipid Kinase Inhibition, and Autophagy Suppression. J Biol Chem *286*, 185-191.

Suzuki, H., Tabata, K., Morita, E., Kawasaki, M., Kato, R., Dobson, R.C.J., Yoshimori, T., and Wakatsuki, S. (2014). Structural basis of the autophagy-related LC3/Atg13 LIR complex: recognition and interaction mechanism. Structure *22*, 47-58.

Suzuki, K., Akioka, M., Kondo-Kakuta, C., Yamamoto, H., and Ohsumi, Y. (2013). Fine mapping of autophagy-related proteins during autophagosome formation in Saccharomyces cerevisiae. J Cell Sci *126*, 2534-2544.

Suzuki, K., Kirisako, T., Kamada, Y., Mizushima, N., Noda, T., and Ohsumi, Y. (2001). The pre-autophagosomal structure organized by concerted functions of APG genes is essential for autophagosome formation. EMBO J *20*, 5971-5981.

Suzuki, K., Kubota, Y., Sekito, T., and Ohsumi, Y. (2007). Hierarchy of Atg proteins in pre-autophagosomal structure organization. Genes Cells *12*, 209-218.

Suzuki, K., and Ohsumi, Y. (2010). Current knowledge of the pre-autophagosomal structure (PAS). FEBS Lett *584*, 1280-1286.

Takahashi, Y., Coppola, D., Matsushita, N., Cualing, H.D., Sun, M., Sato, Y., Liang, C., Jung, J.U., Cheng, J.Q., Mul, J.J.*, et al.* (2007). Bif-1 interacts with Beclin 1 through UVRAG and regulates autophagy and tumorigenesis. Nat Cell Biol *9*, 1142-1151.

Takahashi, Y., Meyerkord, C.L., Hori, T., Runkle, K., Fox, T.E., Kester, M., Loughran, T.P., and Wang, H.-G. (2011). Bif-1 regulates Atg9 trafficking by mediating the fission of Golgi membranes during autophagy. Autophagy *7*, 61-73.

Takahashi, Y., Meyerkord, C.L., and Wang, H.-G. (2009). Bif-1/Endophilin B1: a candidate for crescent driving force in autophagy. Cell Death Differ *16*, 947-955.

Takáts, S., Nagy, P., Varga, Á., Pircs, K., Kárpáti, M., Varga, K., Kovács, A.L., Hegedűs, K., and Juhasz, G. (2013). Autophagosomal Syntaxin17-dependent lysosomal degradation maintains neuronal function in Drosophila. J Cell Biol *201*, 531-539.

Takeshige, K., Baba, M., Tsuboi, S., Noda, T., and Ohsumi, Y. (1992). Autophagy in yeast demonstrated with proteinase-deficient mutants and conditions for its induction. J Cell Biol *119*, 301-311.

Tooze, S.A., Dooley, H.C., Jefferies, H.B.J., Joachim, J., Judith, D., Lamb, C.A., Razi, M., and Wirth, M. (2014). Assessing Mammalian Autophagy. Methods Mol Biol *1270*, 155-165.

Tsukada, M., and Ohsumi, Y. (1993). Isolation and characterization of autophagy-defective mutants of Saccaromyces Cerevisiae. FEBS Lett *333*, 169-174.

Velikkakath, A.K.G., Nishimura, T., Oita, E., Ishihara, N., and Mizushima, N. (2012). Mammalian Atg2 proteins are essential for autophagosome formation and important for regulation of size and distribution of lipid droplets. Mol Biol Cell *23*, 896-909.

Vives-Bauza, C., Zhou, C., Huang, Y., Cui, M., de Vries, R.L.A., Kim, J., May, J., Tocilescu, M.A., Liu, W., Ko, H.S.*, et al.* (2010). PINK1-dependent recruitment of Parkin to mitochondria in mitophagy. Proc Natl Acad Sci USA *107*, 378-383.

Volinia, S., Dhand, R., Vanhaesebroeck, B., MacDougall, L.K., Stein, R., Zvelebil, M.J., Domin, J., Panaretou, C., and Waterfield, M.D. (1995). A human phosphatidylinositol 3-kinase complex related to the yeast Vps34p-Vps15p protein sorting system. EMBO J *14*, 3339-3348.

Walker, E.H., Pacold, M.E., Perisic, O., Stephens, L., Hawkins, P.T., Wymann, M.P., and Williams, R.L. (2000). Structural determinants of phosphoinositide 3-kinase inhibition by wortmannin, LY294002, quercetin, myricetin, and staurosporine. Mol Cell *6*, 909-919.

Weidberg, H., Shvets, E., Shpilka, T., Shimron, F., Shinder, V., and Elazar, Z. (2010). LC3 and GATE-16/GABARAP subfamilies are both essential yet act differently in autophagosome biogenesis. EMBO J *29*, 1792-1802.

White, E., and DiPaola, R.S. (2009). The Double-Edged Sword of Autophagy Modulation in Cancer. Clin Cancer Res *15*, 5308-5316.

Wilz, L., Fan, W., and Zhong, Q. (2011). Membrane curvature response in autophagy. Autophagy *7*, 1249-1250.

Wymann, M.P., Bulgarelli-Leva, G., Zvelebil, M.J., Pirola, L., Vanhaesebroeck, B., Waterfield, M.D., and Panayotou, G. (1996). Wortmannin inactivates phosphoinositide 3-kinase by covalent modification of Lys-802, a residue involved in the phosphate transfer reaction. Mol Cell Biol *16*, 1722-1733.

Yamamoto, A., Tagawa, Y., Yoshimori, T., Moriyama, Y., Masaki, R., and Tashiro, Y. (1998). Bafilomycin A1 prevents maturation of autophagic vacuoles by inhibiting fusion between autophagosomes and lysosomes in rat hepatoma cell line, H-4-II-E cells. Cell Struct Funct *23*, 33-42.

Yamamoto, H., Kakuta, S., Watanabe, T.M., Kitamura, A., Sekito, T., Kondo-Kakuta, C., Ichikawa, R., Kinjo, M., and Ohsumi, Y. (2012). Atg9 vesicles are an important membrane source during early steps of autophagosome formation. J Cell Biol *198*, 219-233.

Yang, Z., and Klionsky, D.J. (2010). Eaten alive: a history of macroautophagy. Nat Cell Biol *12*, 814-822.

Yasumo, H., Masuda, N., Furusawa, T., Tsukamoto, T., Sadano, H., and Osumi, T. (2000). Nuclear receptor binding factor-2 (NRBF-2), a possible gene activator protein interacting with nuclear hormone receptors. Biochimica et biophysica acta *1490*, 189-197.

Young, A.R.J., Chan, E.Y.W., Hu, X.W., Kochl, R., Crawshaw, S., High, S., Hailey, D.W., LIppincott-Schwartz, J., and Tooze, S.A. (2006). Starvation and ULK1-dependent cycling of mammalian Atg9 between the TGN and endosomes. J Cell Sci *119*, 3888-3900.

Yu, L., McPhee, C.K., Zheng, L., Mardones, G.A., Rong, Y., Peng, J., Mi, N., Zhao, Y., Liu, Z., Wan, F.*, et al.* (2010). Termination of autophagy and reformation of lysosomes regulated by mTOR. Nature *465*, 942-946.

Yue, Z., Jin, S., Yang, C., Levine, A.J., and Heintz, N. (2003). Beclin 1, an autophagy gene essential for early embryonic development, is a haploinsufficient tumor suppressor. Proc Natl Acad Sci USA *100*, 15077-15082.

Zalckvar, E., Berissi, H., Mizrachy, L., Idelchuk, Y., Koren, I., Eisenstein, M., Sabanay, H., Pinkas-Kramarski, R., and Kimchi, A. (2009). DAP-kinase-mediated phosphorylation on the BH3 domain of beclin 1 promotes dissociation of beclin 1 from Bcl-XL and induction of autophagy. EMBO reports *10*, 285-292.

Zhang, J., Kan, S., Huang, B., Hao, Z., Mak, T.W., and Zhong, Q. (2011). Mule determines the apoptotic response to HDAC inhibitors by targeted ubiquitination and destruction of HDAC2. Genes Dev *25*, 2610-2618.

Zhong, Y., Morris, D.H., Jin, L., Patel, M.S., Karunakaran, S.K., Fu, Y.J., Matuszak, E.A., Weiss, H.L., Chait, B.T., and Wang, Q.J. (2014). Nrbf2 Suppresses Autophagy by Modulating Atg14L-containing Beclin 1-Vps34 Protein Complex Architecture and Reducing Intracellular Phosphatidylinositol-3 Phosphate Levels. J Biol Chem *289*, 26021-26037.

Zhong, Y., Wang, Q.J., Li, X., Yan, Y., Backer, J.M., Chait, B.T., Heintz, N., and Yue, Z. (2009). Distinct regulation of autophagic activity by Atg14L and Rubicon associated with Beclin 1–phosphatidylinositol-3-kinase complex. Nat Cell Biol *11*, 468-476.

Zoncu, R., Bar-Peled, L., Efeyan, A., Wang, S., Sancak, Y., and Sabatini, D.M. (2011). mTORC1 senses lysosomal amino acids through an inside-out mechanism that requires the vacuolar H(+)-ATPase. Science *334*, 678-683.

Zoncu, R., Efeyan, A., and Sabatini, D.M. (2010). mTOR: from growth signal integration to cancer, diabetes and ageing. Nat Rev Mol Cell Biol *12*, 21-35.